

Frequency Response Characteristics
Of Respiratory Flow-meters

by

Jianchen Hu

A Thesis Presented in Partial Fulfillment
of the Requirements for the Degree
Master of Science in Technology

Approved November 2013 by the
Graduate Supervisory Committee:

Narciso Macia, Chair
Scott Pollat
Bradley Rogers

ARIZONA STATE UNIVERSITY

December 2013

ABSTRACT

Flow measurement has always been one of the most critical processes in many industrial and clinical applications. The dynamic behavior of flow helps to define the state of a process. An industrial example would be that in an aircraft, where the rate of airflow passing the aircraft is used to determine the speed of the plane. A clinical example would be that the flow of a patient's breath which could help determine the state of the patient's lungs. This project is focused on the flow-meter that are used for airflow measurement in human lungs.

In order to do these measurements, resistive-type flow-meters are commonly used in respiratory measurement systems. This method consists of passing the respiratory flow through a fluid resistive component, while measuring the resulting pressure drop, which is linearly related to volumetric flow rate. These types of flow-meters typically have a low frequency response but are adequate for most applications, including spirometry and respiration monitoring. In the case of lung parameter estimation methods, such as the Quick Obstruction Method, it becomes important to have a higher frequency response in the flow-meter so that the high frequency components in the flow are measurable. The following three types of flow-meters were:

- a. Capillary type
- b. Screen Pneumotach type
- c. Square Edge orifice type

To measure the frequency response, a sinusoidal flow is generated with a small speaker and passed through the flow-meter that is connected to a large, rigid container. True flow is proportional to the derivative of the pressure inside the container. True flow is then compared with the measured flow, which is proportional to the pressure drop across the flow-meter.

In order to do the characterization, two LabVIEW data acquisition programs have been developed, one for transducer calibration, and another one that records flow and pressure data for frequency response testing of the flow-meter. In addition, a model that explains the behavior exhibited by the flow-meter has been proposed and simulated. This model contains a fluid resistor and inductor in series. The final step in this project was to approximate the frequency response data to the developed model expressed as a transfer function.

ACKNOWLEDGMENTS

I sincerely express my gratitude towards my advisor Dr. Macia, for his guidance and continued support for my learning and writing for this project.

I also want to say thank you to Rene Fischer. It was with his help in pulmonary instrumentation lab that I was able to get equipment I needed on time, and also have broken things fixed on time. This project would have required much more time without his help. Also I want to thank my committee members Bradley Rogers and Scott Pollat for their valuable advice and suggestions on this project.

I am also grateful to my classmates for their voluntary help and comments, and also with their help to follow the schedule.

My parents have gave me motivation and courage to do this project, Special thanks to them.

There are lots of people behind this project that I cannot list their names, this project would have been impossible without their generous help. Thank you all!

Jianchen Hu

TABLE OF CONTENTS

	Page
ABSTRACT.....	i
ACKNOWLEDGMENTS.....	ii
LIST OF FIGURES.....	vi
Chapter 1.....	1
INTRODUCTION.....	1
1.1 Flow Measurement.....	2
1.2 Research Objectives.....	4
Chapter 2.....	6
LITERATURE REVIEW.....	6
2.1 Flow Type.....	7
2.2 Flow-meter Type and Principles.....	9
2.2.1 Concepts and Physics.....	10
2.2.2 Types of Fluid Flow-meters.....	10
2.2.2.1 Differential Pressure Flow-meters.....	10
2.2.2.2 Velocity Flow-meters.....	14
2.2.2.3 Positive Displacement Flow-meter.....	16
2.2.2.4 Mass flow-meter.....	16
2.3 Respiratory System Monitoring.....	17
2.3.1 Spirometry.....	17
2.3.2 Parameter estimation.....	18
Chapter 3.....	21
SYSTEM MODELING.....	21
3.1 Pneumatic systems and electrical systems.....	21
3.1.1 Electrical system components.....	21
3.1.2 Pneumatic system components.....	22
3.1.3 Modeling physical systems.....	25
3.2 Differential pressure flow-meter.....	25
3.2.1 Fleish Pneumotachometers.....	26
3.2.2 Squared-Edged Orifice Flow-meter.....	28
3.3 Dynamic Characteristics.....	28
3.3.1 Human breathing.....	28

3.3.2 Flow-meter frequency response	30
Chapter 4	36
TEST EQUIPMENT	36
4.1 Test Equipment	36
4.1.1 Flow measurement	36
4.1.1.1 Wet Test Meter	36
4.1.1.2 U-tube manometer	38
4.1.2 Flow generator.....	38
4.1.3 Pressure transducer	39
4.1.4 Low-pass Filter and Amplifier	41
4.1.5 Data Acquisition System (DAQ)	43
4.1.6 Flow-meters.....	46
4.2 Test Loop.....	46
4.2.1 Calibration	46
4.2.1.1 Wet Test Meter calibration	47
4.2.1.2 Linear flow-meter calibration	48
4.2.1.3 Nonlinear flow-meter calibration.....	50
4.2.1.4 Pressure calibration.....	52
4.2.2 Test Loop Setup	53
4.3 Software.....	55
4.4 Potential problem.....	56
4.4.1 Hardware	56
4.4.2 Software	58
4.4.3 Noise and disturbances	60
Chapter 5	61
EXPERIEMTNAL RESULTS	61
5.1 Calibration results	61
5.1.1 Flow calibration.....	61
5.1.1.1 Capillary tube.....	62
5.1.1.2 Square edged orifice	64
5.1.2 Pressure calibration.....	65
5.2 Dynamic Characteristics.....	67
5.2.1 Frequency response of linear flow-meter	67
5.2.1.1 Capillary tube flow-meter.....	68

5.2.1.2 Screen Pneumotach Flow-meter.....	69
5.2.2 Frequency response of non-linear flow-meter.....	70
5.2.3 Factors affect Phase shift.....	70
5.2.3.1 Effect of capacitance difference of pressure transducer	71
5.2.3.2 Effect of inductance	72
5.2.4 Comparison of three flow-meters	75
5.2.4.1 Bandwidth.....	75
5.2.4.2 Phase shift.....	76
5.2.5 PSPICE simulation results	77
5.2.6 First Order system model	78
5.3 Discussion	80
Chapter 6	81
CONCLUSION AND RECOMMENDATION.....	81
REFERENCES	83
APPENDIX A	85
APPENDIX B	89
APPENDIX C	91
APPENDIX D	95

LIST OF FIGURES

Figure	Page
1.1 Approaches to Fluid Mechanics and our approaches	2
1.2 typical pipe flow measurement	3
1.3 Sketch of Square Edged Orifice flow measurement	4
2.1 Traces for Turbulent, Transitional, Laminar flow	9
2.2 Capillary tube.....	11
2.3 Orifice Plate	12
2.4 Venturi tube	13
2.5 Pitot tube.....	15
2.6 Ultrasound-Acoustic flow-meter	16
2.7 Test Setup for Quick Obstruction Method	19
3.1 Symbol for Fluid Resistor	23
3.2 Symbol for pneumatic tank.....	24
3.3 hydraulic and electrical systems.....	25
3.4 linear flow-meter relationship test setup.....	27
3.5 Data collected for linear flow-meter relationship	27
3.6 Data collected for non-linear flow-meter relationship.....	28
3.7 Human breath and Tidal volume definition.....	29
3.8 Capillary tube modeling circuit	30
3.9 Capillary tubing flow-meter.....	31
3.10 Capillary tube modeling with pressure transducer circuit.....	31
3.11 linear frequency response modeling	32
3.12 Capillary tube simulation results.....	33
3.13 Pressure transducer calibration process	34
3.14 Signal conditioning circuit coefficient.....	34
3.15 nonlinear flow-meter modeling process.....	35
3.16 Square edged orifice tube simulation result.	35

Figure	Page
4.1 Wet Test Meter and stopwatch.....	37
4.2 Wet Test Meter flow measure.....	37
4.3 U-tube manometer.....	38
4.4 Function generator and audio amplifier.....	39
4.5 Pressure transducer device.....	40
4.6 Cross section of pressure transducer.....	40
4.7 4th order Butterworth filter with $f_c=375$ HZ frequency response.....	41
4.8 4th order Butterworth filter with $f_c=375$ HZ step response.....	42
4.9 Signal conditioning circuit.....	43
4.10 NI USB-6009 Device.....	44
4.11 block diagram of NI USB-6009.....	45
4.12 DAQ analog channel setup.....	46
4.13 Capillary, screen pneumotach and square edge orifice type flow-meters.....	46
4.14 Structure of Wet Test Meter.....	47
4.15 Structure of Wet Test Meter.....	49
4.16 nonlinear flow-meter calibration process.....	50
4.17 Pressure calibration process.....	52
4.18 Test loop setup.....	53
4.19 Nonlinear flow-meter data recorded.....	54
4.20 Front panel of labview.....	55
4.21 Part of backend labview code.....	56
4.22 moister air in flow calibration process.....	57
4.23 Flow rate calculator from Wet Test Meter.....	59
5.1 Linear flow-meter calibration coefficient (from Excel).....	62
5.2 Linear flow-meter calibration coefficient (from LabVIEW).....	63
5.3 nonlinear flow-meter calibration coefficient (from Excel).....	64

Figure	Page
5.4 Nonlinear flow-meter calibration coefficient (from LabVIEW).....	65
5.5 Pressure calibration coefficient (from LabVIEW)	66
5.6 Setup for frequency response	67
5.7 Frequency response of capillary tube	68
5.8 Frequency response of Screen Pneumotach flow-meter	69
5.9 Frequency response of Square edged orifice	70
5.10 Capillary tube cross-section	71
5.11 Phase difference affected by pressure transducer capacitance difference	72
5.12 RLC Circuit	72
5.13 PSPICE simulation for pneumatic system with inductance.....	73
5.14 PSPICE simulation for inductance effect of phase angle.....	74
5.15 PSPICE frequency response for phase difference.....	74
5.16 Magnitude frequency response of three devices	75
5.17 Phase shift frequency response of three devices	76
5.18 PSPICE simulation for frequency response process setup.....	77
5.19 AC analysis of magnitude and phase difference	78
5. 20 equivalent electrical model for flow-meter	79
5. 21 Comparison with first order system	79
6.1 frequency response data for three devices	81

ACRONYMS AND ABBREVIATIONS

A	Cross sectional area (m ²)
t	Time (sec)
π	Constant Pi (3.14)
P	Pressure (Pascal or N/m ² or kg/(m*s ²))
V _{tv}	Tidal Volume (cm ³)
f	Frequency
V	Volume (cm ³)
Q	Flow (cm ³ /sec)
R	Reynolds number
R _{LF}	Linear flow-meter coefficient
K _{NF}	Nonlinear flow-meter coefficient
ΔP	Pressure difference
μ	Absolute viscosity of the gas
L	Length of the tube (cm)
l	Length of the orifice(cm)
r	Radius of the orifice
d	Diameter of orifice
n	Polytrophic coefficient
D	Diameter of tube
v	Speed at a point on a streamline
g	Acceleration due to gravity
z	Elevation of the point above a reference plane
ρ	Density of the fluid
β	Ratio of diameter in a tube (D ₂ /D ₁)
C _d	Discharge coefficient

Chapter 1

INTRODUCTION

Exploring a way to assess the condition of the lungs of a diseased patient using a technique that is minimally invasive, quick to perform and low cost has always been desirable. There are several clinical approaches that have been used, including spirometry and lung parameter estimation. A special parameter estimation approach called the Quick Obstruction Method (QOM) doesn't need expensive and complicated equipment [22]. Instead, it uses inexpensive equipment including a mask, a flow-meter, a pressure sensor for mouth pressure, and a fast acting valve used to create the quick obstruction. The method consists of obstructing the airflow during normal respiration for a fraction of a second (approximately 1/20s) while recording the resulting flow and mouth pressure.

The parameter Q is used to indicate flow rate in the commonly used approach, referred to as the Control Volume approach. In this approach, the volumetric flow-rate is measured through a fixed shape restriction.

Flow rate is typically determined by measuring pressure drop across the fixed shape restriction.

For laminar flow through a capillary flow-meter or a screen pneumotach flow-meter, a linear relationship of pressure and flow exist from Poiseuille's equation, which can be expressed as $\Delta P = R_{LF} * Q$, where R_{LF} is the linear coefficient. [2] The narrow bandwidth of this type of flow-meter is the main limitation for high frequency measurement. In order to obtain the necessary bandwidth, a non-linear flow-meter, called square edge orifice was ultimately recommended in this project. The equation that characterizes this nonlinear flow-meter is $\Delta P = K_{NF} * Q|Q|$, where K_{NF} is the non-linear coefficient. This type of flow-meter has the higher bandwidth which is more suitable for respiratory parameter estimation method.

Two LabVIEW programs were developed in this project:

- a) The first program calibrates the flow-meter and pressure transducer. The resulting coefficients are plotted and saved in user defined locations. Coefficient substitution is done in sub-VIs (both linear and nonlinear flow-meter).

- b) The second program records dynamic flow data for different frequencies. Magnitude and phase angle are recorded in user defined locations. Frequency response data is formatted for plotting in MATLAB.

The fluid system and flow-meters are all modeled by electrical circuits so that electrical simulation tools including PSPICE and LabVIEW can be used to model the dynamic behavior of the system. Simulation results are compared to experimental results.

1.1 Flow Measurement

Typically there are three approaches in fluid mechanics, experimental, theoretical and computational. In this project, experimental approach is heavily used since access is available to the equipment necessary to get experimental results. Additionally, the theoretical approach will be used to develop mathematical equations that govern the flow. Finally, the experimental results are related to the theoretical results, as shown in **Figure 1.1**.

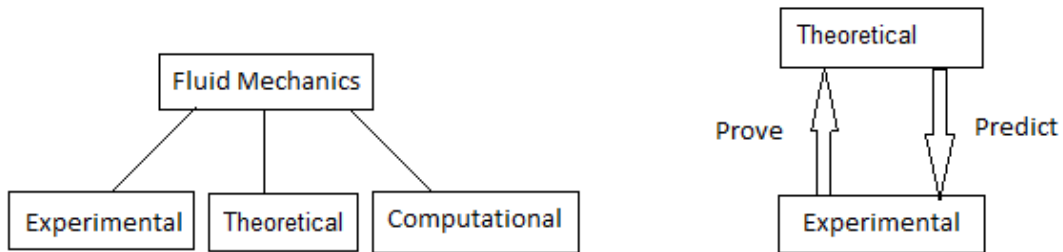


Figure 1.1 Approaches used in fluid mechanics and approaches in this project

Fluid flow is caused by pressure differences and gradients, in human body, human breath is the result of pressure difference generated by expansion and contraction of diaphragm and chest. Nowadays, there are many different ways to measure flow rate. Pipe flow is the basic flow type in almost everywhere. Pipe flow measurement requires a technology which placed in a short section of pipe which should not block the flow of fluid. Because molecules are in random motion, the fluid fills the conduit completely, the main force that drives the flow is the pressure difference. In

this project, the fluid is not compressed, so the fluid is treated as an incompressible fluid, and also gravity is ignored. Pipe flow is the most convenient and basic technology used in the market.

Figure 1.2 shows the idea of pipe flow measurement.

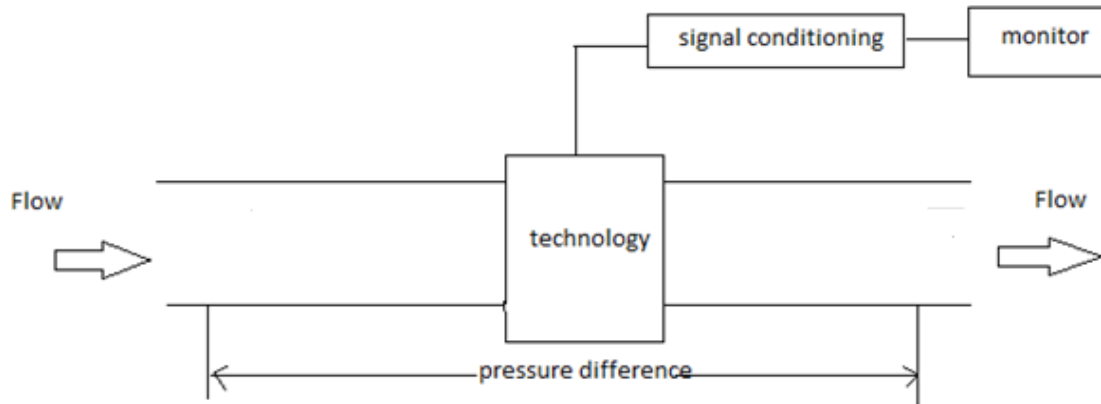


Figure 1.2 typical pipe flow measurement

In this project, differential pressure type flow-meter is used to measure flow rate Q_{flow} . The first simple device available is the capillary flow-meter. Capillary tube is constructed by putting many small diameter tubes in parallel, across a large diameter tube, Poiseuille's equation shows a linear pressure-flow relationship of this capillary tube, $\Delta p = K_{LF} * Q_{flow}$, K_{LF} is the linear coefficient.

Figure 2.2 shows the basic structure of capillary tube.

Another kind of device which is simple and suitable in this project is the square-edge orifice. It is constructed by introducing a constriction in the flow, and then the pressure difference caused by the constriction can be related to Q_{flow} by applying Bernoulli's theorem. It shows a quadratic relationship which can be simply expressed by $\Delta P = K_{NF} * Q_{flow}^2$. This equation adequately describes flow in the direction that makes Q positive. However, to capture negative flow, this equation is modified to be $\Delta P = K_{NF} * Q_{flow} * |Q_{flow}|$. Detail information about the factor K_{NF} will be discussed later. **Figure 1.3** shows the squared-edge orifice technology. When the fluid moves through the orifice, it contracts and then expands. This results in a pressure drop across the orifice, the decrease in pressure as the fluid passes through the orifice is the result of velocity increase as the fluid passes through the reduced area, which can be captured by the pressure

difference flow-meter.

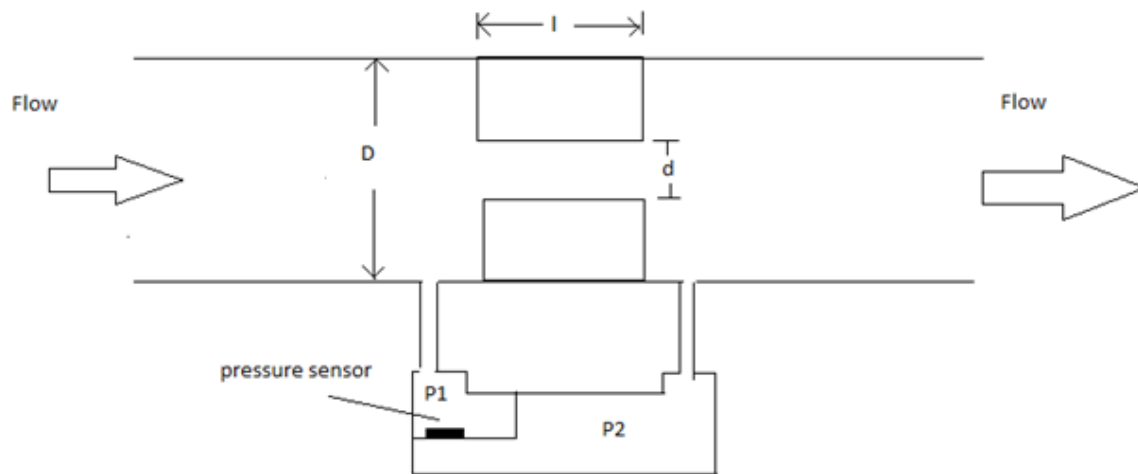


Figure 1.3 Sketch of Square Edged Orifice flow measurement

Due to the fact that human breath is non-steady flow, the dynamic behavior of flow-meter has to be determined. The Laplace transform is used to determine frequency response of the system, by obtain a transfer function captures the ratio of measured flow to true flow. Equations introduced in this project are frequency domain.

1.2 Research Objectives

This research requires some basic understanding of fluid mechanics and control theory, because behind the fluid physics, the most critical thing is the frequency response of respiratory flow-meters. There is a need to understand orifice flow for certain orifice geometries, and the frequency response characteristics. Therefore, the research objectives of this project are defined as follows:

1. Setup the equipment for flow measurement includes calibration. Confirm that the flow rate indicated by sensor, amplification circuit, and the data acquisition software is the true flow rate.

2. Perform frequency response tests of three flow-meters, two linear type flow-meters: Capillary flow-meter and screen pneumotach flow-meter, a nonlinear flow-meter: Square-edge orifice.
3. Develop LabVIEW programs for calibration and frequency response measurement. Program should accommodate user defined coefficient save and load location, data accuracy and readability for MATLAB data handling.
4. Develop an equivalent electrical model that can be used to explain the behavior of flow-meters. Model and simulate in PSPICE, and compare the behavior of the ideal model's frequency response to the experimentally frequency response.
5. Fit an ideal first order model to experimental data in the MATLAB. Observe if the ideal electrical model can capture adequately the behavior of real flow-meters.

Chapter 2

LITERATURE REVIEW

Fluid mechanics is an old subject, after Archimedes found liquid balancing which is the foundation of hydrostatics, this subject has not been developed for thousands of years until 15 century, Da Vinci started to talk about pipe flow, water wave, then in 17 century, Newton discussed object's movement in fluid, until the development of Euler's equation and Bernoulli's equation, fluid mechanics then formally became a science subject to be developed. In 20 century, aircraft industry promote the development of fluid mechanics. Now, more and more new technologies are being developed in this area.

Flow rate Q is the most critical factor to indicate the properties of flow, how to get the flow rate under some certain conditions is the question to be answered for most engineers working in this area.

Flow can be expressed by 3 different types, Laminar, Turbulent and Transitional, This is a very important classification expressed by Osborne Reynolds' experiment [2], he injected a dye to observe the nature of a flow, when speed is small, the flow pass as a straight line, called Laminar flow, when the speed is faster, some intermittent bursts occurred, this is called Transitional flow, as the speed continue to increase, the dye is blurred, this is called Turbulent flow. He also expressed a Reynolds number as $R = \frac{\rho * V * d}{\mu}$, It is a ratio of the inertial force to the viscous damping force. It is also proved that if the Reynolds number is less than 2100 then it is Laminar, if it is greater than 4000 it is Turbulent, it is Transitional if it is in between. Reynolds number is a critical factor to express properties of a flow itself.

The idea of flow measure is straight forward, measure the flow rate without disturbing the flow, some techniques have been developed, like pressure differential flow-meter, ultrasonic flow-meter and so on, different types can be used under different conditions, in this project, pressure-flow type flow-meter is used.

In respiratory system, lungs behavior is the most critical part to analysis health condition of patient, lungs are part of a group of organs and tissues that all work together to help breathe, the

resulting flow of human breath can indicate health status. There are two ways to measure the flow and volume of human lungs in clinical areas, 1. Spirometry is the most commonly used technique in clinical area, it is used to diagnose asthma, chronic obstructive pulmonary disease (COPD) and certain other conditions that affect breathing, spirometry may also be used periodically to check how well lungs are working for chronic lung conditions. Indicators such as tidal volume (TV) and vital capacity (VC) provide a glimpse of the range of motion of the lungs. Forced Expiratory Volume (FEV) and other parameters are used together to compare to the average value based on age, sex. Below the average means lungs are not working properly as it should be. This method requires patients' cooperation. 2. Parameter estimation method is to deal with noninvasive measurement of components descriptive of the mechanical characteristics of the respiratory apparatus. Parameters include resistance (R), elastance ($E=1/C$), inertance (L). Interrupter technique (IT) is introduced by von Neergaard and Wirz [23]. It consists in execution of a short duration occlusion at the mouth and pressure and flow measurement in the mouthpiece. This method requires large computation, but this technique doesn't need patients' cooperation and can be applied to unconscious patients.

Due to the fact that interrupter technique assumes that mouth and alveolar pressure equilibrate almost instantaneously during the interruption process, this interruption process should be fully detected from flow-meter through pressure sensor, this yields high bandwidth flow-meter, frequency response of flow-meters shows important bandwidth limitation which can be compensated in software.

2.1 Flow Type

Flow can be classified into two types, compressible and incompressible flow, a more visualize example would be liquid and gas, liquid is incompressible flow which doesn't have a fixed shape but fixed size, compressible flow such as gas doesn't have fixed shape and size. Technically, all fluids are compressible to some extent, which means changes in pressure would result in changes in density, however, in some cases the changes in pressure are very small that the

changes in density is negligible, which means the density of the fluid doesn't change with time in the process, then it can be defined incompressible flow. For gas, Mach number is the parameter to define if a flow of gas is compressible or not. The Mach number is named after physicist Ernst Mach, it is a dimensionless quantity representing the ratio of speed of an object moving through a fluid and the local speed of sound.^[3] M is the Mach number, v is the velocity of the source, v_{sound} is the speed of sound, $M = \frac{v}{v_{\text{sound}}}$. Usually, at low Mach number, say lower than 0.3, the compressible effect can be ignored, we can define the flow incompressible. For small Mach number flow, incompressible Navier Stokes equations can be used, for large Mach number flow, the compressible flow equation can be used to get numerical solution. However, nothing is perfect, both compressible and incompressible effect exist in real world flow, there is a numerical method to compute compressible flow with low Mach number regions on a staggered grid using a pressure correction method extended for compressible flow proposed ^[4]. There are also many interesting papers talking about simplified equations for low Mach number under different conditions. ^[5]

As been introduced earlier, Reynolds number which can be defined as $R = \frac{\rho * V * d}{\mu}$, ρ is the density of the fluid, V is the mean velocity of the object relative to the fluid, μ is the dynamic viscosity of the fluid, d is the hydraulic diameter of the pipe. It can be used to define if a flow is laminar or turbulent or transitional, **Figure 2.1** shows the traces of three types of flow. The Reynolds can be used to evaluate if a fluid is viscous or inviscid, that means if the fluid friction has significant effects on the fluid motion. Some papers testing different Reynolds number square edged orifice results have proven that Reynolds number is critical factor especially for liquid.^[6]

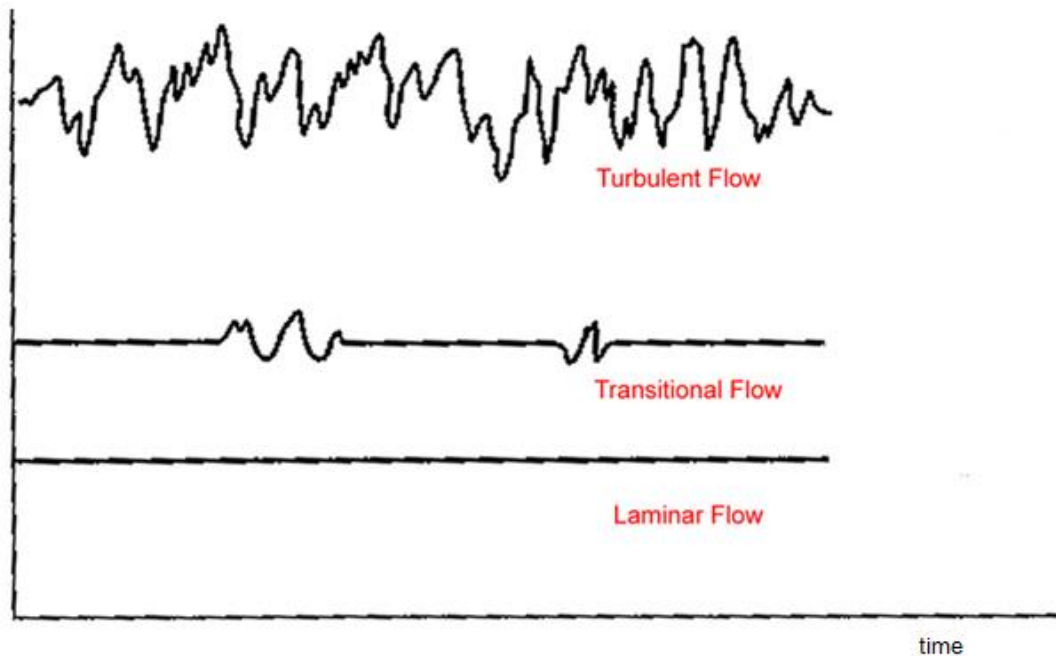


Figure 2.1 Traces for Turbulent, Transitional, Laminar flow

Another important classify of flow which is especially crucial for this project is steady and unsteady flow. Steady flow is the condition where the fluid properties at a point doesn't change over time, otherwise flow is unsteady. Technically all flows are unsteady, it only depends on how to analysis the flow, the unsteady flow analysis is usually the case for most process especially in medical area, because of the human lung behavior, and steady flow is used for analysis and device calibration, steady and unsteady flow in different processes can be obtained. [7]

2.2 Flow-meter Type and Principles

Flow-meter is the type of device which can measure the flow rate of fluid indirectly by using some techniques. From a business point of view, cheap, accurate, convenient flow-meter is the one we should be shooting for, in this section we will introduce different types of flow-meters that have and continue to be used for measuring respiratory flow in industrial world [8], even though some are not been used widely, they are under studied and are great paths to access respiratory systems. Also in this chapter we will introduce the physics and techniques behind them, we will start this section by introduce some basic equations we will be using.

2.2.1 Concepts and Physics

The method we use to access the respiratory system is control volume approach, focus on a fixed boundary, mass, momentum and energy are allowed to cross the boundary, call CV [9].

For low Mach number gases, it can be considered to be incompressible, so the density is constant, an important equation in fluid physics is Bernoulli equation [10]:

$$\frac{v^2}{2} + gz + \frac{p}{\rho} = \text{constant}$$

v is speed of flow, g is acceleration due to gravity, z is the elevation of the point above a reference plane, p is the pressure, ρ is the density .

For laminar flow in capillary tubing, the pressure drop can be found using Poiseuille's equation [11]:

$$\Delta P = \frac{128\mu LQ}{\pi D^4 N}$$

This shows a linear relationship between pressure difference P_{diff} and flow rate Q, μ is the viscosity of fluid, L is the length of tube, r is radius, Q is the volumetric flow rate. N is the number of small diameter pipes.

2.2.2 Types of Fluid Flow-meters

The different types of common used flow-meters and their principles will be introduced in this section, generally speaking, there are 5 types of flow-meters, (1) Differential Pressure Flow-meters. (2) Velocity Flow-meters. (3) Positive Displacement Flow-meters. (4) Mass Flow-meters. (5) Open Channel Flow-meters.

2.2.2.1 Differential Pressure Flow-meters

For a differential pressure flow-meters, the flow is calculated by measuring the pressure drop over an obstructions inserted in the flow, through the relationship between pressure drop and volumetric flow, flow rate can be calculated accurately, (within 5% according to American Thoracic society)[12].

Capillary tube

In capillary tube, if the flow is laminar, the pressure drop can be found through Poiseuille's equation:

$$\Delta P = \frac{128\mu L Q}{\pi D^4 N}$$

Which have been introduced above. In reality, flow is not totally laminar, there are always some turbulent flow exist, as far as our concern, we treat it laminar now to have a pure linear relationship expressed as:

$$\Delta P = R_{LF} Q$$

R_{LF} is the linear fluid resistive coefficient, which is equal to $\frac{128\mu L}{\pi D^4 N}$ in Poiseuille's equation. See

Figure 2.2

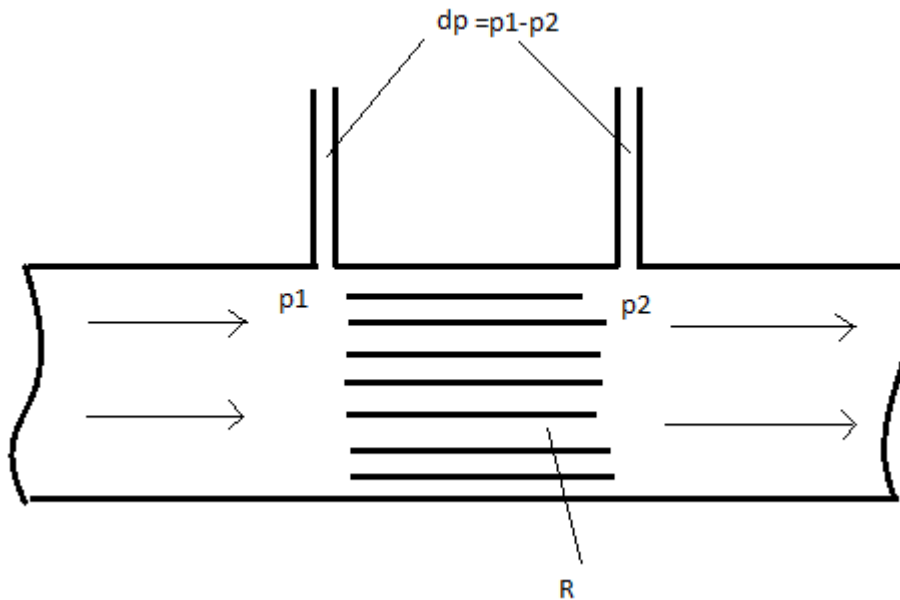


Figure 2.2 Capillary tube

Orifice Plate

An orifice plate is the thin plate with a hole in the middle, it is placed in a pipe in which fluid flows, when the fluid reaches the orifice plate, it is forced to converge to go through the small hole, and the fluid flow is measured through the difference in pressure from the upstream side to the downstream side. This is a very precisely method to measure the flow [13].

By assuming steady-state, incompressible, inviscid, laminar flow in a horizontal pipe with negligible frictional losses, we can use a simplified Bernoulli's equation to get the relationship between two points on the same streamline:

$$P_1 + \frac{1}{2}\rho V_1^2 = P_2 + \frac{1}{2}\rho V_2^2$$

The orifice plates are simple, cheap and convenient, however, large nonlinearity is a big question, and also, because of the squared factor, the accuracy is poor at low frequency, a high accuracy depend on sizing, a typical orifice plate is shown in **Figure 2.3**^[13]

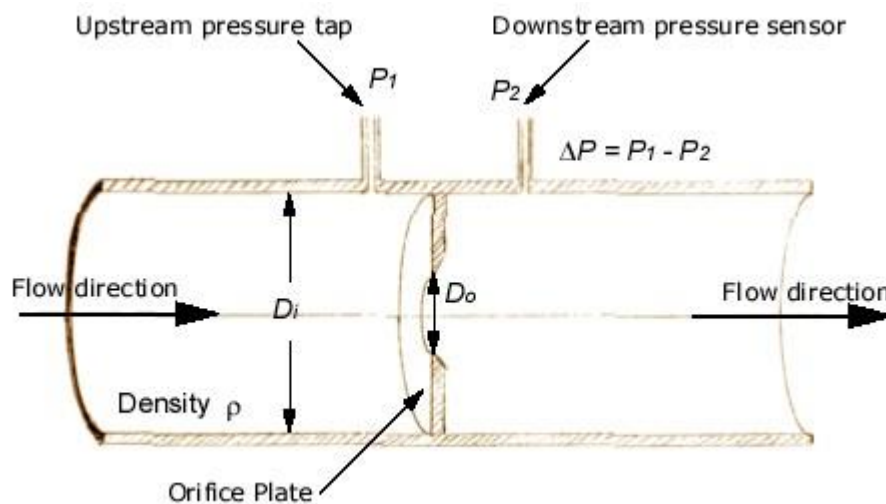


Figure 2.3 Orifice Plate

To start calculate the square edge orifice equation we need to have some assumptions to use simplified Bernoulli equation and continuity equation. Assume the flow is steady and incompressible, pipe is horizontal, no friction losses. Now we can use Continuity equation:

$$\rho_1 A_1 V_1 = \rho_2 A_2 V_2$$

And Bernoulli equation:

$$\frac{p_1}{\rho} + \frac{V_1^2}{2} = \frac{p_2}{\rho} + \frac{V_2^2}{2}$$

Derive from these two equations we have:

$$p_1 - p_2 = \frac{\rho V_2^2}{2} \left[1 - \left(\frac{A_2}{A_1} \right)^2 \right]$$

Solve for V_2 we have:

$$V_2 = \sqrt{\frac{2(p_1 - p_2)}{\rho[1 - (\frac{A_2}{A_1})^2]}}$$

Flow rate $Q=A_2V_2$, so we get:

$$Q = A_2 \sqrt{\frac{2(p_1 - p_2)}{\rho[1 - (\frac{A_2}{A_1})^2]}}$$

For a certain technology, all the dimension parameters are well defined, we write p_1-p_2 as Δp , and we can get:

$$\Delta p = R_{NF}Q^2$$

To make this even function an odd function, so that the negative flow can result in negative pressure, we modify this equation to get the nonlinear relationship:

$$\Delta p = R_{NF}Q|Q|$$

Where R_{NF} is the nonlinear coefficient.

Venturi tube

Venturi tube is a kind of tube with a constricted section, the pressure difference is measured between the normal tube cross section and reduced area cross section, similar to orifice plate, Bernoulli equation is also used to analysis the flow information. **Figure 2.4** shows this kind of technique.

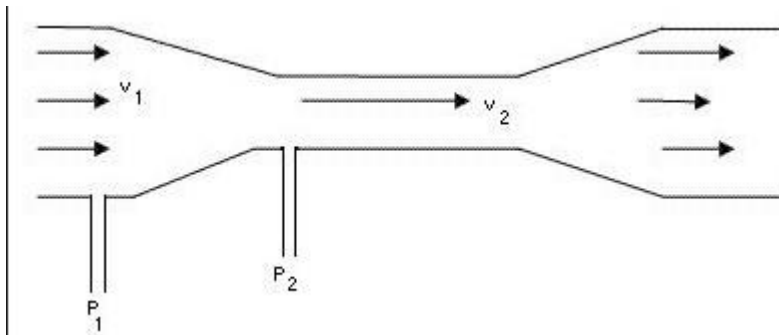


Figure 2.4 Venturi tube

Flow Nozzles

Flow nozzles is also a kind of pressure difference flow creator, it has a smooth elliptical inlet leading to a throat section with a sharp outlet. This restriction in the fluid flow causes a pressure drop, which would related to the flow through Bernoulli equation.

There are many different kinds of pressure difference flow-meters, they all basically use the same mechanism, create a pressure difference through sizing the tube. This is the most commonly used type of flow-meter

2.2.2.2 Velocity Flow-meters

For a velocity flow-meter, the basic idea to calculate flow is to measure the speed in one or more points in the flow, then integrate the flow speed over the flow area.

Pitot tube

The Pitot tube focus on point measure, the basic Pitot tube consists of a tube pointing directly into the fluid flow, then the pressure at this point can be measured, the moving fluid is brought to rest as there is no outlet to allow flow to continue, now use a simplified Bernoulli equation:

$$P_t = P_s + \left(\frac{\rho V^2}{2}\right)$$

Solve for V, get

$$V = \sqrt{\frac{2(P_t - P_s)}{\rho}}$$

Figure 2.5 shows this kind, this is a very popular flow-meter to measure the speed of flow, especially in air applications [14].

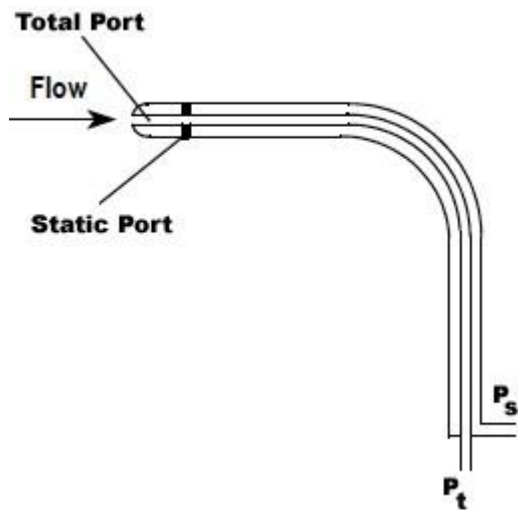


Figure 2.5 Pitot tube

Calorimetric flow-meter

The calorimetric flow-meter is to place two temperature sensors in close contact with each other within the fluid but thermal insulated from each other, one of the sensors is constantly heated, another is cool, when the fluid flow increases, heat is transferred from one to the other, temperature difference between the sensors is reduced, this reduction is proportional to the flow rate. As we can see that, response times will vary due to the thermal conductivity of the fluid.

Turbine flow-meter

The basic idea for turbine flow-meter is this, if a fluid moves through a pipe and acts on the vanes of a turbine, the turbine will start to spin and rotate. The rate is measured to calculate the flow. This kind of device is used for large flow, not suitable for small load flow-meter due to friction problem [15].

Electromagnetic flow-meter

Based on Faraday's law of electromagnetic induction, when a conductor moves through a magnetic field, voltage will be induced, the fluid acts as the conductor and the magnetic field is generated by energized coils outside the flow tube.

So this kind of flow-meter has a huge limitation, which is it can only be used for electrical conductive fluid.

Ultrasound-Acoustic flow-meter

This flow-meter uses the Doppler phenomenon, which states that sound travels faster if the medium is also moving, it provides a property independent measurement of flow, and the measurement is independent of gas composition, pressure, temperature, and humidity. In this flow-meter as shown in **Figure 2.6**, a pair of transmitters sends and receives sound. The difference between these two transit times is used for calculating flow. [16]

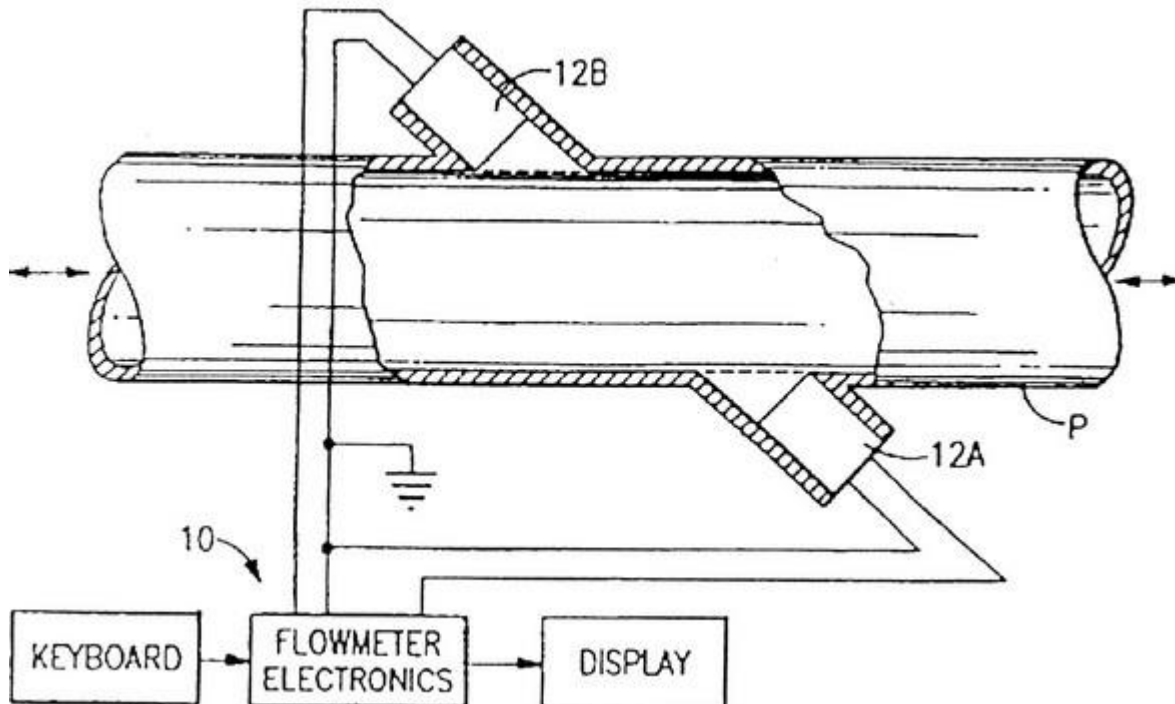


Figure 2.6 Ultrasound-Acoustic flow-meter

2.2.2.3 Positive Displacement Flow-meter

The positive displacement flow-meter measures process fluid by precision-fitted rotors as flow measuring elements. Known and fixed volumes are displaced between the rotors. The rotation of the rotors are proportional to the volume of the fluid being displaced.

2.2.2.4 Mass flow-meter

Mass flow-meter measure the mass flow rate directly. The mass flow rate is the mass of fluid traveling past a fixed point per unit time. This can be very accurate.

Thermal flow-meter

Thermal flow-meter uses thermistors to measure the flow. Thermistors are electrical resistors made of a material whose resistance decreases with temperature. As the flow passes by the thermistor bead, it attempts to decrease its temperature, which translates to an increase in resistance, as a result, the change in current is proportional to fluid flow.

The accuracy of thermal mass flow device depends on the calibrations reliability of the actual process [17].

Coriolis flow-meter

Coriolis mass flow-meter uses the Coriolis Effect to measure the amount of mass moving through the element. The fluid to be measured runs through a U-shape tube is caused to vibrate in an angular harmonic oscillation. Due to this effect, phase shift on some places of the tubes can be measured with sensors.

2.3 Respiratory System Monitoring

To detect respiratory diseases in patients having the symptom of running out of breathe, or in patient suspected of having asthma, monitoring respiratory system becomes crucial.

Measurement of flow rate, tidal volume during a breathing procedure can capture the characteristics of lungs, chest wall and overall respiratory process. The basic idea is to determine how much air patient's lungs can hold, how quickly patient can move air in and out of lungs, how well patient's lung can absorb oxygen and release carbon dioxide out of blood. In short, the behavior of the lungs indicates the health status of the patient.

2.3.1 Spirometry

Spirometry is the most commonly used method for measuring lung functions. It is a measure of maximum volume and speed that air that can be inhaled and exhaled. Basically, patient is asked to take a deep breath and a quick exhaling into spirometer. Parameters are recorded during this process, Forced Vital Capacity (FVC) shows the maximum amount of air can be exhaled, Forced

Expiratory Volume (FEV) shows the maximum amount of air can be exhaled in one breath, for a specific duration in time, for example FEV₁, in the volume that can be exhaled during the first second. For healthy persons these parameters should be larger or equal to the predicted. Normally this test is performed several times to ensure repeatable values. However, this method depends highly on patient's cooperation and effort. Also FVC can easily be underestimated. Peak flow-meter test is one of the most critical aspect in spirometry, since a peak flow-meter measures the Peak Expiratory Flow (PEF), PEF is used to measure Peak Expiratory Flow Rate (PEFR), a good flow-meter should detect flow in a short rise time and short dwell time. Rise time is define as time it takes to go from 10% to 90% of PEF, while dwell time is the during the flow excess 95% of PEF. The expected value of parameters through this method depends on patients' height, sex and age.

2.3.2 Parameter estimation

Parameter estimation is another type of approach to access the respiratory system, respiratory system resistance, compliance and inertance can be determined from this approach. In interrupter method, a short period obstruction is introduced, assume that mouth and alveolar pressure are equilibrate instantaneously during this process, then the pressure measured at mouth equals to the alveolar pressure, so that, knowing the value of initial pressure drop (Δp_{ao}) and flow rate Q_{flow} before interruption, interrupter resistance can be calculated through:

$$R_{ini} = \frac{\Delta p_{ao}}{Q_{flow}}$$

This method was tested on children aged 2-7 years old [24].

Quick Obstruction Method consists of partial obstruction to the airflow during normal inspiration for a fraction of a second (1/20s approximately), while recording the resulting flow and mouth pressure. Through comparing the disturbed (actual flow and pressure signal) and undisturbed (obtained by extrapolating the pre-obstruction waveform) system, the difference between these two signals are fitted into a simplified respiratory model:

$$R_{resp}\dot{V} + I_{resp}\ddot{V} = P_{mouth}$$

The equipment used to estimate respiratory resistance R_{resp} , and respiratory inertance I_{resp} [22]. Using the Quick Obstruction Method is shown in **Figure 2.7**. This method requires a high frequency response flow-meter.

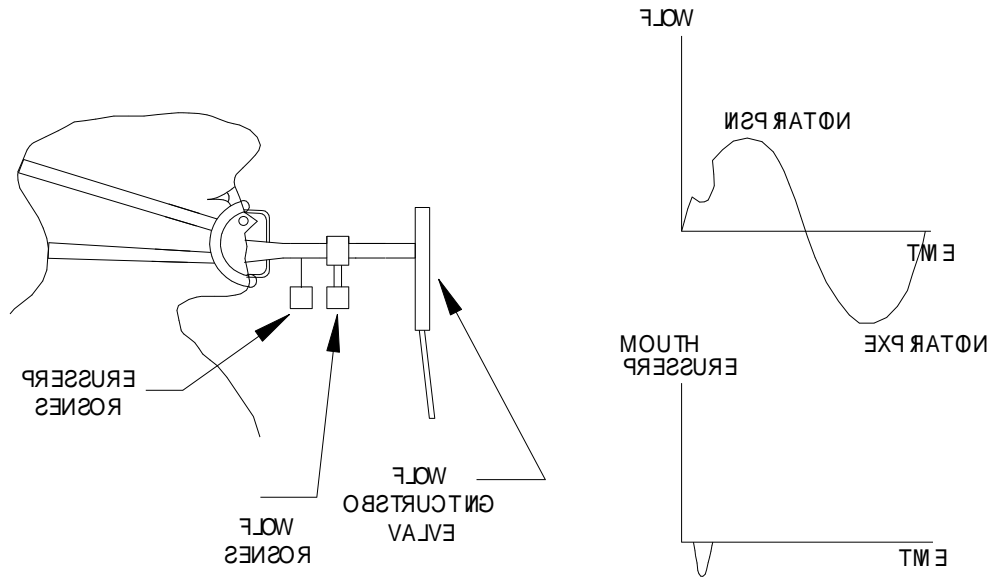


Figure 2.7 Test Setup for Quick Obstruction Method [22]

2.4 Frequency response of respiratory flow-meters

For a typical respiratory flow-meter, dynamic response characteristics can be determined by a frequency response test. There are two classical approaches to determine the frequency response of flow-meter. The first test is response to a transient, a step response is monitored and analysis, for a first order system, time constant τ is sufficient to describe the response of a first order lag to transient input. The second test is response of sinusoidal input over a range of frequency. In such a test a sinusoidally varying input is applied to the device and the output is compared to the input, parameters of interests are magnitude and gain. The gain is a measure of how much the output of flow-meter is amplified compared to the input, phase shift is a measure of time lead of flow-meter output follows the input.

Two different methods can be employed to quantify the true flow through a flow-meter. The first method is by using a piston pump as a flow source, however, the unavoidable compliance between the piston and the flow-meter may shunt enough away from the flow-meter to cause error. The second method is to allow the gas flow into a rigid chamber of known compliance, measure the pressure in the chamber and calculate the flow-rate.^[25]

Chapter 3

SYSTEM MODELING

As been introduced above, certain behaviors of pneumatic systems are similar to electrical systems. To perform analysis and predict the dynamic behavior of pneumatic systems, system modeling and simulation is required. This chapter introduces how to perform an analysis to capture the behavior of pneumatic systems.

Pneumatic systems are usually dynamic systems---system for which the input causes the output to vary with time. Dynamic systems are encountered in every engineering discipline. Due to the difficulties in modeling and analysis the behavior of pneumatic system, often devices and systems are modeled using analogous electrical components. Equivalent electrical parameters like resistance, inductance, and capacitance are used to describe the pneumatic system. The resulting electrical schematic can be easily modeled in SPICE for DC and AC analysis. The following section introduces how to transfer a pneumatic system into an electrical system.

3.1 Pneumatic systems and electrical systems

There are two types of inputs to dynamic systems, AC and DC signal for electronic systems, steady and unsteady flow in pneumatic systems. In the respiratory system, human breathing is an unsteady flow similar to a sinusoidal waveform. To understand the behavior of this pneumatic system, electrical simulation can be obtained by transferring the pneumatic system into equivalent electrical system. AC analysis in electrical system is equivalent to analysis of the frequency dependent characteristics of the devices in pneumatic systems. Also through comparison of frequency response, equivalent electrical model can be derived. This chapter is started by introducing equivalent electrical and pneumatic components.

3.1.1 Electrical system components

Electrical system components mentioned here are all ideal passive components, including resistors, capacitors and inductors. The pneumatic system can be represented with electrical

analog components. For this reason, the elementary equation describing electrical components are introduced here.

A Resistor can be described mathematically by:

$$V = IR$$

A Capacitor is an energy storing component, can be described by:

$$I = C \frac{dV}{dt}$$

The inductor stores energy in a magnetic field, and the voltage across it is given by

$$V = L \frac{dI}{dt}$$

3.1.2 Pneumatic system components

Similar to electronic systems, in pneumatic system, there are also three components to be discussed.

The Fluid Resistor

The fluid resistor is a component that exhibits resistance when the flow pass. It can be constructed by inserting additional fluid resistance inside the fluid conductor, usually small diameter tubes. The mathematical equation is given by:

$$p = Rq$$

Where p is the pressure difference, q is the flow, R is the fluid resistance. A schematic of the fluid resistor is shown in **Figure 3.1**.

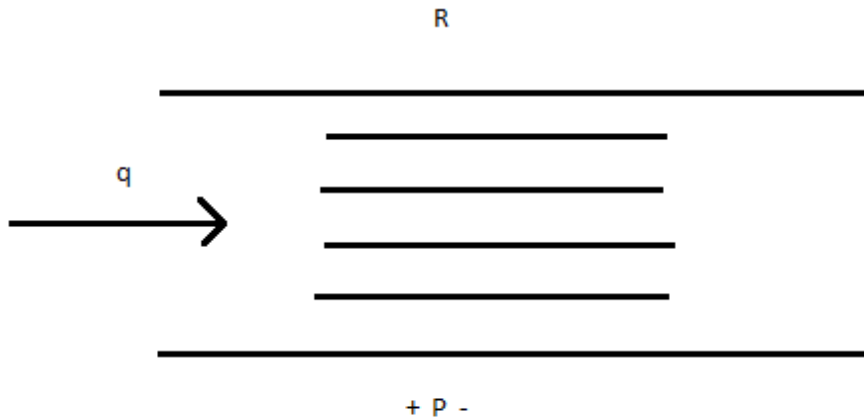


Figure 3.1 Schematic of a fluid resistor

The Pneumatic Tank

A Pneumatic tank is an energy-storing component, made up of a large tank. Because of the compressibility of the gas, a large volume of gas embodies this compressibility effect, making a tank act as an accumulator. The capacitance of this tank is given by:

$$C = \frac{V_{\text{tank}}}{n\bar{p}}$$

Where V_{tank} is the volume of the tank, \bar{p} is the average pressure, n is the polytropic exponent, a parameter that is related to the heat transfer in and out of the tank. For adiabatic process, $n=1.4$, for isothermal process, $n=1.0$. [12]

The real flow q into the tank is given by:

$$q = C \frac{dp}{dt}$$

In most applications if the dynamic are slow, the process is isothermal; if fast, the process adiabatic (no heat transfer).

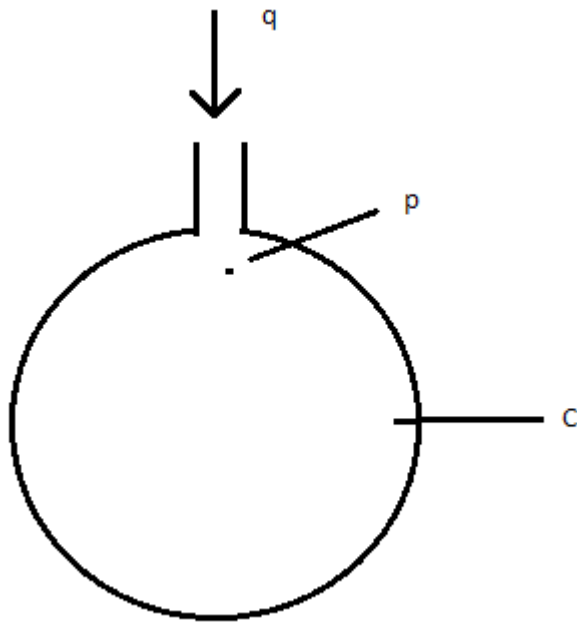


Figure 3.2 Symbol for pneumatic tank

The pneumatic tank, in the experiments performed here is called a “Glass jar”, it is used to measure true flow in our system, because it is placed at the end, it will act as a load capacitor in electrical system, so that the output current can be obtained through the elemental equation for a capacitor. In pneumatic system, true flow can be accessed using the above equation, can expressed in terms of the Laplace operator s ,

$$Q_{true} = CsP$$

A sinusoidal flow is generated with a small speaker and passed through the flow-meter under test which is connected to the “Glass Jar”. True flow is proportional to the derivative of the pressure inside the container.

Hydraulic Line with Inertia

A fluid moving inside a pipe has a certain amount of inertia. The inertial characteristic is described by the elemental equation:

$$p = \frac{\rho L}{A} \frac{dq}{dt}$$

Where L is the length of the conduit, A is the cross-sectional area, and ρ is the fluid's density. The fluid inertia can then be defined I_f as. $I_f = \frac{\rho L}{A}$.

Since air is much less dense than water, the effect of inductance is often negligible and rarely considered. However, in our project we have found out that inductance plays a major role in affecting the dynamic characteristics of the flow-meter..

3.1.3 Modeling physical systems

For structural modeling of pneumatic systems and electronic systems, some governing equations are obeyed by these systems.

Electronic system: Kirchhoff's voltage and current laws (also known as KVL and KCL).

Pneumatic system: Conservation of mass.

Through comparing the pneumatic and electric equation under similar conditions, the equivalent equation and parameters are shown in **Figure 3.3**^[22]

type	hydraulic	electric
quantity	volume V [m^3]	charge q [C]
potential	pressure p [$Pa=J/m^3$]	potential ϕ [$V=J/C$]
flux	Volumetric flow rate Φ_V [m^3/s]	current I [$A=C/s$]
flux density	velocity v [m/s]	current density j [$C/(m^2 \cdot s) = A/m^2$]
linear model	Poiseuille's law $\Phi_V = \frac{\pi r^4}{8\eta} \frac{\Delta p^*}{\ell}$	Ohm's law $j = -\sigma \nabla \phi$

Figure 3.3 hydraulic and electrical systems

3.2 Differential pressure flow-meter

The previous sections have provided some basic physics and analogy fundamentals which will be used throughout this project.

Pressure difference type flow-meters are used throughout the medical community due to its cost, low distortion, accuracy, portability and lab condition. This type device is the mostly commonly

used in clinical area like spirometry, to access the condition of the human breathing apparatus. The governing principle is that when gas passes through this type of device, there is a pressure difference across the device, similar to a resistor in electronic system. The relationship can be linear or nonlinear, depending on the type of device used.

3.2.1 Fleish Pneumotachometers

This type of device is made up of capillary tubes, with a pressure sensor used to measure the pressure difference across the capillary tubes, shown in **Figure 3.4**.

According to Poiseuille's equation, for laminar flow, the pressure drop across a single tube can be expressed as a function of flow rate:

$$\Delta p = p_1 - p_2 = \frac{8\eta QL}{\pi r^4}$$

Where $p_1 - p_2$ is the pressure drop along tube, η is the kinematic viscosity of the gas, Q is the true flow rate, L is the length of the tube, r is the radius of the tube. The above equation can be expressed as:

$$\Delta p = R_{LF}Q$$

Where, R_{LF} is the linear coefficient, Q is the flow rate and Δp is the pressure drop. As **Figure 3.4** shows the setup and the test equipment. A pressure regulator and a needle valve to generate the flow, then let the flow pass our flow-meter, in addition a u-tube manometer is used to measure the pressure difference across the flow-meter. The other end of the flow-meter connect to a wet test gas meter. The wet test meter's dual indicator completes one revolution every time that 1 ft³ passes through it, by timing this process, the real flow rate Q_{flow} can be calculated.

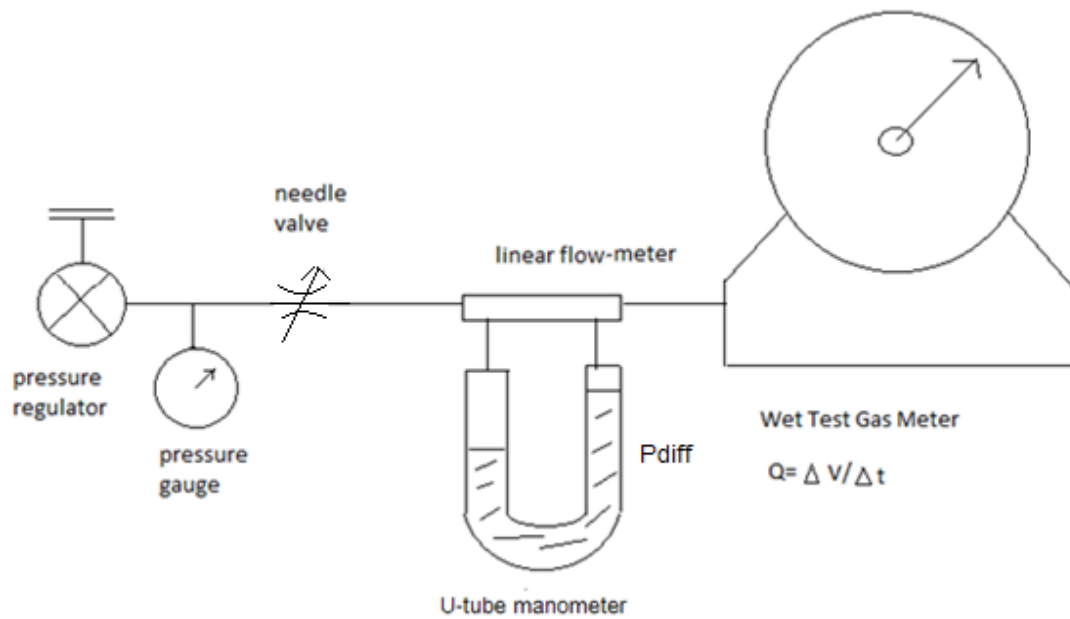


Figure 3.4 linear flow-meter relationship test setup

The results are shown in **Figure 3.5**. It can be seen from the graph that this device acts as a linear device as expected. In a later chapter, it will be shown the calibration process.

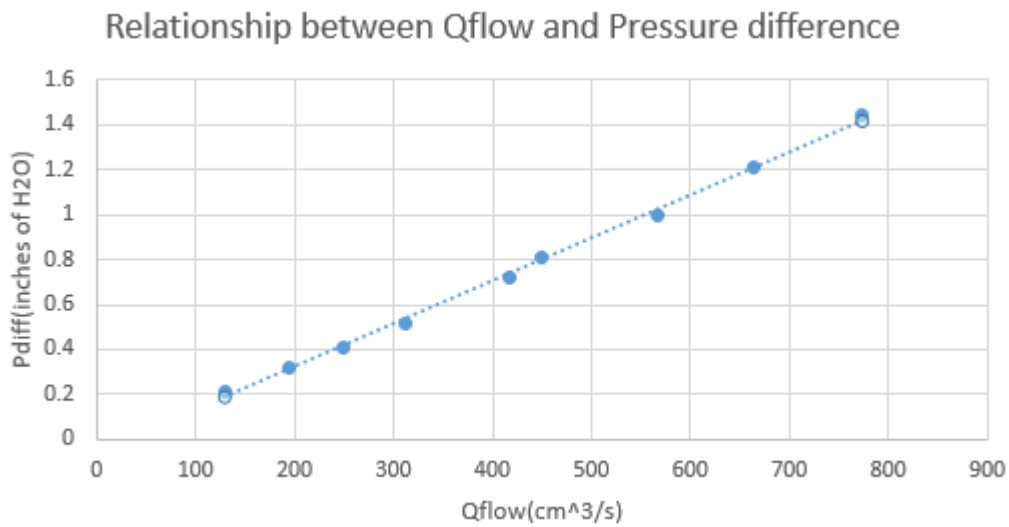


Figure 3.5 Data collected for linear flow-meter relationship

3.2.2 Squared-Edged Orifice Flow-meter

This flow-meter is used because it is expected to have a larger bandwidth than the fleish flow-meter discussed previously. This type of pressure difference flow-meter, called squared edge orifice is introduced here, a cross section of the device is shown in **Figure 1.3**. Because the large diameter of the device, the flow here is turbulent.

See **Figure 3.4** for the test setup. The collected data is shown in **Figure 3.6**. Notice that the flow-pressure relationship is an odd function. So the way that the theoretical equation manipulate is correct.

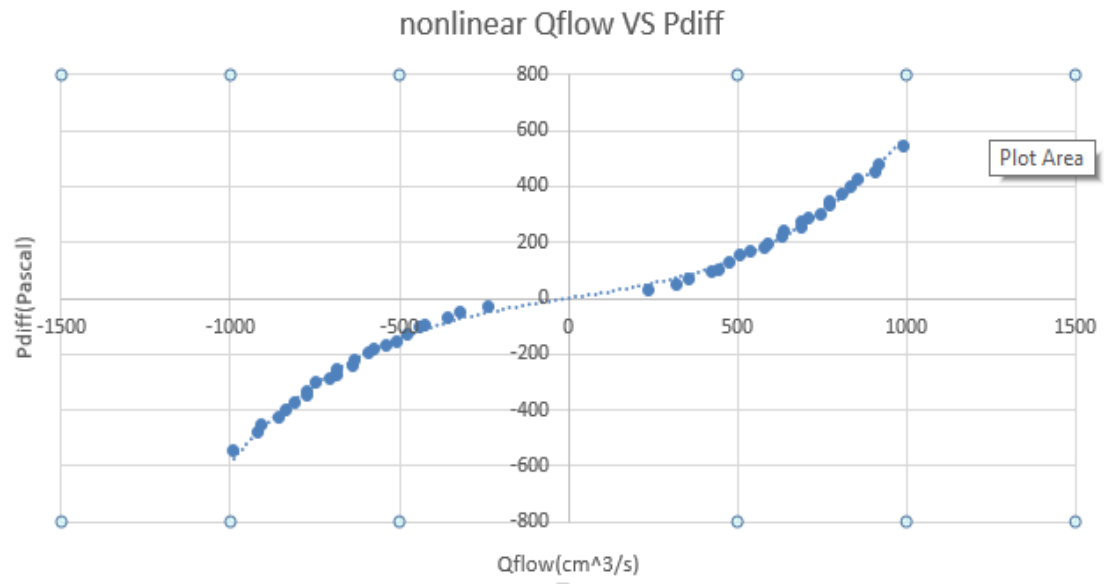


Figure 3.6 Data collected for non-linear flow-meter

From the above graph it can be seen that for square-edged orifice, presents a large nonlinearity. However notice that there are enough points for flows less than 200 cm³/s. It is because the flow is small, a condition that can barely generate a measurable pressure difference.

3.3 Dynamic Characteristics

3.3.1 Human breathing

Human breathing are the users for flow-meters. Human breathing is a result of motion of human lungs and diaphragm. The actual performance of the respiratory system is reflected by the

volumes that the lung can realize, and the speed in which these volumes can be moved in and out of the lungs. For the average human beings, Tidal volume is about $500\text{cm}^3/\text{breath}$ _[18], and the normal breathing frequency is about 12 breath/min. Lung volume changes due to cyclic expansion and contraction of the diaphragm. This lung volume closely resembles a sinusoidal wave, as shown in **Figure 3.7**.

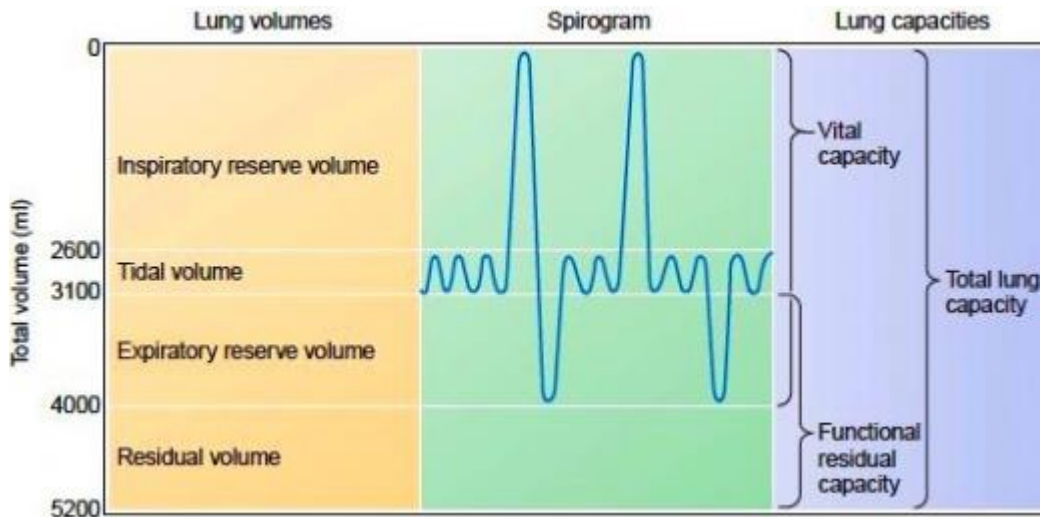


Figure 3.7 Human breath and Tidal volume definition

Lung volume can be described by the following equation:

$$V = \frac{V_T}{2} \sin 2\pi f t + \frac{V_T}{2} + FRC$$

$$V = 250 \sin 2\pi f t + 250 + FRC$$

The flow rate can be found by differentiating the previous equation:

$$Q = 250 * 2\pi f * \cos 2\pi f t$$

Which implies that the maximum flow is:

$$\max(Q) = \pi * 10^2$$

Notice that the flow into the flow-meter is not a DC flow but a sinusoidal flow. To analyse the behavior of a rapidly changing flow, It is necessary to explore the dynamic behavior in frequency domain.

3.3.2 Flow-meter frequency response

To determine the dynamic response characteristics of a device, it is needed to understand the underlying physics behind the device. The first thing that needs to be done is to model the pneumatic system with electrical circuit for a dynamic system modeling.

Capillary tube modeling

For our capillary tube was previously shown in **Figure 2.2**. The relationship between flow and pressure is linear, and given by:

$$\Delta p = R_{LF} Q$$

The testing set up used to evaluate the dynamic characteristics of the flow-meters can be modeled by electrical circuit shown in **Figure 3.8**.

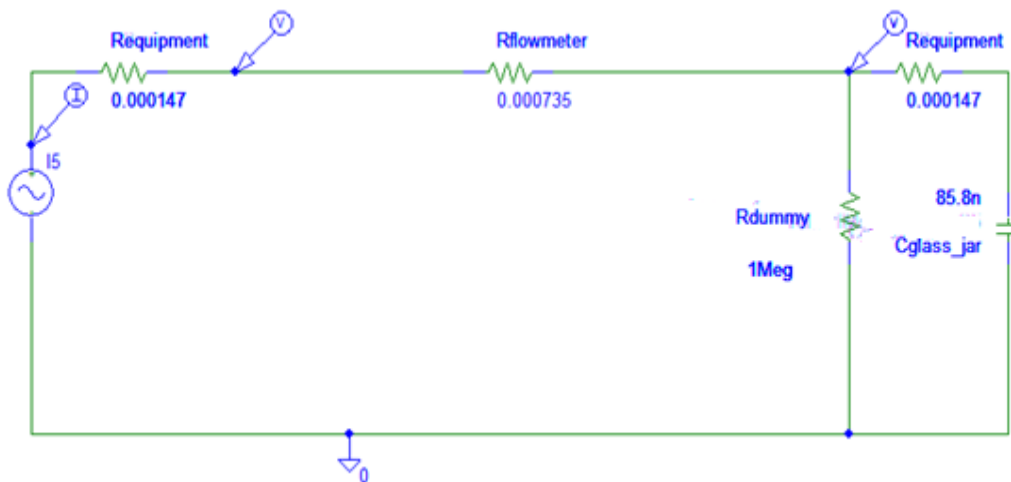


Figure 3.8 Capillary tube modeling circuit

This circuit is modeled in PSPICE. The flow describing human breathing is modeled as an AC current source, which generates a sinusoidal wave. A large resistor R_{dummy} is used to avoid simulation problem due to floating node because of the current source appeared. Capacitor C_{glass_jar} is the glass jar at the end of our process, radius of the glass jar is 5 inch. Notice that this is just a simplified version, because of our pressure transducer terminal is connected to the capillary tube as shown in **Figure 3.9**.

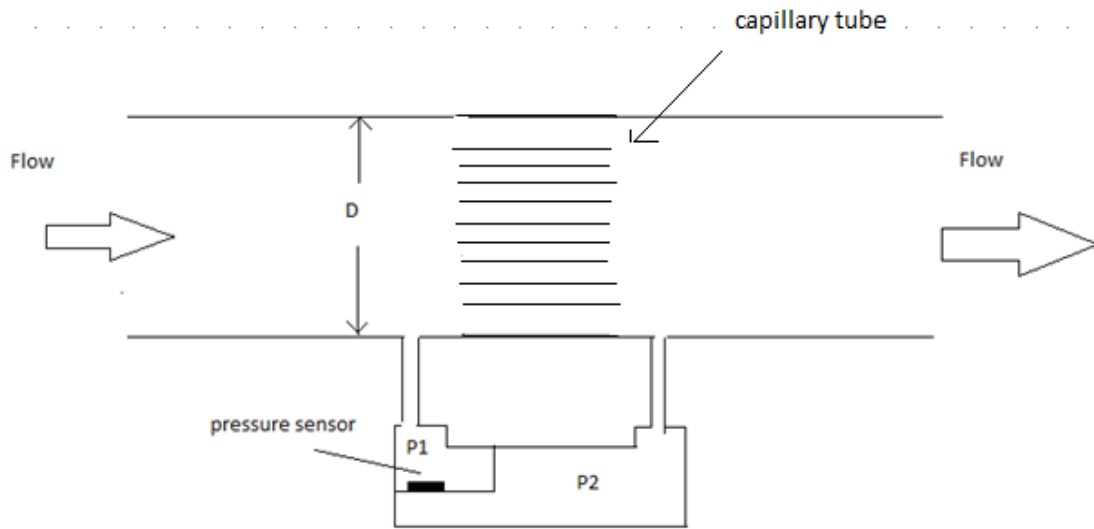


Figure 3.9 Capillary tubing flow-meter

The capacitance inside the pressure transducer may effect system behavior, so we modified our electronic circuit to be more realistic shown in **Figure 3.10**.

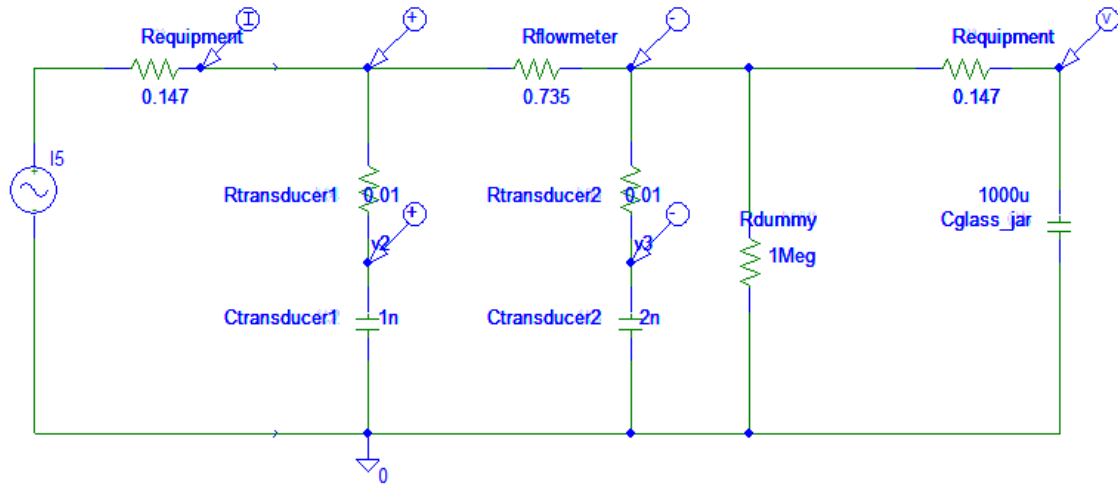


Figure 3.10 Capillary tube modeling with pressure transducer circuit

As we know that for an RC circuit, it generate a first order delay as:

$$H(s) = \frac{1}{1 + \tau s}$$

$$\tau = RC$$

And our real measure point is not across R1, but across the pressure transducer, at V2 and V3, where the pressure at that point is equivalent to voltage, so that RC circuit can be modeled as first order transfer function above, process can be expressed as **Figure 3.11**.

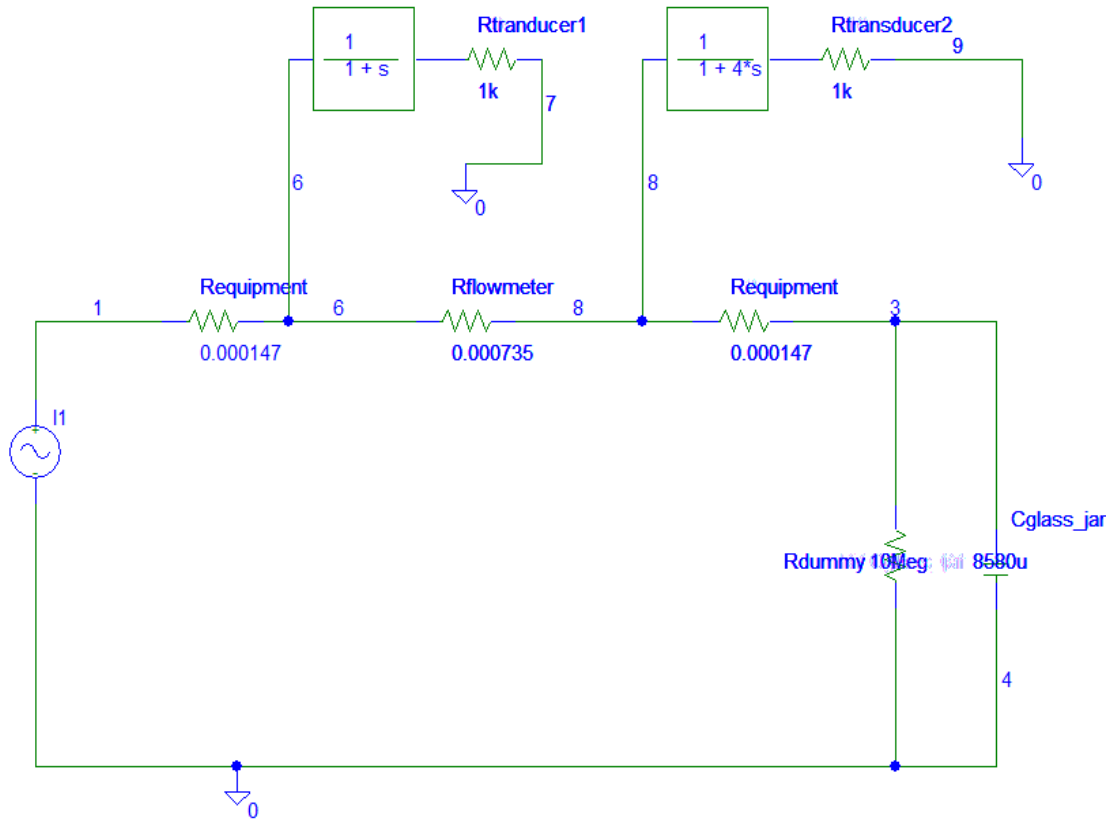


Figure 3.11 linear frequency response modeling

The response for capillary modeling as we can predict that, because of the linear relationship between V_{diff} and Q , the current source and Voltage across R1 should be in phase, the voltage at the end of the glass jar should have a 90° phase shift due to capacitance, because the equation:

$$I = C \frac{dV}{dt} = CsV$$

$$V = \frac{I}{Cs}$$

$$\angle V = \angle I - 90^\circ$$

The simulation results shown in **Figure 3.12**.

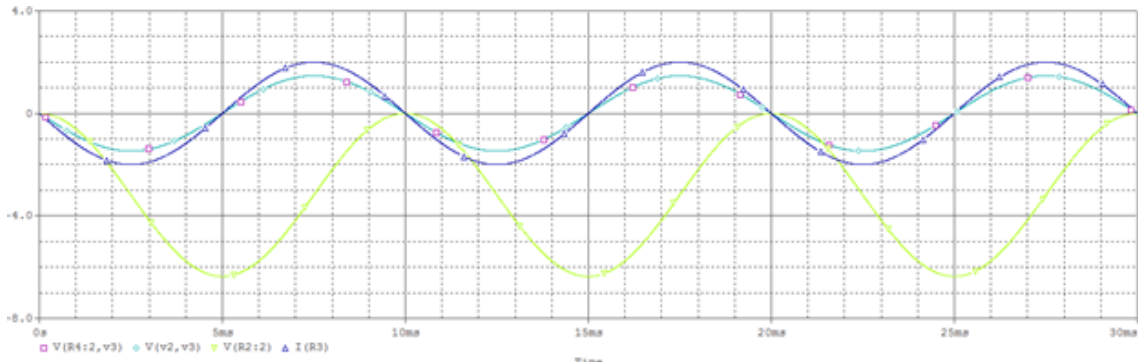


Figure 3.12 Capillary tube simulation results

To see and compare all three signals, signals are amplified so they can all be shown in one graph, the phase relationship can be seen directly.

Square edged orifice tube modeling

Compare to the linear process modeling, it is not straight forward to model the nonlinear relationship between pressure and flow rate:

$$\Delta p = R_{NF}|Q|Q$$

Because there is not a single device that can capture this relationship in electronic circuit, what we can do is a system level block diagram that can easily model this process. Before going into modeling the process, we need to know the coefficient of our pressure transducer, low pass filter, and amplifier, detail explanation of those devices will be introduced in next chapter, and here we set up the test to calculation the coefficient. Whole test process is shown in **Figure 3.13**.

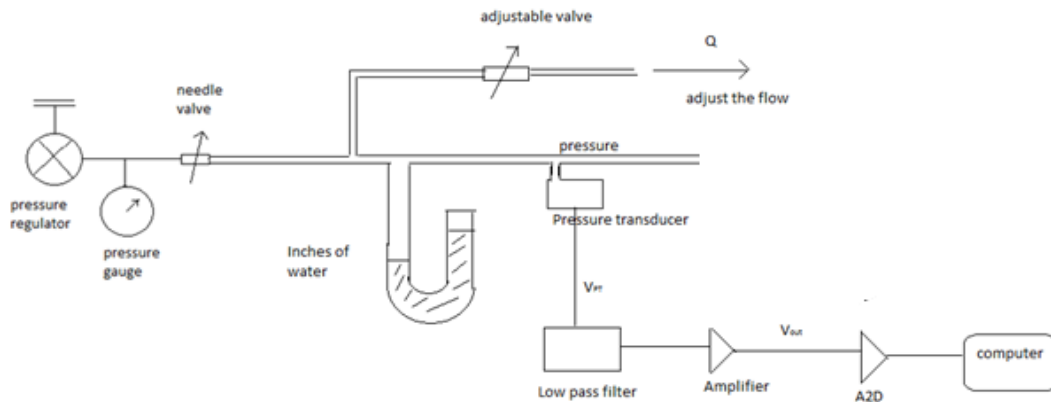


Figure 3.13 Pressure transducer calibration process

This pressure transducer calibration process shows the way devices are connected, then we can use a Voltmeter across terminals of low pass filter, amplifier, and A2D to get the value of those devices under different pressure conditions, and do a curve fitting to get the coefficient. **Figure 3.14** shows the data collected.

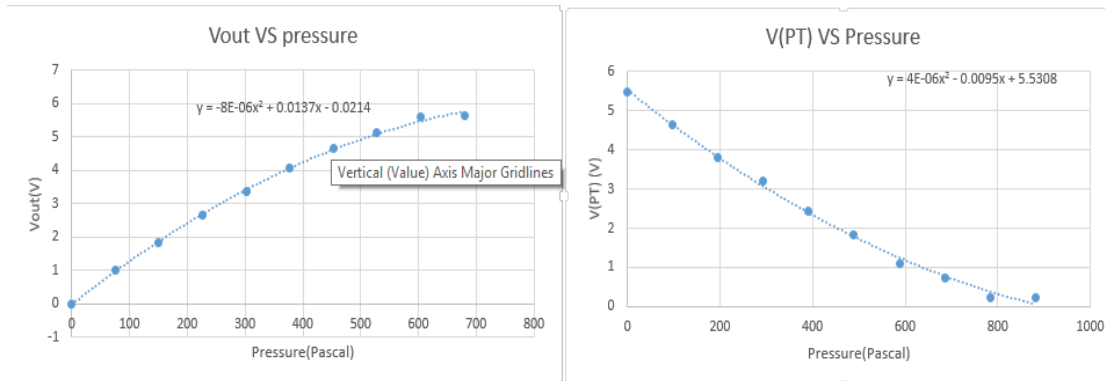


Figure 3.14 Signal conditioning circuit coefficient

Through the curve fitting we can tell that the higher order is negligible, so those devices are linear, this is a very important statement in nonlinear flow-meter process, and we can state that the only nonlinear relationship is from the nonlinear flow-meter. Since we now have all coefficient, we can do modeling of nonlinear flow-meter process in SPICE. **Figure 3.15** shows the block diagram.

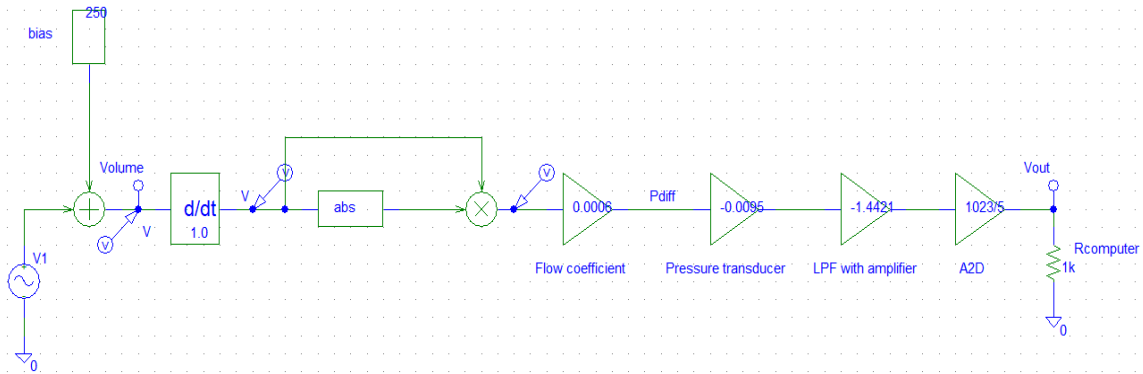


Figure 3.15 nonlinear flow-meter modeling process

Notice in this diagram, V (volume) is the voltage at end of glass jar, V after the differentiator is the real flow, and V after the multiplier is the pressure difference across the square edged orifice. As shown before for the linear case, phase angle between those parameters are similar, simulation result is shown in **Figure 3.16**.

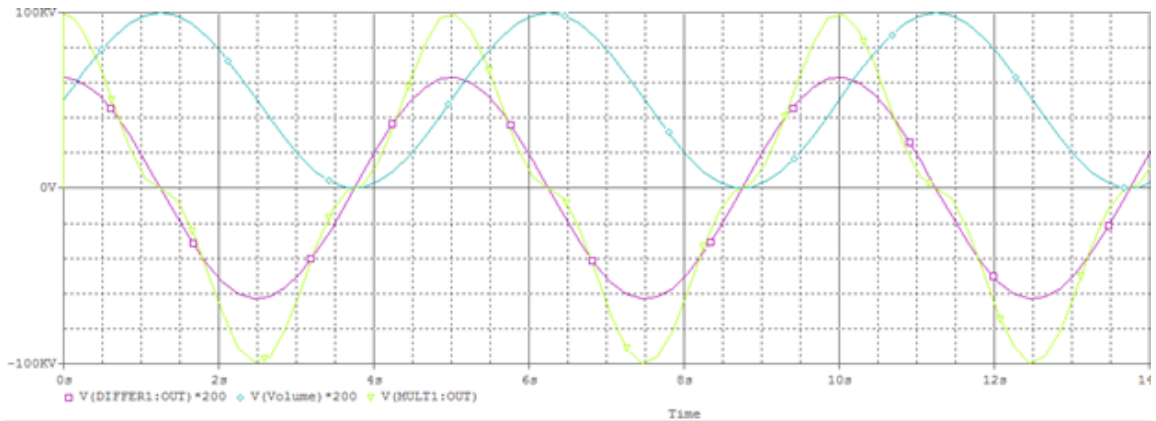


Figure 3.16 Square edged orifice tube simulation result.

From this simulation result we can see the phase shift between Qflow and pressure, and also the little strange sine wave plot of the pressure difference across square edged orifice, this is easy to understand when you think about the quadratic relationship between flow and pressure shown in **Figure 3.6**.

Chapter 4

TEST EQUIPMENT

In this chapter we will introduce the test equipment in lab, and the test method we use for data collection and analysis, experimental method we use here can be compared to the theoretical method through predicting the results. We will use mechanical device and analog device for data collecting, and will also use some statistical methodology for data handling, we will introduce all in this chapter.

4.1 Test Equipment

4.1.1 Flow measurement

The goal of this project is to measure true flow. What we want to achieve is that as long as a flow appeared in our system, flow rate has to be shown directly, this yields a fast and convenient approach-through a simple device. These test procedures are to be developed to achieve this goal.

In our lab, there are two ways to measure flow, control volume approach and pressure drop approach, both have limitations, and we will introduce these two in different sections.

4.1.1.1 Wet Test Meter.

A wet test meter is a precision device that can measure the volume of fluid. Usually we measure the flow rate by getting the volume of fluid over a fixed period of time by a stopwatch. **Figure 4.1** shows the wet test meter and a stopwatch.

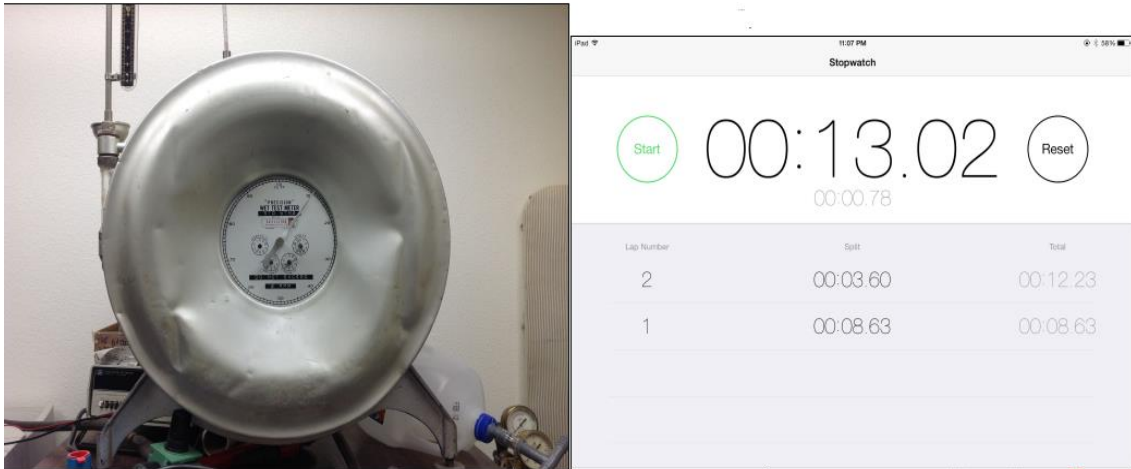


Figure 4.1 Wet Test Meter and stopwatch

We can see that the volume of wet test meter is large, it can handle large flow, a whole revolution of wet test meter is $1 \text{ ft}^3 (28316 \text{ cm}^3)$, for a fixed volume, like 1 ft^3 , divide by the time it take to pass wet test meter, is the true flow rate, unit cm^3/s .

The graph on right side is a typical stopwatch with lap function, the reason we need that is to have a linear line of time and volume relationship, to increase the accuracy. The method we use is to record the time it take for half a cycle and the time it take for a whole cycle, plot a linear line, to have an accurate flow rate measured. A typical line is shown in **Figure 4.2**.

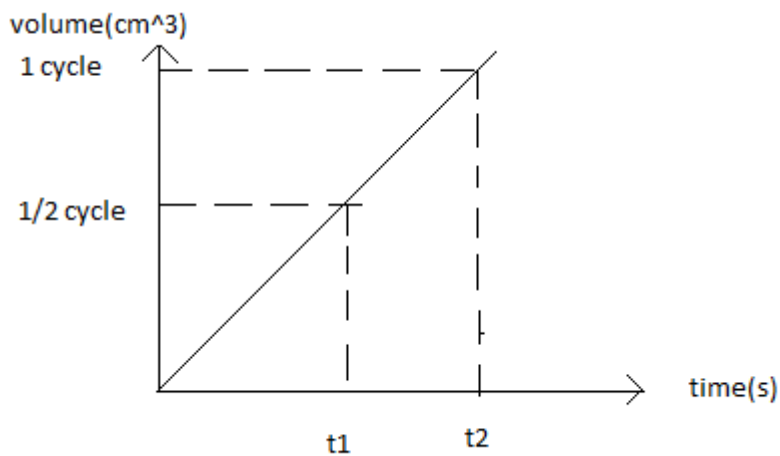


Figure 4.2 Wet Test Meter flow measure

Due to the mechanical friction, there is a limitation about the Wet Test Meter, flow cannot exceed 2 cycle per minute, the maximum calibration flow we can calculate through:

$$Q_{max} = \frac{V}{t} = \frac{28316cm^3 * 2}{60s} \approx 943 cm^3/s$$

4.1.1.2 U-tube manometer

Another type of device to calibrate the pressure is U-tube manometer, this device can measure pressure difference between two terminals, unit is in inches of water, and we can transfer that to cm of water. It is shown in **Figure 4.3**.

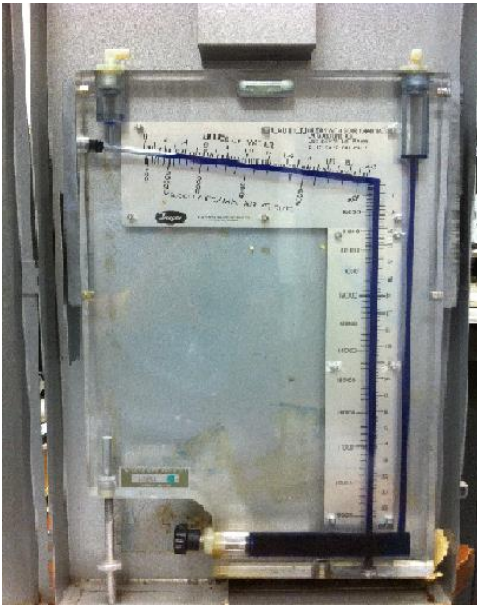


Figure 4.3 U-tube manometer

4.1.2 Flow generator

The sine wave generator is to model the human breath in a standard way, there are two major parts of flow generator, a function generator and an audio amplifier. A standard function generator can be used to produce a sine output with the desired frequency ranges for test (from 10 HZ to 200 HZ). Maximum device capability is 100 kHz. With variable frequency and amplitude adjustment, the function generator is the stimulus for the system input. The output of the device will feed an audio amplifier with a 50Ω load.

Figure 4.4 shows the function generator and audio amplifier.

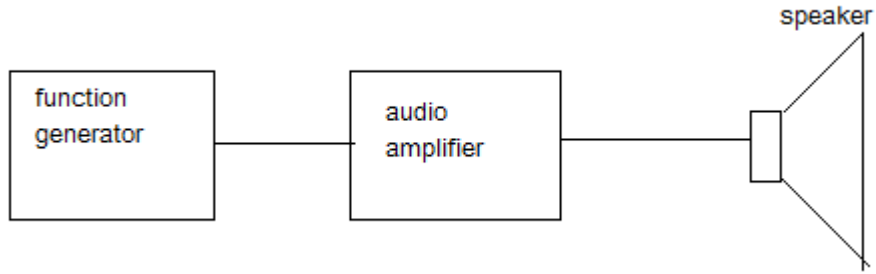


Figure 4.4 Function generator and audio amplifier

4.1.3 Pressure transducer

Two pressure transducer are used in this system, one for measuring the pressure difference across flow-meter, resulting in estimate flow measure, one for measuring the pressure of whole closed loop system placed near glass jar. **Figure 4.5** shows the pressure transducer.



Figure 4.5 Pressure transducer device

Both of these pressure transducers (Honeywell 163PC01D75) have an operating pressure range of $\pm 2.5 \text{ inH}_2\text{O}$ ($\pm 17.2 \text{ kPa}$). The linearity depends on the terminal, when $P_1 > P_2$, linearity $\pm 1\%$, when $P_1 < P_2$, linearity $\pm 2\%$, so the way we connect the transducer is place P1 as the input terminal. Max overpressure is 5 psi.

Because this device is connect directly to flow-meter, we need to understand how it works to avoid error. **Figure 4.6** shows the cross section of this pressure transducer.

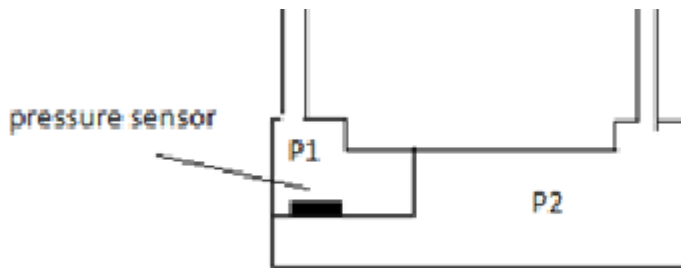


Figure 4.6 Cross section of pressure transducer

We can see that volume of two sides are different, this can be modeled as capacitance difference as shown in **Figure 3.16**. The volume difference and parasitic capacitance should be considered in experiment. To have better linearity, we use P1 terminal as our input, P2 for output, so the pressure difference would be:

$$\Delta p = p_1 - p_2$$

4.1.4 Low-pass Filter and Amplifier

The output of each transducer (pressure and flow) is connected to a single filter. Both of these filters are low-pass, 4-pole Butterworth filter (D74L4B-375Hz)^[19]. The -3dB corner frequency (f_c) point is 375Hz. DC gain is 0 ± 0.1 dB, The input source voltage used in this application is +12 Vdc (+Vs) and -12 Vdc (-Vs).

From Matlab code shown below:

```
[z,p,k] = butter(4,375/500,'low');  
[sos,g] = zp2sos(z,p,k);  
Hd = dfilt.df2tsos(sos,g);  
h = fvtool(Hd);  
set(h,'Analysis','freq')
```

The frequency response can be plotted in Matlab as shown in **Figure 4.7**. The plot shows data sampled at 1000 HZ.

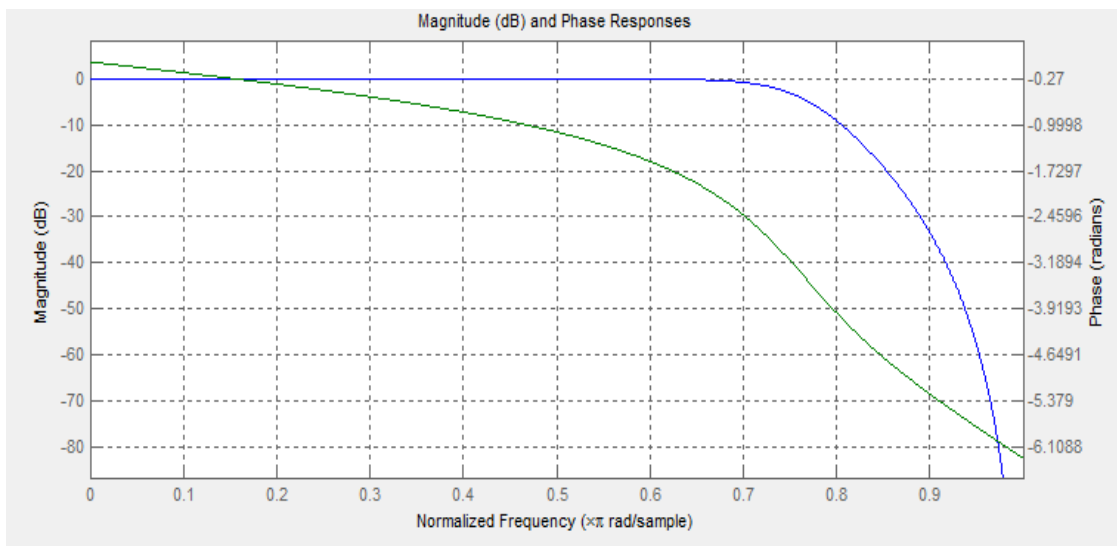


Figure 4.7 4th order Butterworth filter with $f_c=375$ HZ frequency response

Step response is shown in **Figure 4.8**. We can see that the response is fast but a little oscillation.

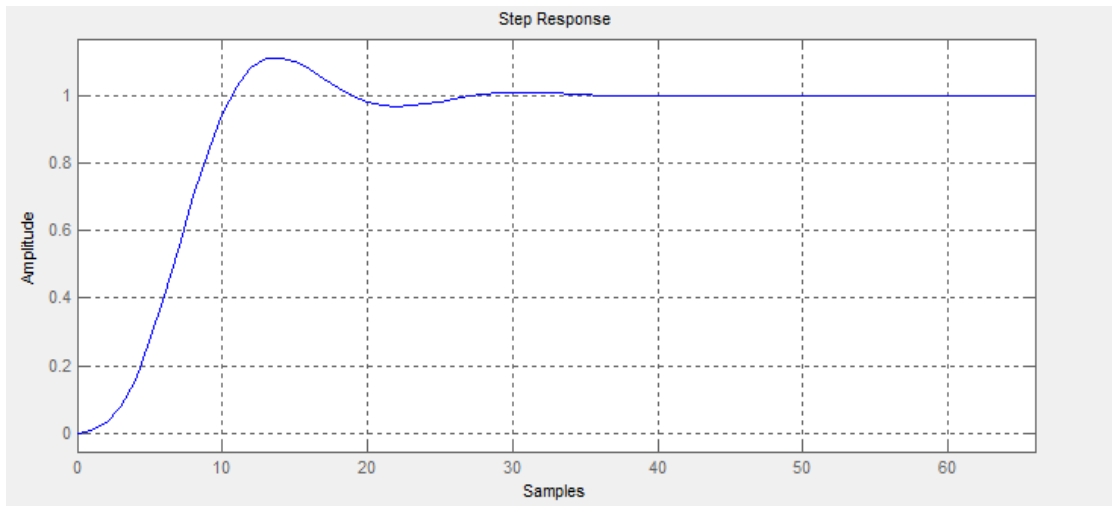


Figure 4.8 4th order Butterworth filter with $f_c=375$ HZ step response

We know that this device is suitable for our experiment, because the bandwidth of our flow-meter is far lower than 375 HZ, plus, the human breath frequency is far away from this cut-off frequency, so this cut-off frequency is efficient for our pneumatic system.

The output of each filter (pressure and flow) feeds a Junction Field Effect Transistor (JFET) op-amp with nominal input resistance (r_{in}) exceeding $10^{12}\Omega$. The op-amp (NTE858) is biased to achieve enough circuit gain in order to reliably measure the incoming signal at the DAS. Like the filters described above the source input voltage used is +12 Vdc ($+V_{DD}$) and -12 Vdc (V_{EE}). This amplifier has high slew rate, and high unity gain bandwidth, with slew rate $13\text{ V}/\mu\text{s}$, low distortion, unity gain bandwidth of 100MHZ, CMRR and PSRR of 100dB. Open loop gain of 250V/mV.

The whole signal conditioning circuit is shown in **Figure 4.9**

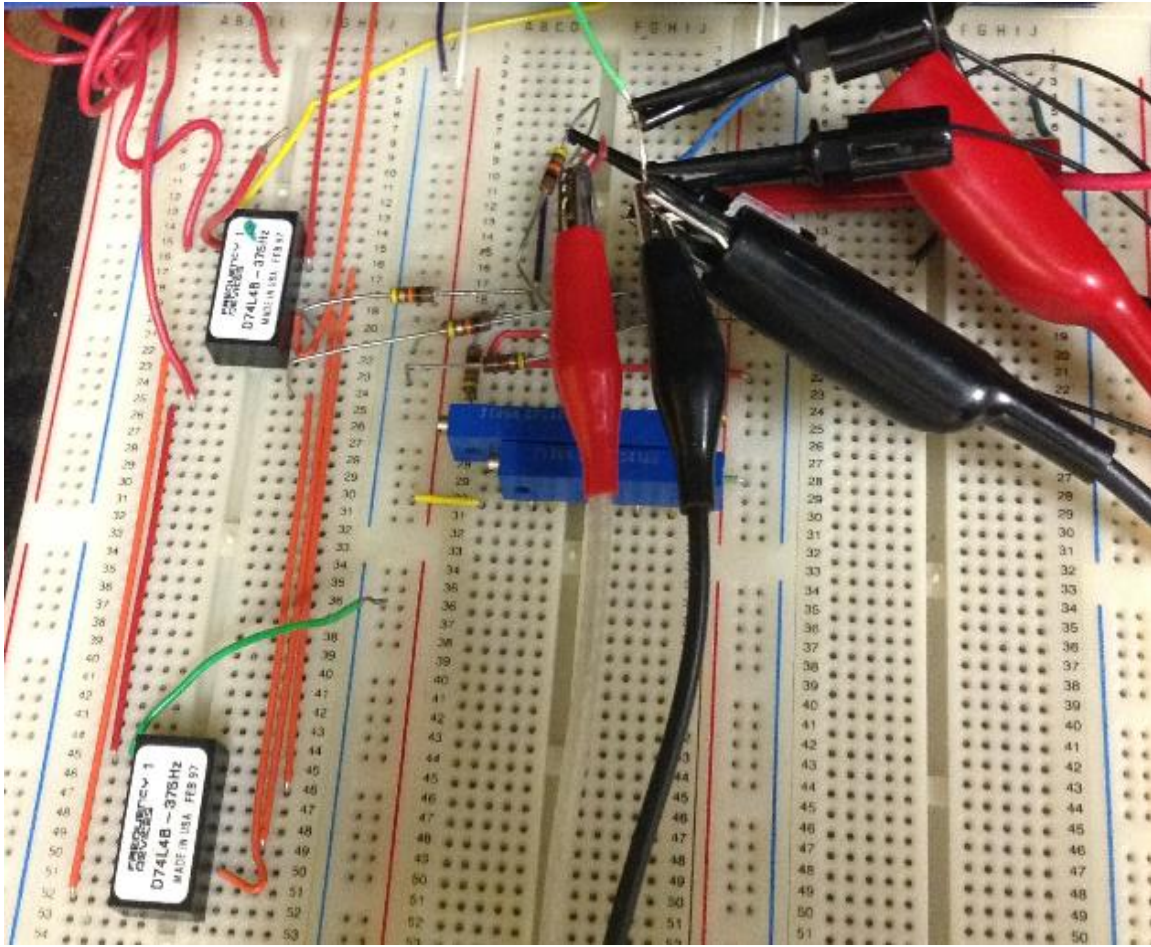


Figure 4.9 Signal conditioning circuit

4.1.5 Data Acquisition System (DAQ)

The data acquisition system we use to transfer signal from hardware to software is National Instrument part number USB-6009^[20], this device uses a Serial Universal Bus that can be controlled from a software in PC called National Instrument Labview. The further software setup will be introduced in later section 4.3.

The structure of USB-6009 can be shown in **Figure 4.10**



Figure 4.10 NI USB-6009 Device

This DAQ has 8 analog input with 14-bits resolution, 48 kS/s sampling rate, 2 analog output of 12-bits resolution and 150 kS/s sampling rate, 12 digital I/O and 32-bits counter. Block diagram is shown in **Figure 4.11**. The function we will use is two monitoring the output of signal conditioning circuit, which are two channels of pressure transducer input (one for flow measure, one for pressure measure). Specifically, analog input AI0 and AI1, AI0 is for channel 1(flow) measure, AI1 is for channel 2(pressure) measure.

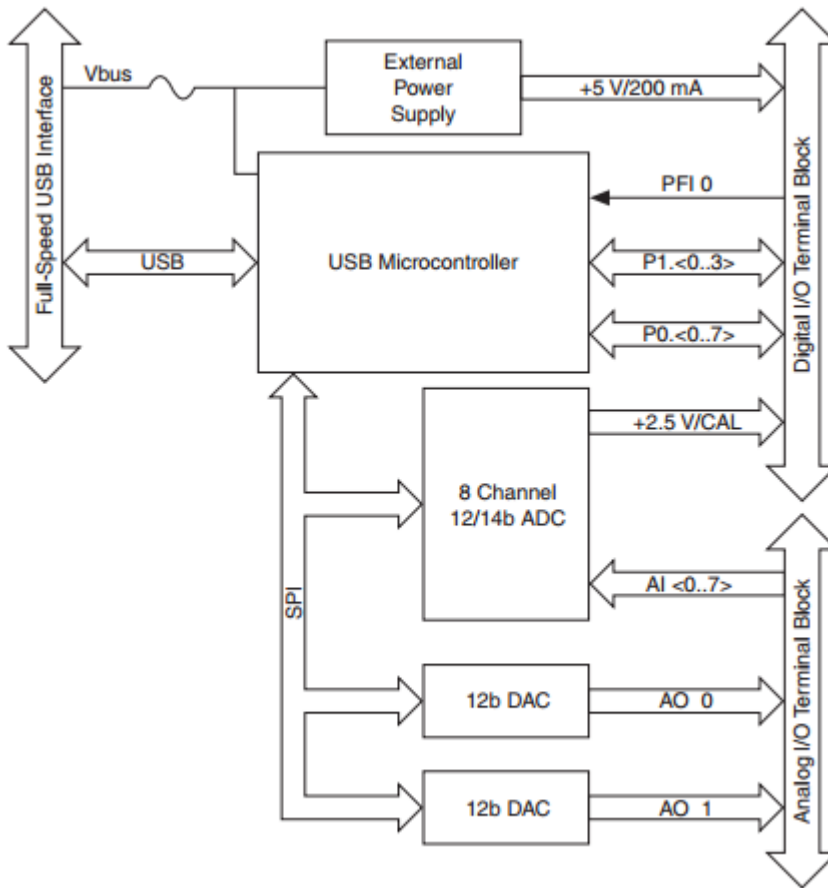


Figure 4.11 block diagram of NI USB-6009

DAQ configuration process is through Labview build in function, The analog channels were configured as Referenced Single Ended (RSE), with a range between 0 to 10Vdc and sampling rate of 5 kHz. RSE mode (as opposed to differential) effectively references the input signal to the DAS board internal ground reference. DAQ analog setup is shown in **Figure 4.12**.

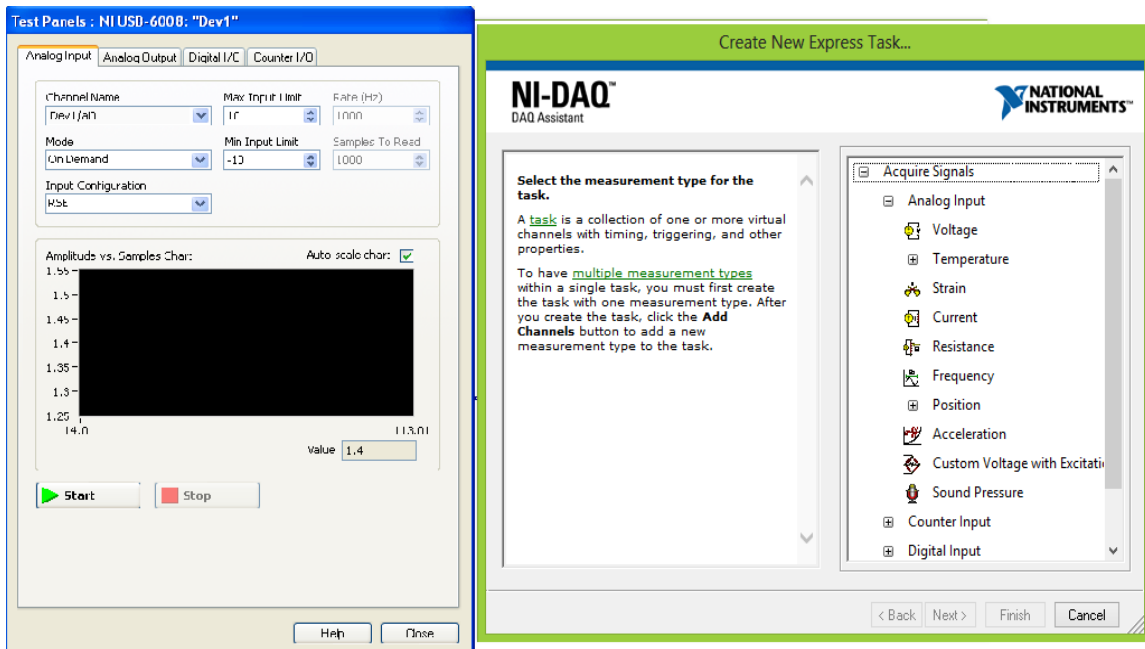


Figure 4.12 DAQ analog channel setup

4.1.6 Flow-meters

Three flow-meters are tested in this project, Capillary type, screen pneumotach type, square edge type, shown in **Figure 4.13**.



Figure 4.13 Capillary, screen pneumotach and square edge orifice type flow-meters

4.2 Test Loop

4.2.1 Calibration

Calibration Process is the major part in this experiment, Accuracy and reliability of our data depends on this process, Notice that we will use computer software to indicate flow rate, all mechanical parts, MEMS and software coefficients should be considered, and all those parts can

easily pick up bias, results in accuracy problems, so get the coefficient and cancel out bias are our goals in calibration process.

Calibration process can be down separately in 4 different processes, in 4 sub-sections, we will introduce the method we use to do calibration.

4.2.1.1 Wet Test Meter calibration

Wet Test Meter calibration is the first we should do because it brings a problem and would affect future flow rate calibration process.

All our experiments depend on the assumption that we can measure real Q_{flow} in our lab, and that based on the assumption that using Wet Test Meter, through equation:

$$Q = \frac{dV}{dt}$$

We can get the real flow rate, however, the fact is that this is not all true because of the structure the Wet Test Meter was built. The structure of Wet Test Meter is shown in **Figure 4.13**

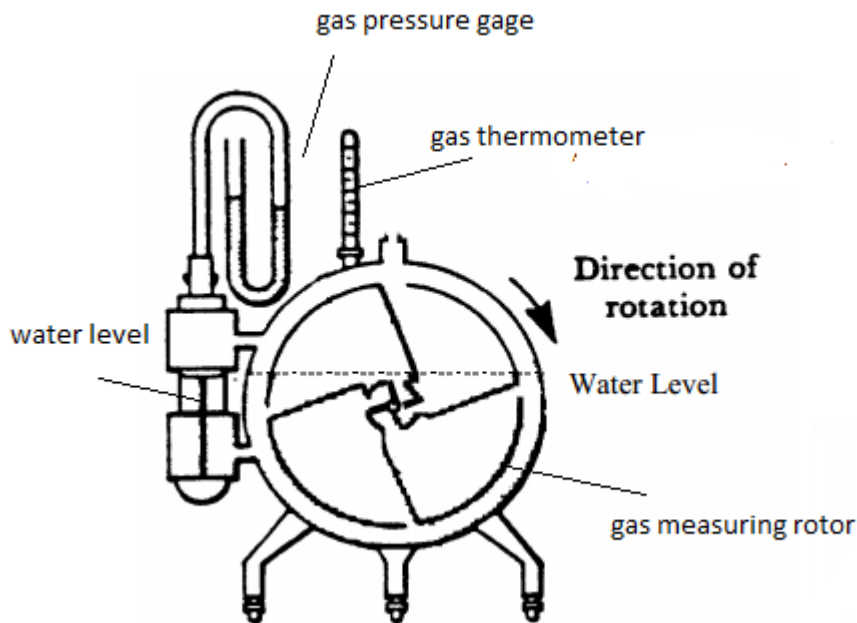


Figure 4.14 Structure of Wet Test Meter

The main body of Wet Test Meter contain a cylindrical rotor made as 4 buckets, the rotor is immersed in water to a level just above the axis, the gas being metered is introduced into the

water, as gas passes through the meter, it will pick up water vapor. However, in our experiment, the real flow generated by flow generator is dry flow. What we need to do is to transfer the moister flow into dry flow.

When the dry flow passes water, it will pick up water molecule, make the pressure larger, so we can define a correction factor C.F:

$$C.F = \frac{P_{dry} - P_{vapor}}{P_{dry}}$$

$$Dry\ gas\ volume = Metered\ Volume * C.F$$

P_{dry} is the dry flow pressure, P_{vapor} is the adds-in water molecule pressure, define this coefficient is very helpful for measuring true dry flow in our system, a table of saturation vapor pressure over water is given in **APPENDIX B**.

4.2.1.2 Linear flow-meter calibration

From our previous introduction we know that if we use the linear capillary flow-meter, then all devices in our system are linear devices with some coefficient, noise, and offset added, then calibrate this process so that our software shows the real flow rate is critical in this experiment, **Figure 4.14** shows the setup for linear flow-meter calibration.

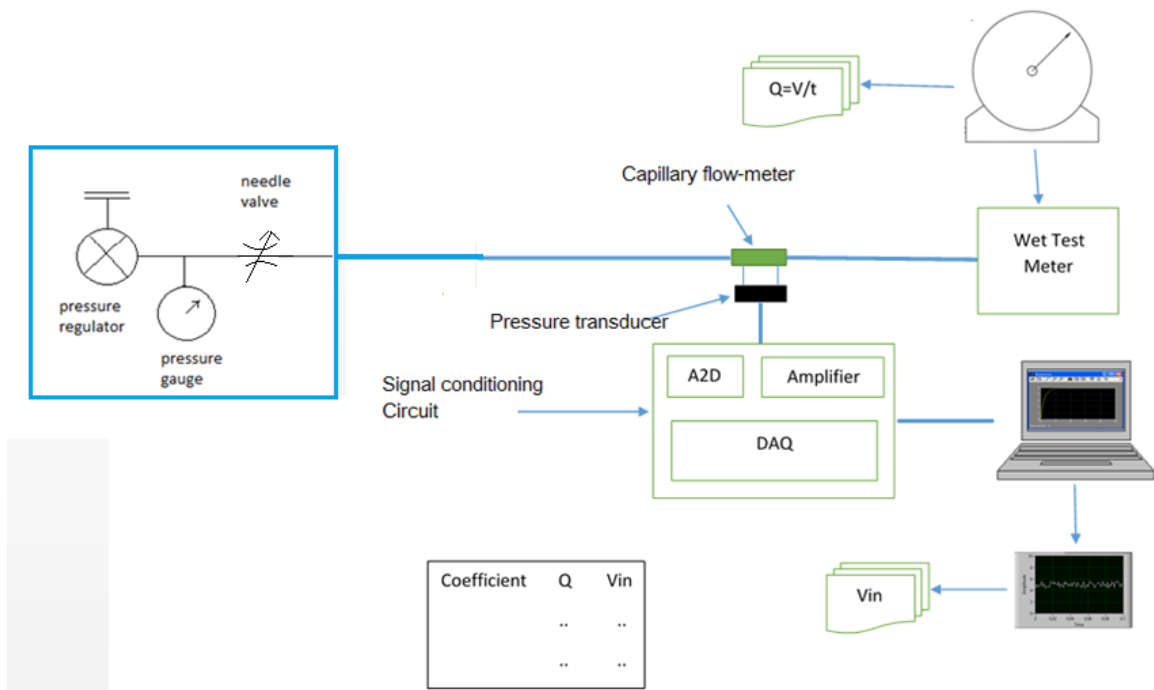


Figure 4.15 Structure of Wet Test Meter

From the above diagram we can see that there is much to do in this process, the critical part is data handling, due to the non-ideal process error and human failure, we need to use some statistical method like linear regression, missing data handling and so.

The real flow rate we record is from the Wet Test Meter, time for dc flow to pass half ft² or 1 ft² is recorded, using the method we introduced in section 4.1.1.1, we can calculate the moisture flow rate, Q. Then from the LabVIEW result, we have a sets of dc voltages Vin calculated using average data. The voltage Vin indicates the pressure difference across capillary flow-meter with some gain added. Then we know there is a linear relationship between Q and Vin, plot the Vin in terms of Q, use linear regression analysis, after a linear curve fitting, we have a relationship:

$$V_{in} = Q_0 + K_1 Q$$

The coefficient we want to record is the bias Q_0 and linear coefficient K_1 . With the aid of these linear parameters, real flow rate Q can be indicated in labview by invert above equation:

$$Q = \frac{V_{in} - Q_0}{K_1}$$

4.2.1.3 Nonlinear flow-meter calibration

Nonlinear flow-meter calibration use the similar process as the linear calibration one, however, due to the nonlinearity of the device, it is much harder to achieve, some mathematical tools have been used to get the nonlinear coefficient and calculate through labview result.

Process of nonlinear flow-meter calibration is shown in **Figure 4.15**.

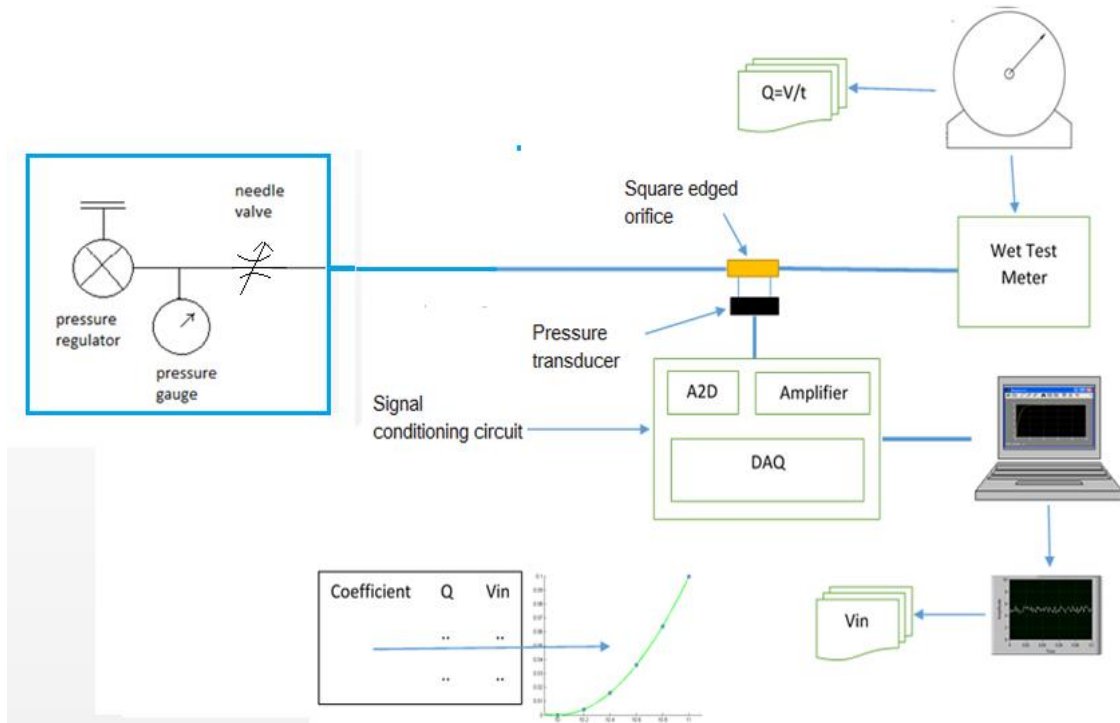


Figure 4.16 nonlinear flow-meter calibration process

Notice that the major difference between nonlinear and linear flow-meter calibration process is the curve fitting, for nonlinear process, the relationship between LabVIEW result V_{in} and real flow rate Q is quadratic, as shown:

$$V_{in} = b_0 + b_1Q + b_2Q^2$$

This equation yields quadratic polynomial curve fitting, in this case, specifically, we use least square method through SVD (singular value decomposition), SVD can be found in any linear algebra books [21]. In our case, we know that our system's order is two, so after we get all the sets of $(V_{in0}, Q_0), (V_{in1}, Q_1) \dots$, we can write the equation that:

$$\begin{bmatrix} 1 & Q_0 & Q_0^2 \\ 1 & Q_1 & Q_1^2 \\ \vdots & \vdots & \vdots \\ 1 & Q_{15} & Q_{15}^2 \end{bmatrix} \begin{bmatrix} b_0 \\ b_1 \\ b_2 \end{bmatrix} = \begin{bmatrix} V_{in0} \\ V_{in1} \\ \vdots \\ V_{in15} \end{bmatrix}$$

We can call it $Ab = Y$, The Maximum group we can have here are 15 groups, The least square yields that we should have minimum Euclidian norm of error, which is that:

$$\|e\|_2 = \|Ab - Y\|_2 \text{ is minimum}$$

The general thoughts is that error vector $e = Ab - Y$ must be perpendicular to column space of A, so basic idea is to project Y onto the column space of A, b can be determined:

$$b = (A^T A)^{-1} A^T Y$$

For invertible $A^T A$, However, in our system, if we have more data, optimal solution of b is the one that has minimum length.

Here comes the SVD, A can be shown as:

$$A = U \Sigma V^T$$

U and V are orthogonal matrices. All solutions to $Ab = Y$ have the same row space component, after knock out the null space, it can be determined by:

$$b = V \Sigma U^T Y = \begin{bmatrix} b_0 \\ b_1 \\ b_2 \end{bmatrix}$$

Now that is the coefficient we need for nonlinear curve fitting.

Now the problem comes up, how do we put the coefficient back to get the flow rate Q from V_{in} .

We already know that:

$$V_{in} = b_0 + b_1 Q + b_2 Q^2$$

So we can determine Q:

$$Q = \frac{-b \pm \sqrt{b^2 - 4ac}}{2a} = \frac{-b_1 + \sqrt{b_1^2 + 4b_2(V_{in} - b_0)}}{2b_2}$$

However, this only holds for dc input, and specifically, only positive input, because LabVIEW cannot show a complex number from square root. What we can do is though this:

$$Q = \frac{-b_1 + \sqrt{b_1^2 + 4b_2(V_{in} - b_0)}}{2b_2} * \text{sign}(b_1^2 + 4b_2(V_{in} - b_0))$$

Notice that in real test process, there is always a V_{bias} added to LabVIEW results, so modify above equation, we can get that:

$$Q = \frac{-b_1 + \sqrt{b_1^2 + 4b_2(V_{in} + V_{bias} - b_0)}}{2b_2} * \text{sign}(b_1^2 + 4b_2(V_{in} + V_{bias} - b_0))$$

This will be the equation we use in software to get the estimate flow rate.

4.2.1.4 Pressure calibration

Pressure calibration is to calibrate the pressure, so that our pressure sensor would indicate pressure in labview, Unit is cmH2O, the relationship is linear, so the curve fitting is not so hard to do, **Figure 4.16** shows the whole process.

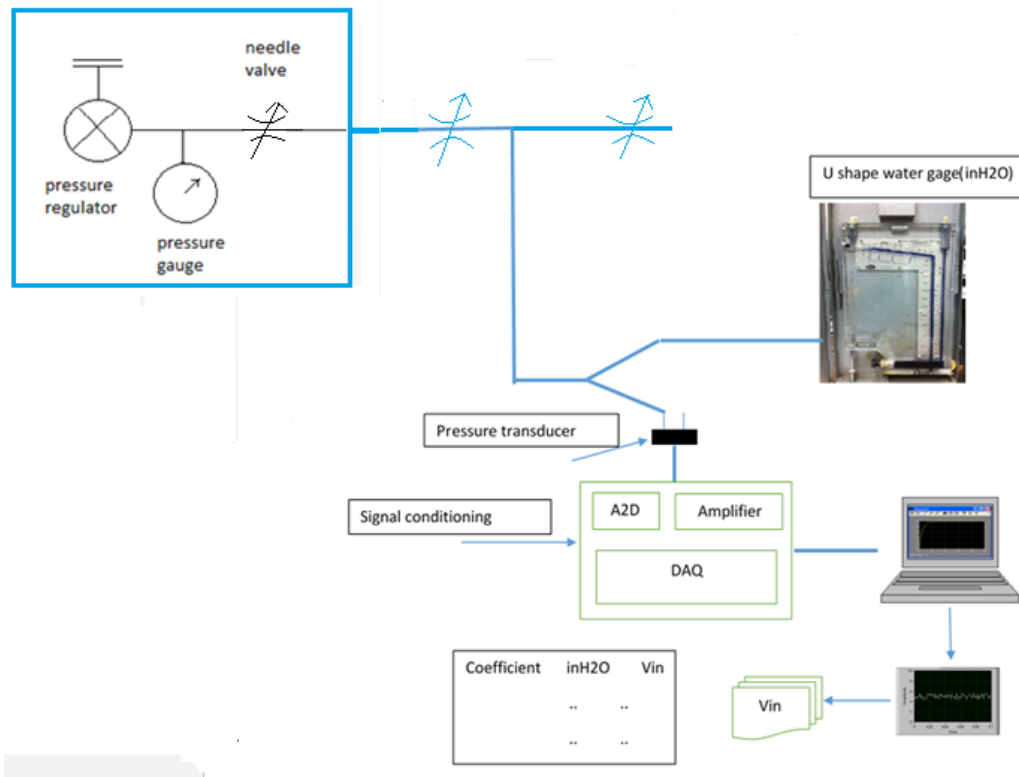


Figure 4.17 Pressure calibration process

In this calibration process, it is very important keep the pressure in a small range, or it will damage our pressure transducer, and spill out the liquid in U-tube manometer.

4.2.2 Test Loop Setup

After the calibration process, we already have the coefficient for linear, nonlinear flow-meter and pressure transducer saved separately. In our test loop, LabVIEW will read those parameters and show the graph and properties of each different types of flow.

Figure 4.17 shows the whole process of test loop.

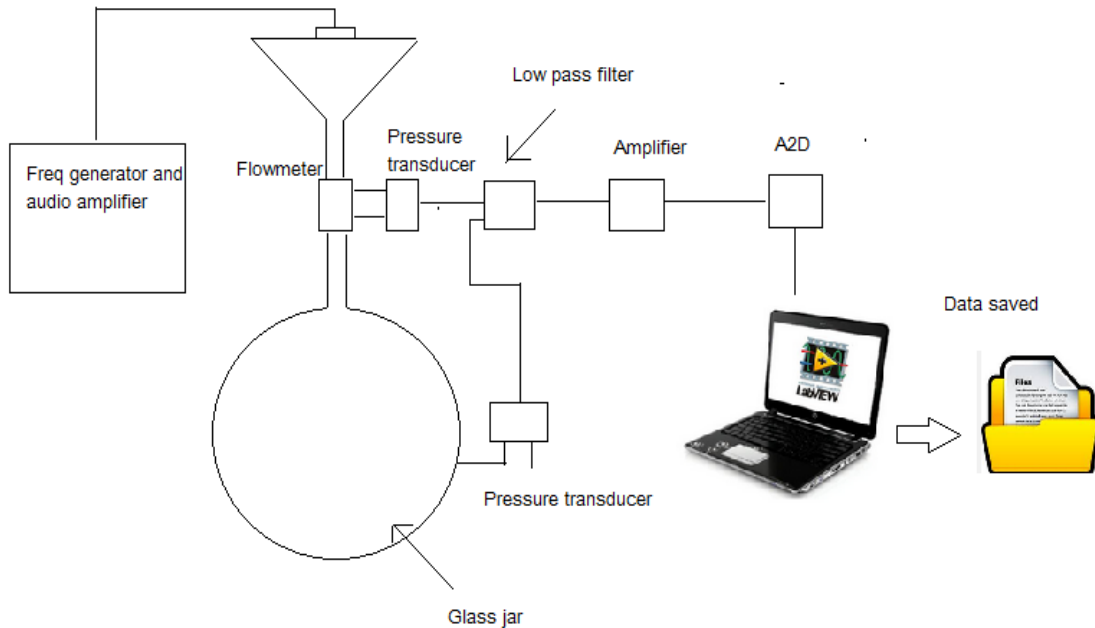


Figure 4.18 Test loop setup

In our process, the distance from flow source to glass jar is not far, this reduce long distance parasitic capacitance, resistance, inductance. Estimated flow is recorded by the pressure transducer through flow-meter, real flow is recorded by pressure transducer next to the glass jar, the parameters are all from calibration process, the data computer recorded are amplitude, frequency, phase of those two channels, a sample recorded data is shown in **Figure 4.18**.

Amplitude	Freq	Phase	Phase Diff of Q^ and Q		
Qflow	261.474315		20.324156	-119.892503	see below
Pressure	1.043047		20.324505	134.460194	15.647303
Qflow	279.715075		30.170878	30.111436	see below
Pressure	0.711241		30.171041	-80.902960	21.014396
Qflow	249.481786		40.152021	85.636136	see below
Pressure	0.482110		40.152930	-32.623897	28.260033
Qflow	211.561243		50.067072	-89.127577	see below
Pressure	0.336124		50.066547	144.229552	36.642871
Qflow	186.854355		60.045575	202.019093	see below
Pressure	0.242755		60.044289	67.145751	44.873342
Qflow	173.732615		69.999061	-18.101733	see below
Pressure	0.184065		70.000484	199.279813	52.618454
Qflow	169.431764		80.001841	-51.468558	see below
Pressure	0.145233		80.003550	159.860975	58.670467

Figure 4.19 Nonlinear flow-meter data recorded

Now for plotting the frequency response, assume real flow rate is the input, measured flow is the output, so that the transfer function can be found:

$$H(s) = \frac{\hat{Q}(s)}{Q(s)} = \frac{k_1 V_Q(s)}{C k_2 s V_p(s)}$$

Since from our previous calibration process, the LabVIEW results can show the true flow and pressure, so the equation is simplified to:

$$H(s) = \frac{Q_{flow}(s)}{CsPressure(s)}$$

C is the capacitance of glass jar, $s = j\omega = j2\pi f$, f is the frequency, the imaginary part of this in the transfer function only act as a 90 degree phase shift, doesn't affect the magnitude, we handled that in software, so the phase difference we see from data collected is the phase different from estimated flow rate to real flow rate, as been discussed earlier, is the result of inductance.

4.3 Software

In our experiment, the software we use is LabVIEW, due to its convenient communication between software and hardware. As been introduced earlier, DAQ we use is USB-6009, Labview has a built in VI to use this device.

The front panel of LabVIEW software is shown in **Figure 4.3.1**.

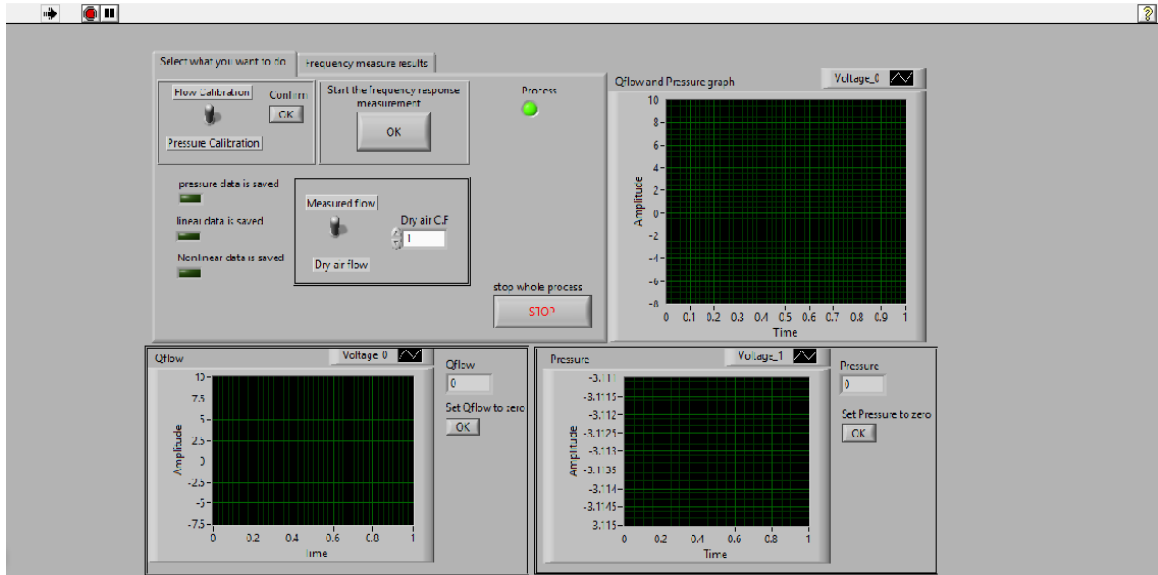


Figure 4.20 Front panel of labview

It has all instruction for user to select behavior. To be easier to debug, we separate different parts into different subVIs, the main panel will call different subVIs, and they will close after invoked, **Figure 4.20** shows a glimpse of backend code.

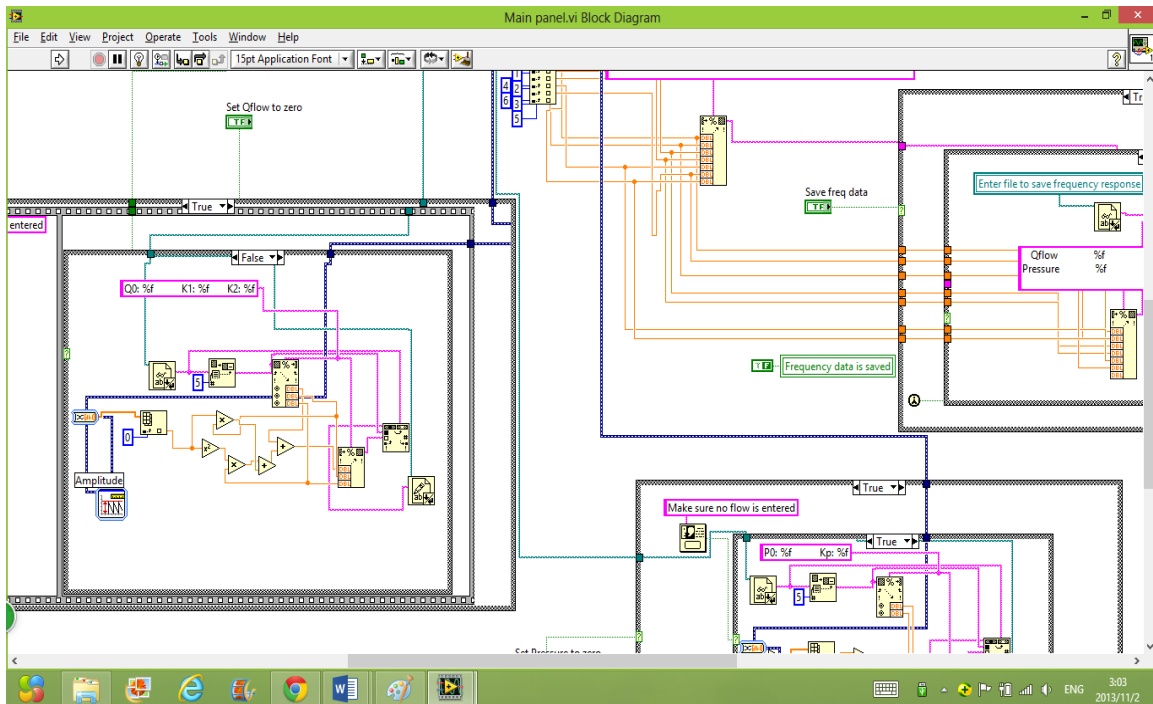


Figure 4.21 Part of backend labview code

Whole idea of our programming structure can be found in flowchart in **APPENDIX A**.

4.4 Potential problem

During our process, there are several problems occurs that needed to be handled carefully, some we can concur some we can minimize the effect to our system, they are divided into four sub-sections.

4.4.1 Hardware

Due to the fact that nothing is ideal, the difference from theory to experiment can cause some problem sometime, especially for hardware connection. Several problems occur in this experiment, list below. The noise and disturbances are general case that we will introduce in Noise and disturbances section.

4.4.1.1 Wet Test Meter correction factor

As been introduced in section 4.2.1.1, in calibration process, the true flow as measured by Wet Test Meter detected is the moister air, the viscosity and pressure can be different from the true air, however, the flow our flow-meter detected is dry air from the flow generator, that difference can cause inaccurate result, the solution is to moister the dry air before it pass the flow-meter, as shown in **Figure 4.21**.

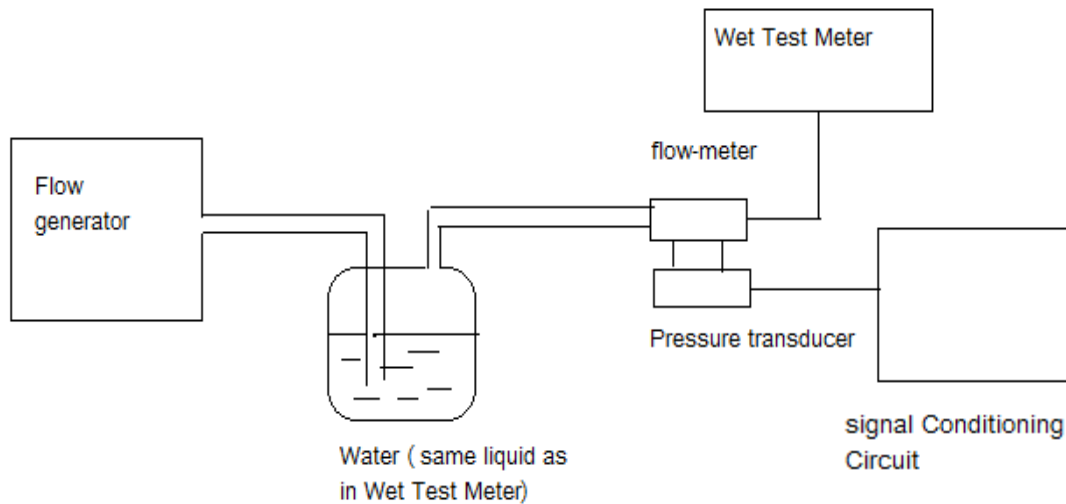


Figure 4.22 moister air in flow calibration process

This method guarantee the consistency of the flow through flow-meter and Wet Test Meter, it is necessary in flow calibration process. Through calibration process, the flow rate we get is the moister air, to transfer that into dry air to be used in frequency response measurement, we can use the C.F introduced in section 4.2.1.1.

4.4.1.2 Fluid restriction between flow-meter and Wet Test Meter

Ideally, we have all tube with the same diameter, so no pressure will be generated from the tube connection corner, however, in our experiment, those tubes have different diameters, so at the adjoin corner, it may become a sharp edge orifice, that will increase the resistance. This phenomenon is really bad if it happens between flow-meter and Wet Test Meter, the flow generator is non an ideal flow source, it's a pressure source, so large resistance after the flow-

meter will load the source, it will decrease the pressure difference we expected across the flow-meter.

This effect can be eliminated through using the same diameter tube, keep the flow well-distributed through our system.

This folded tube problem is a general case that happens in our system, it will cause the flow non-equally distributed in our system, check the tube connection is very important.

This folded tube is becoming a real problem when it comes to the connection between flow-meter and pressure sensor, if the tube is folded, resistance is increased, and the pressure difference we get will be drastically different from the well-handled results.

This can be solved by using a clamp to fasten the pressure sensor.

4.4.2 Software

Software problem are basically occurs in LabVIEW programming, we can have different techniques to solve the problem.

Using Built-in VI in LabVIEW is a convenient way to achieve behavior we want, however, in our case, we need to measure the frequency response of the system, build-in VI tends to slow down our system, using build-in VI can result in decrease of frequency about 1000 times. This becomes an issue when our program reads the coefficient and outputs the frequency of the input. We can solve that by using direct calculation in programming during the read coefficient process.

Another problem occurs during the non-linear flow-meter coefficient load process, because LabVIEW cannot output a complex number from square root of negative flow rate, we need to modify the way we calculate flow rate from quadratic form. As been introduced in section 4.2.1.3.

We can absolute the whole part under the square root, then use the result times the sign of that part, as shown:

$$Q = \frac{-b_1 + \sqrt{\text{abs}(b_1^2 + 4b_2(V_{in} + V_{bias} - b_0))}}{2b_2} \text{sign}(b_1^2 + 4b_2(V_{in} - b_0))$$

b_0, b_1, b_2 are coefficient factors generated from LabVIEW nonlinear curve fitting, V_{bias} is the bias voltage in data collected, V_{in} is the input voltage of LabVIEW.

Due to the noise in our system from different parts, the coefficient we get may not successfully offset LabVIEW result to zero when there is no flow passing through, we need to have a button that can read the bias at that point where there is no flow passing through, then added that additional part to offset coefficient, so that when no flow is entered, the LabVIEW shows zero flow on the screen.

In calibration process, to compare the results of flow we read from LabVIEW and we collected from Wet Test Meter quickly, we can use a program made by Dr. Macia, front panel is shown in

Figure 4.22

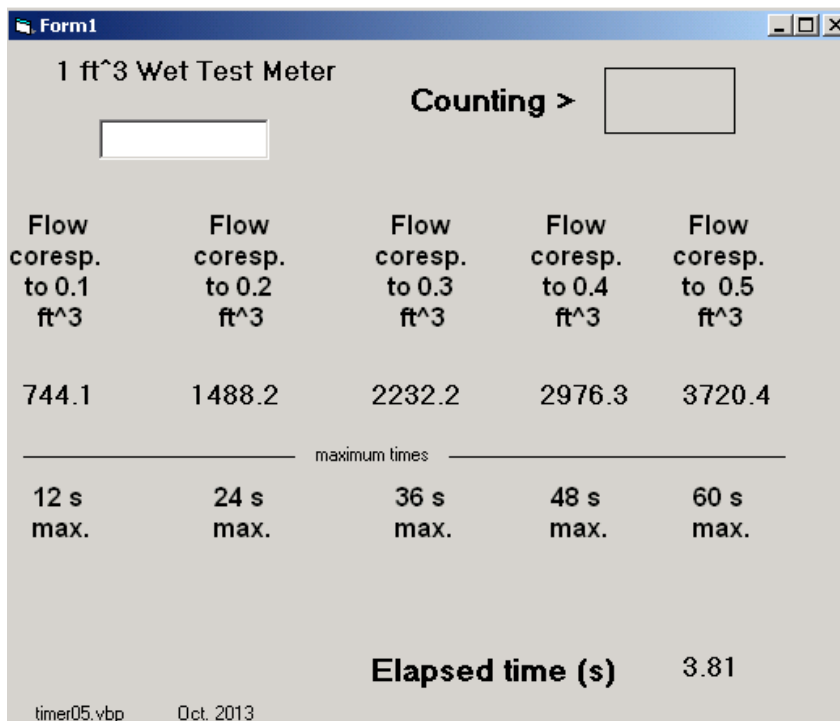


Figure 4.23 Flow rate calculator from Wet Test Meter

What this program does is when you enter a time period, it will show the result for flow rate for different amount of flow passing Wet Test Meter during this period.

4.4.3 Noise and disturbances

Noise and disturbances are general cases that cannot be avoided, and they may come from different parts of our experiment, we can eliminate noises and disturbances by carefully improving our setup.

In our system, signal conditioning circuit is achieved on a breadboard, all the external connections are from passive devices, like passive resistors, passive capacitors. First of all, naked wires on a breadboard are one of the sources to introduce noise, then loose connections of all passive devices can cause noise and disturbances, these problems can be solved by fastening all the devices and making it a PCB board.

Also, unavoidable noises and disturbances can come from different aspects, we know that for passive devices, the range is limited, resistors are about $10 \sim 10^5 \Omega$, with variance of $\Delta R = \pm 30\% \sim 50\%$, capacitors are about $10^{-2} \sim 10^2 \text{pF}$, with variance of $\Delta C = \pm 20\% \sim 30\%$. And also in filters and amplifiers, transistors can have thermal noise and flicker noise.

Hardware noises and disturbances are also huge, the pressure in the lab may change as we pass more flow through the flow generator, that will affect the result, and the flow friction against the tube may result in noise.

Noises and disturbances are unavoidable, but we can eliminate the effect by carefully handling the device and process, or using some statistical methods during data collection.

Chapter 5

EXPERIMENTAL RESULTS

Over the experiment of this study, pressure drops across the flow-meter were measured using linear and nonlinear flow-meters, under AC and DC flow source, for DC flow source, calibration factor is collected for computer software coefficient, both channels have to be calibrated for AC condition, calibration for flow rate is through Wet Test Meter, calibration for pressure is through U-tube manometer. For AC flow source, calibration coefficient is read and calculated in software, transfer function between estimate flow and true flow can be obtained through the data collected, Phase difference, amplitude and bandwidth can be seen from the data collected.

In this experiment, all the results are obtained at temperature 75°F in lab condition. Errors introduced above are minimized. The fluids in this experiment are dry air and air moistened by water. Reynolds number is fixed, viscosity differences of these two different types of fluids are handled by calibration coefficient. Graphs plotted are by LabVIEW graph or Excel.

5.1 Calibration results

Calibration process can be done by software through data recording, also it can be done by external hardware connection and data recording, software way is more accurate, hardware is more reliable, in this experiment, we do both and compare, to make sure that through coefficient calculation, flow rate indicated on the screen is the real flow rate.

Two major types of calibration are shown, flow calibration is to calibrate the estimate flow rate, and pressure calibration is to calibrate the real flow rate in close loop systems. Flow unit is cm^3/s . pressure unit is cmH_2O .

5.1.1 Flow calibration

5.1.1.1 Capillary tube

Screen Pneumotach flow-meter calibration uses the similar process as capillary flow-meter, here we only introduce the capillary tube calibration process.

Process of Capillary tube calibration process was shown in previous chapter

For each different flow rates input to the system by adjusting pressure valve, a sets of data are collected, real flow rate from Wet Test Meter, and LabVIEW result. As been introduced in earlier chapter, we know this relationship is linear, so through a linear curve fitting coefficients can be accessed.

Data collected and plotted through Excel is shown in **Figure 5.1**

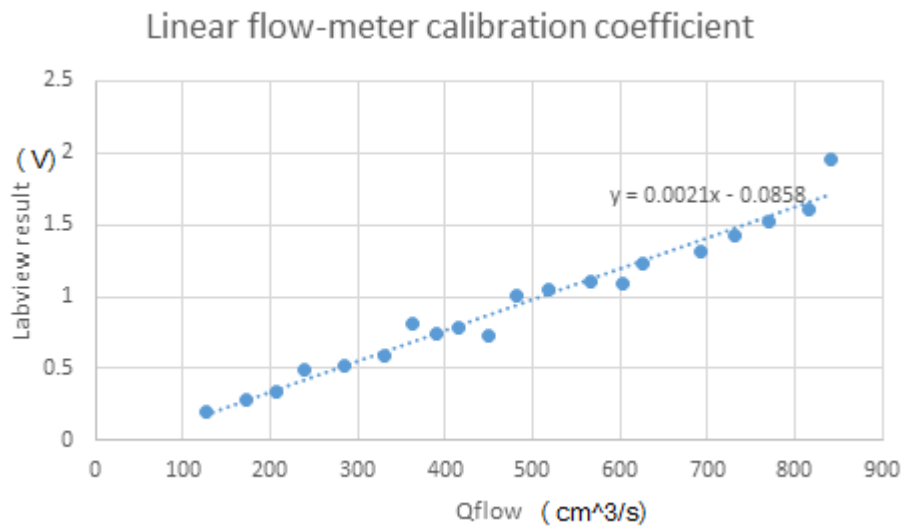
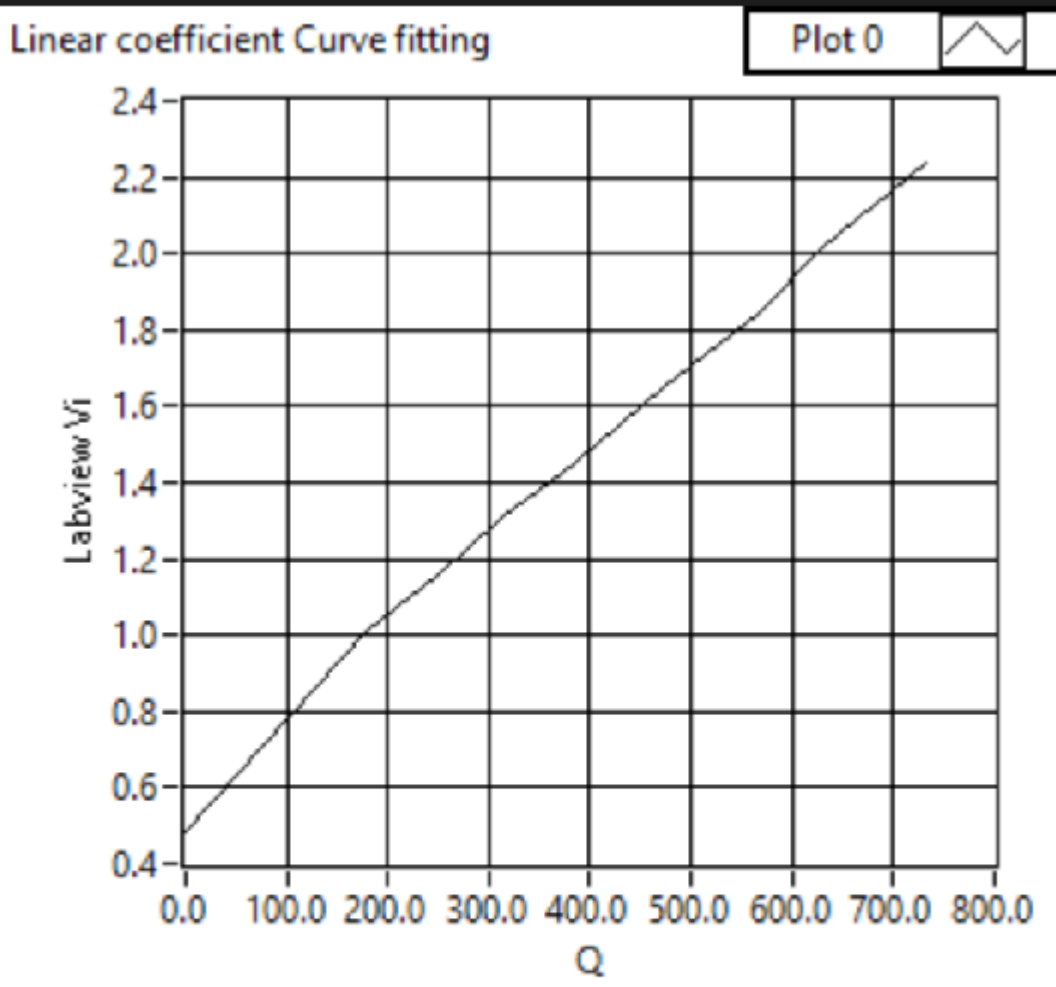


Figure 5.1 Linear flow-meter calibration coefficient (from Excel)

Data collected from LabVIEW software is saved and shown in **Figure 5.2**



```

File Edit Format View Help
Arizona State University at Polytechnique campus
Pneumatic system flow measure using capillary tube
linear flowmeter calibration

The linear coefficient:
Q0: 1.293234      K1: 0.002318
Horace -10/30/2013|

```

Figure 5.2 Linear flow-meter calibration coefficient (from LabVIEW)

The data generated from LabVIEW shows the valid coefficient which can be easily load and used in next stage, through comparing the flow rate generated from software to real flow rate, we find these coefficients are valid and indeed accurate.

5.1.1.2 Square edged orifice

Setup for square edged orifice plate calibration process is similar to capillary tube, shown in previous chapter. The major different part is the way we get the calibration coefficient is much harder than linear process, as been introduced in previous chapter, use least square technique through SVD process. Data collected and plotted from Excel is shown in **Figure**

5.3

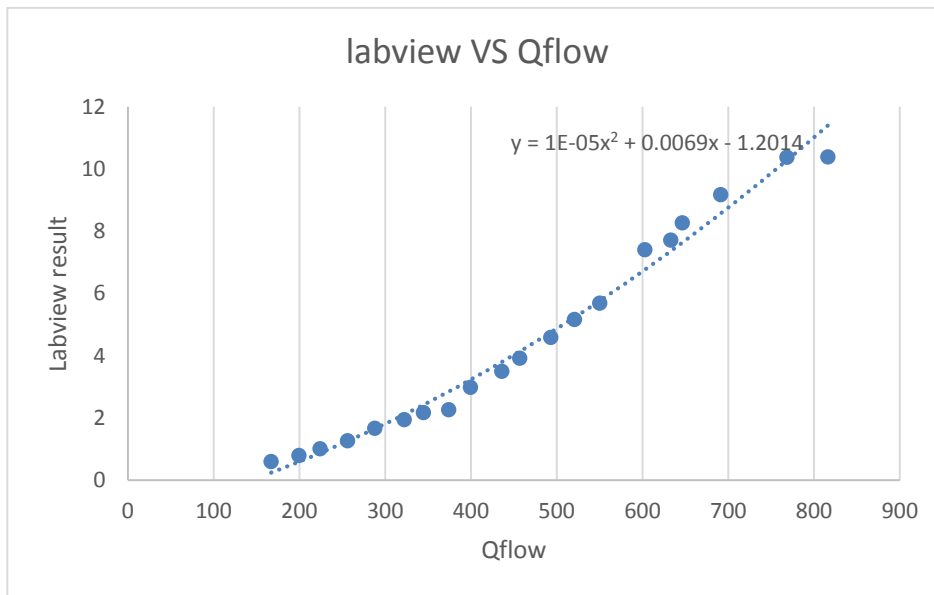
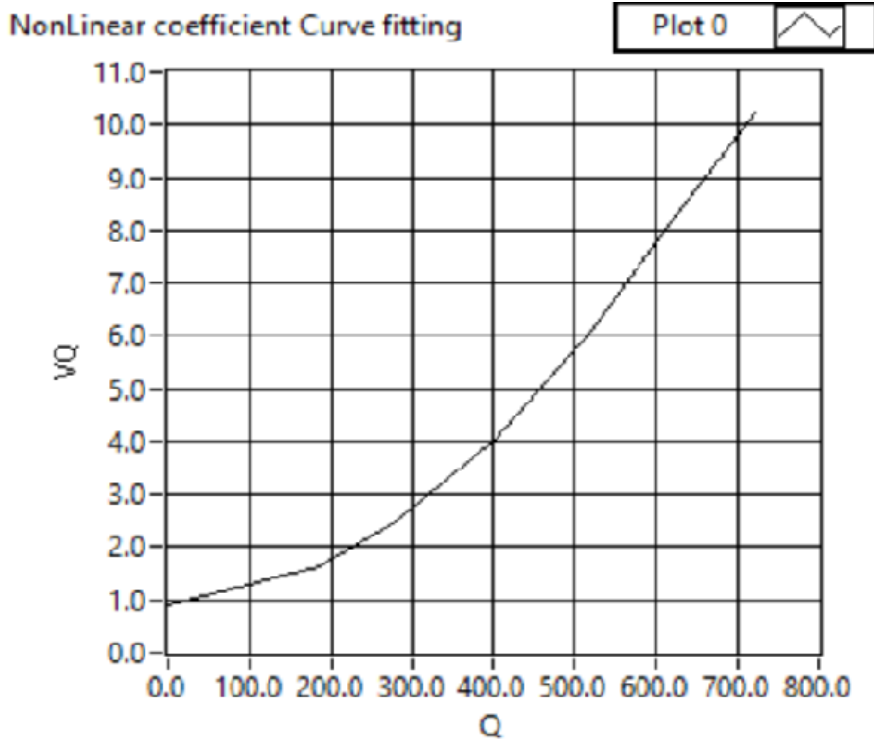


Figure 5.3 nonlinear flow-meter calibration coefficient (from Excel)

Data collected from LabVIEW result is shown in **Figure 5.4**



Arizona State University at Polytechnique campus
Pneumatic system flow measure using Square edged orifice tube
Nonlinear flowmeter calibration

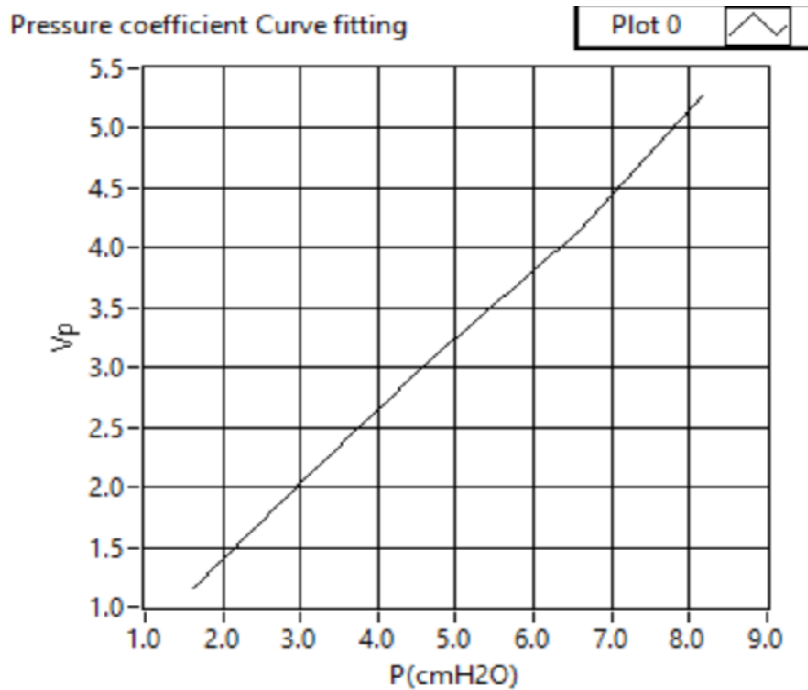
The Nonlinear coefficient:
Q0: 1.010934 K1: 0.002597 K2: 0.000015
Horace-10/30/2013

Figure 5.4 Nonlinear flow-meter calibration coefficient (from LabVIEW)

The data generated from software is valid and as shown above, pure quadratic relationship can be observed, Offset LabVIEW result can be cancelled out in read coefficient process by LabVIEW offset voltage V_{bias} .

5.1.2 Pressure calibration

Real pressure is measured by U-tube manometer, compare to the pressure transducer from channel 2. LabVIEW data is shown in **Figure 5.5**



Arizona State University at Polytechnique campus
Pneumatic system flow measure using U-shape for pressure calibration
pressure calibration

The pressure coefficient:
P0: 0.153708 Kp: 0.619311
Horace 11/01/2013}

Figure 5.5 Pressure calibration coefficient (from LabVIEW)

In this process, we already know that all the hardware devices in this process are linear the linear line relationship is what we expected, this pressure calibration process is for next step real flow rate measurement.

In pressure calibration process, voltage in LabVIEW cannot be over 6 Volts, or it will saturated.

5.2 Dynamic Characteristics

The performance parameters related to flow-meter usually are determined by steady state condition, however, due to real-world application, dynamic characteristic of flow-meter have to be determined.

Frequency response of our devices are determined by function generator and audio amplifier, a sine wave dry air flow is injected into the system, through adjusting frequency of function generator, frequency response can be obtained through channel 1 and channel 2, which are estimate flow and real flow, setup is shown in **Figure 5.6**

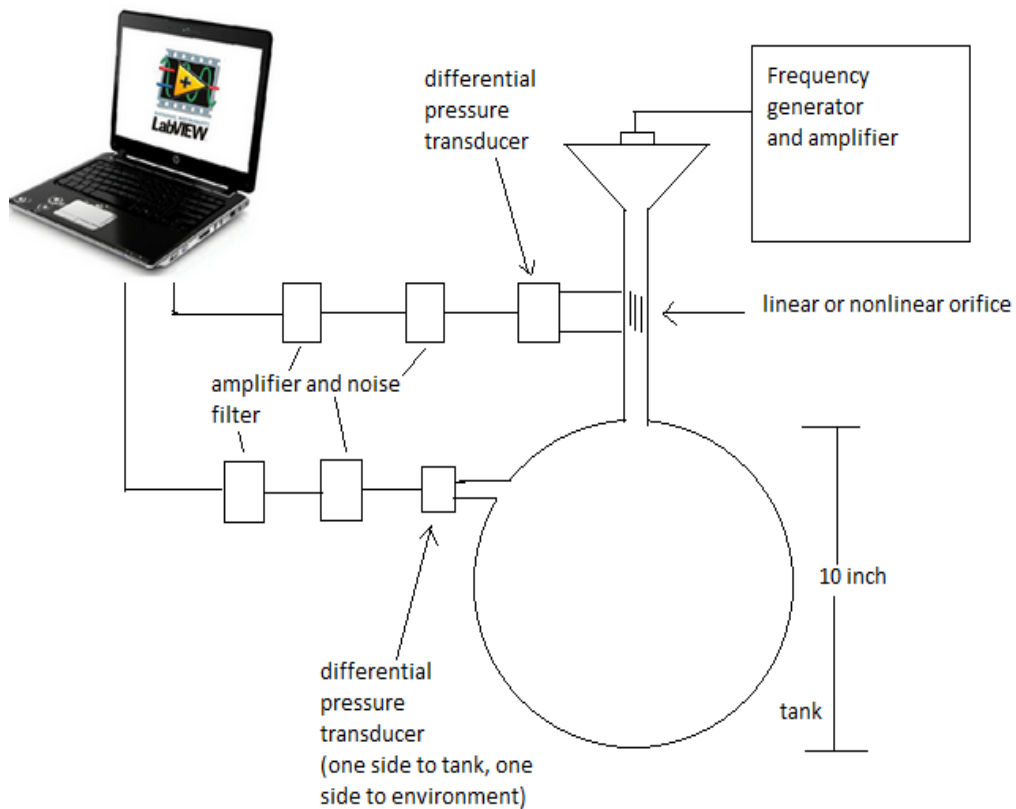


Figure 5.6 Setup for frequency response

5.2.1 Frequency response of linear flow-meter

Two kinds of linear flow-meters are used, all generate linear relationship between pressure and flow rate, flow is laminar in both flow-meters, flow source is pure sine wave with low distortion,

cut-off frequency through Butterworth filter is 375 HZ, under room temperature 75°F, detail coefficient factor and constants will be introduced in subsections.

5.2.1.1 Capillary tube flow-meter

Capillary tube flow-meter data is collected from labview and processed and plotted in Matlab.

Frequency response is shown in **Figure 5.7**:

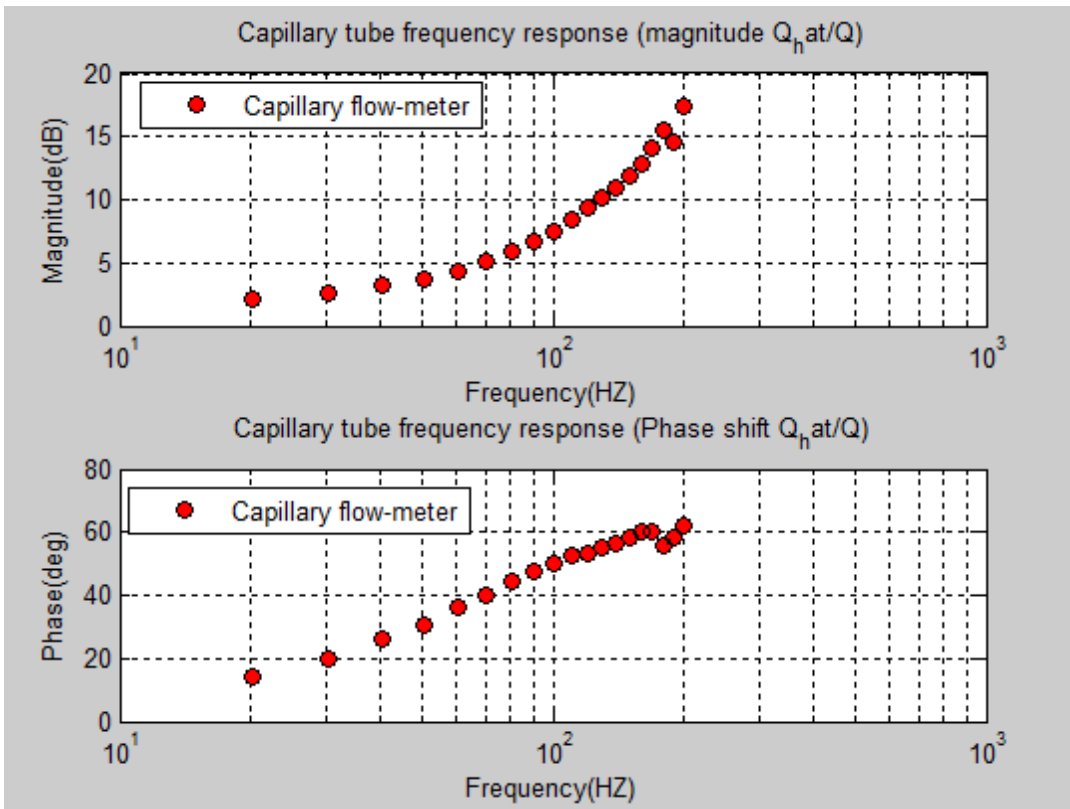


Figure 5.7 Frequency response of capillary tube

Data is processed so this shows a bode plot with phase in degree magnitude in Decibel, equation we use for data processing is the equation we introduced in earlier chapter:

$$H(s) = \frac{Q_{flow}(s)}{Cj2\pi f Pressure(s)}$$

Notice for a frequency response, transfer function from input to output is not decreased with increased frequency, this is due to the effect of inductance, the physic is simple to understand, because of the flow-meter inductance, as frequency increases, it has a trend to reject the change

of direction, that results in a large resistance appear, then the voltage, in this case, the pressure difference across the flow-meter, will increase, so at high frequency, estimated flow cannot accurately reflect the real flow, because it is increased. Later in this chapter we will introduce SPICE simulation which can capture this behavior.

Bandwidth of this type is then 3dB frequency, around 40~50 HZ, can be observed from the graph.

5.2.1.2 Screen Pneumatich Flow-meter

Screen Pneumatich is another kind of linear flow-meter, frequency response is shown in **Figure**

5.8.

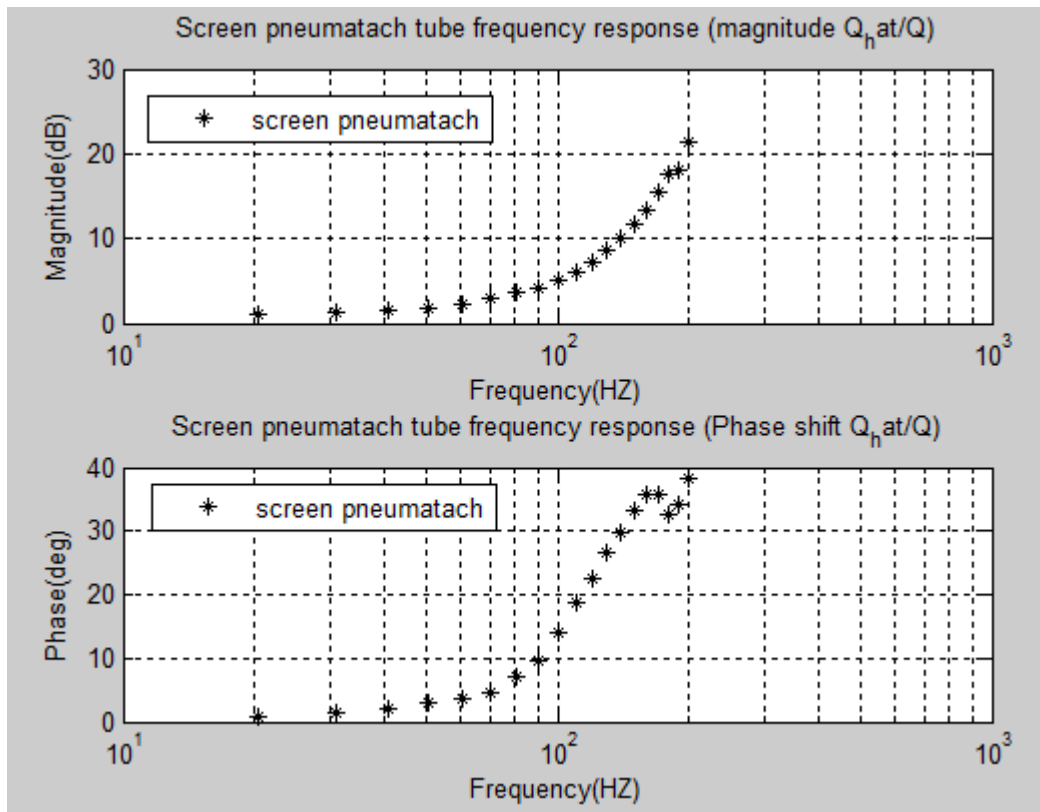


Figure 5.8 Frequency response of Screen Pneumatich flow-meter

This flow-meter use a different kind of technology but use the same mechanism to generate a resistance. Behavior is similar to capillary flow-meter.

5.2.2 Frequency response of non-linear flow-meter

Square edged orifice is the typical type of non-linear flow-meter we use in our lab, frequency response is shown in **Figure 5.9**.

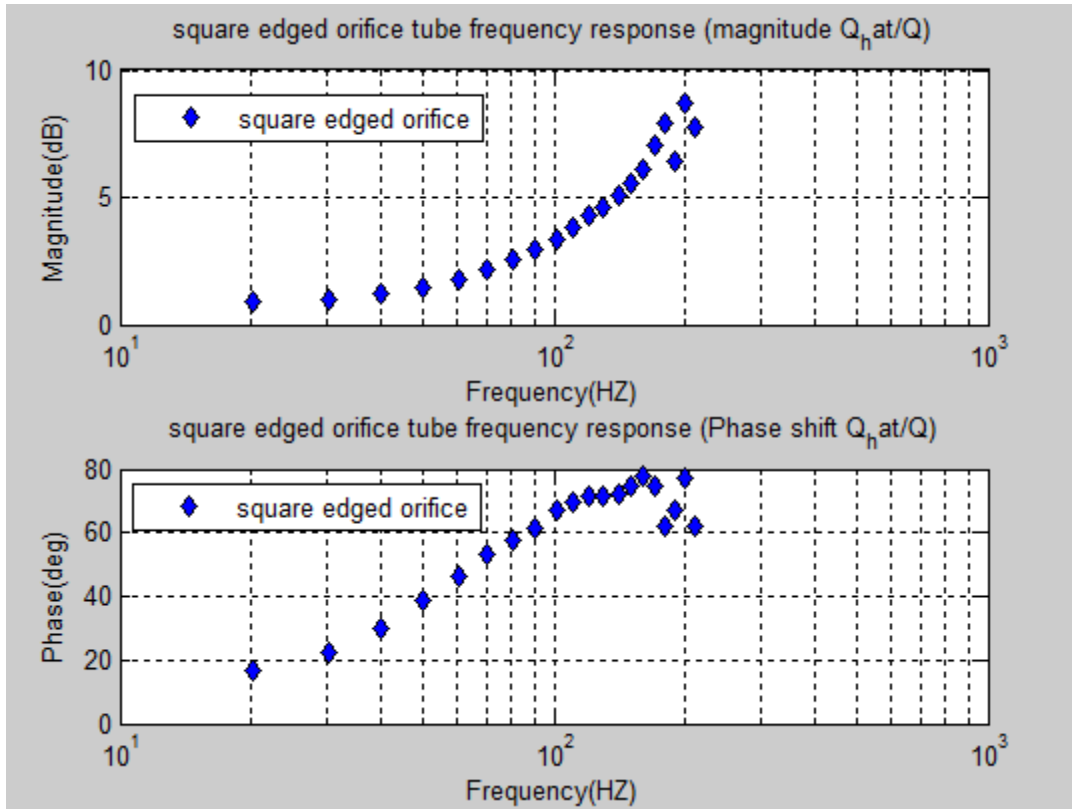


Figure 5.9 Frequency response of Square edged orifice

5.2.3 Factors affect Phase shift

Frequency response data yields that there is a phase difference between estimated flow and real flow, and this difference is time variant, with the increased frequency, phase difference become larger and larger. From our previous theoretical equation, for capillary tube:

$$\frac{\hat{Q}(s)}{Q(s)} = \frac{R * V_Q(s)}{C * s * V_p(s)} = \frac{R * V_Q(s)}{C * j * w * V_p(s)}$$

$$\angle \frac{\hat{Q}(s)}{Q(s)} = 0^\circ - 90^\circ + \angle \frac{V_Q(s)}{V_p(s)}$$

This shows that if our estimate flow can really reflect the real flow, they should be in phase, phase angle should be zero, and this phase difference phenomenon may come from two different possibilities. We need to test in two sub-sections

5.2.3.1 Effect of capacitance difference of pressure transducer

The effect is a general case, we use capillary to explain this behavior.

Capillary tube is shown in **Figure 5.10**.

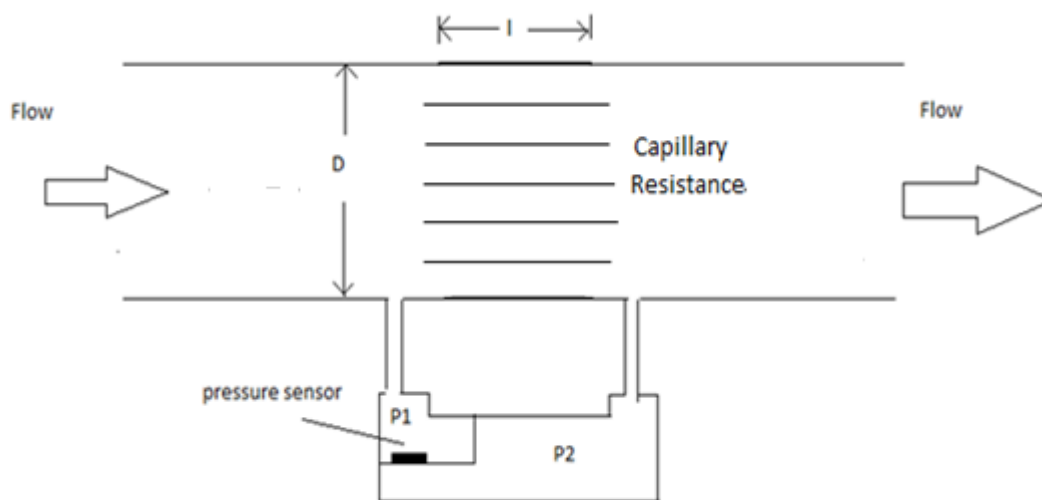


Figure 5.10 Capillary tube cross-section

As been introduced in pressure transducer section, the way we connect the pressure transducer can result in accuracy difference, this is because of the structure of pressure transducer, the capacitance of two sides are different, $C_1 < C_2$, due to this reason, the pressure measured from the pressure transducer should account for capacitance difference effect. We setup this experiment to measure and compare the phase angle difference by invert the connection of pressure transducer. In this case, we use oscilloscope record the data.

Data is shown in **Figure 5.11**

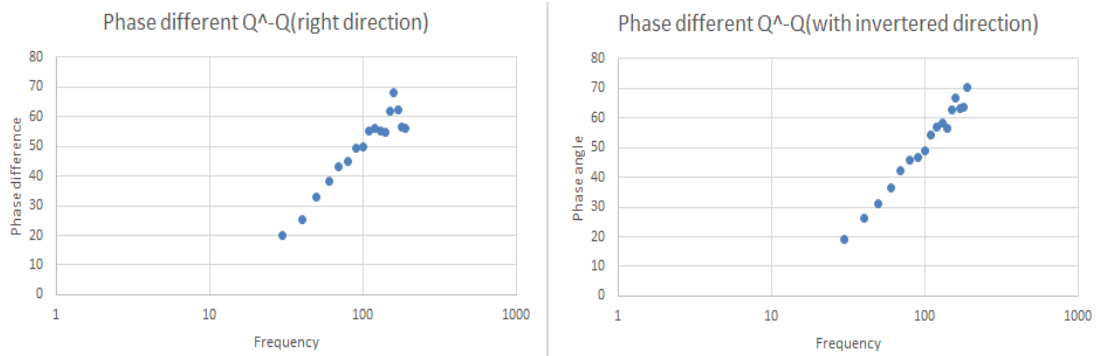


Figure 5.11 Phase difference affected by pressure transducer capacitance difference

From the data collected, it is clearly that these data have the same trend, and invert direction of pressure transducer didn't affect phase angle difference, the capacitance difference in pressure transducer is negligible.

5.2.3.2 Effect of inductance

Another possible source that generates this phase difference is the inductance, we know that for a pure inductance circuit, voltage should lead current by 90° . This is clear because we know:

$$V = L \frac{dI}{dt} = sLI = j\omega LI$$

$$\angle V = 90^\circ + \angle I$$

Then for our system, parasitic inductance exists, that will make our system an RLC system, it can be modeled in SPICE. Typical RLC circuit is shown in **Figure 5.12**

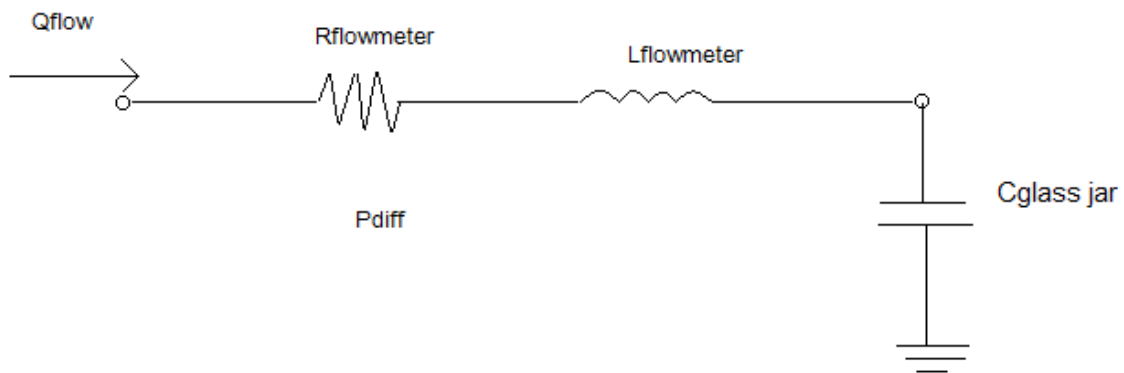


Figure 5.12 RLC Circuit

Equivalent resistance from V_{in} to V_{out} can be expressed as $sL + R$, so the current can be expressed as $I = \frac{V_{out}-V_{in}}{sL+R}$, now turn back to dynamic fluid system, equation can be revised as:

$$\frac{\hat{Q}(s)}{Q(s)} = \frac{V_Q(s)}{C * s * V_p(s) * (sL + R)}$$

$$\angle \frac{\hat{Q}(s)}{Q(s)} = 0^\circ - 90^\circ - \arctan\left(\frac{\omega L}{R}\right) + \angle \frac{V_Q(s)}{V_p(s)}$$

Factor added is $\arctan\left(\frac{\omega L}{R}\right)$, all the parameters are positive, so this is a positive number depends on the resistance, inductance and frequency value.

SPICE modeling is shown below in **Figure 5.13**

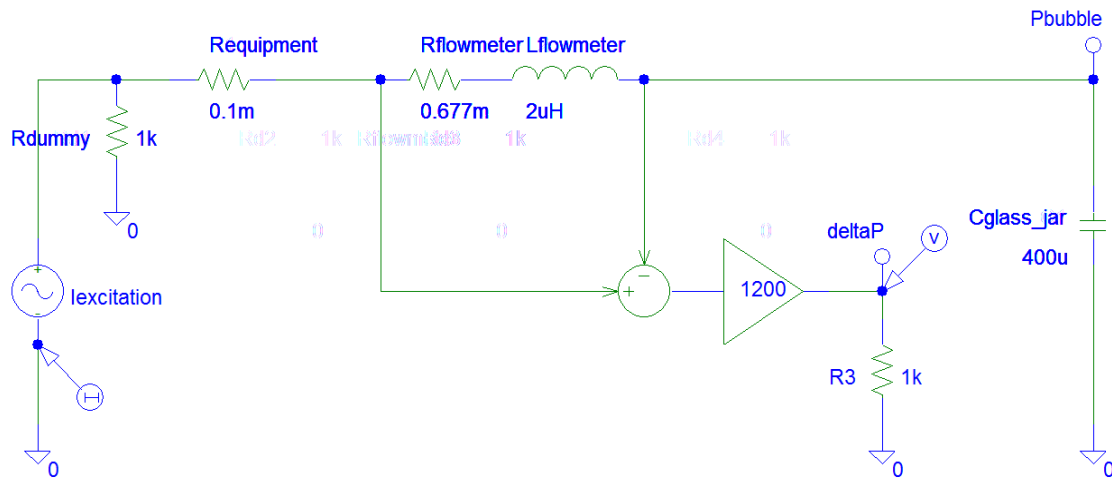


Figure 5.13 SPICE simulation for pneumatic system with inductance

Because in SPICE, current source direction is define from the current source positive terminal, through current source, to negative terminal. So we put the measure pin in negative terminal to have this 180° shift back. Simulation result is shown in **Figure 5.14**

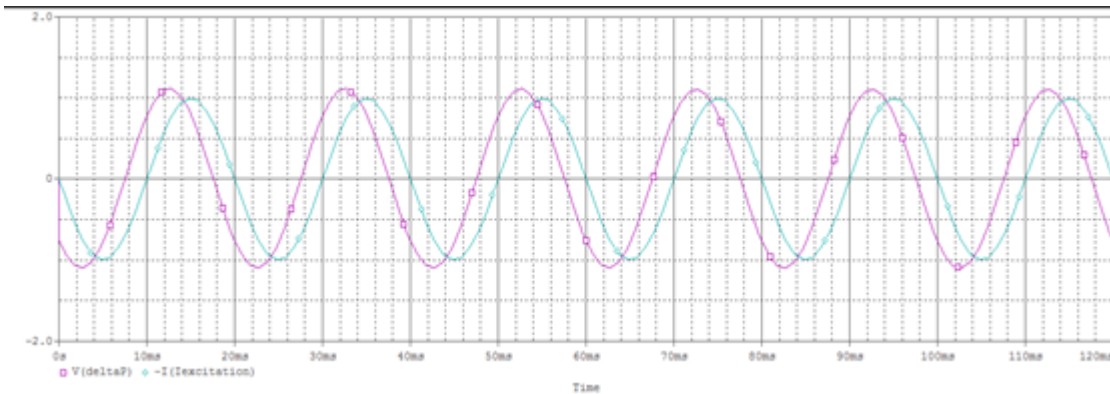


Figure 5.14 SPICE simulation for inductance effect of phase angle

Notice in this case, voltage across RL leads current, this matches the fact that in our pneumatic system, pressure difference across flow-meter lead the real flow rate.

Frequency response is shown in **Figure 5.2.3.2.D**

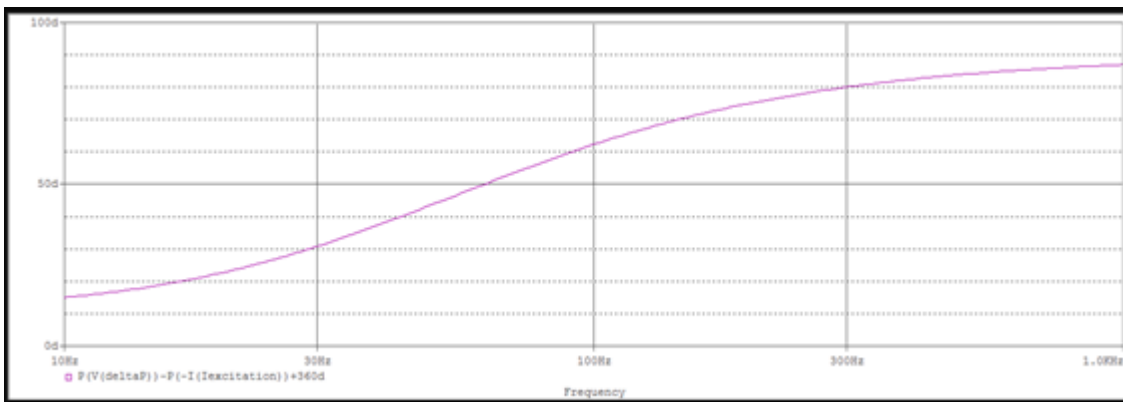


Figure 5.15 SPICE frequency response for phase difference

This shows the phase difference with frequency change for a fixed resistance and inductance, as frequency increases, phase difference of estimate flow and true flow increases, it fits our data correctly, also notice that this difference can never pass 90° due to the fact that

factor $\arctan\left(\frac{\omega L}{R}\right) \leq 90^\circ$, it can also be observed from the data we collected, and the frequency response for phase difference.

5.2.4 Comparison of three flow-meters

Three flow-meters have been introduced and tested, in this section we plot the frequency response of three devices, both for magnitude and phase plot, the dynamic characteristics can be determined from these comparison.

5.2.4.1 Bandwidth

Magnitude plot of three devices is shown in **Figure 5.16**.

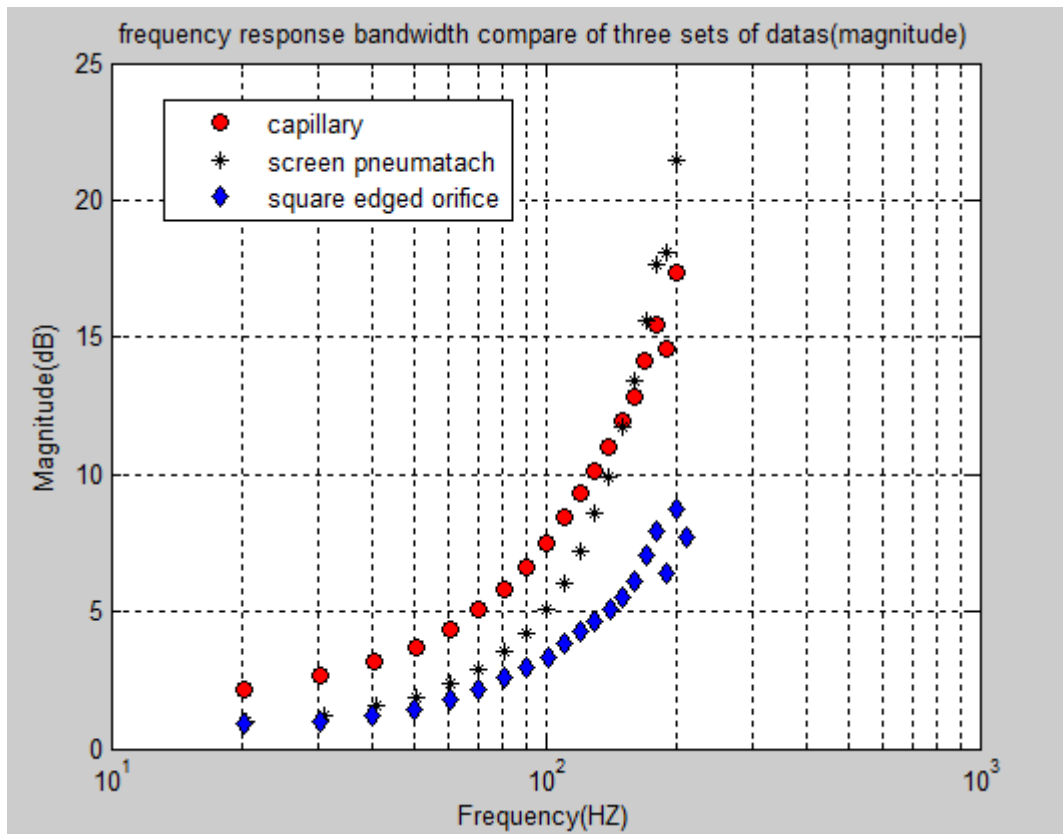


Figure 5.16 Magnitude frequency response of three devices

From the above graph, we can see that nonlinear flow-meter has a higher bandwidth, over 100 HZ, and the slope is not to large, which indicates that this device have better high frequency behavior. For linear flow-meter, Screen Pneumotach flow-meter has a higher bandwidth, about 70~80 HZ, slightly higher than capillary tube flow-meter, both Screen Pneumotach and square edged orifice have a good low frequency behavior, at low frequency, magnitude is close to zero,

this indicates that the flow rate captured from these devices at low frequency is close to true flow-rate. Capillary tube has the lowest bandwidth, worst low frequency behavior. The results of these behavior indicates the parasitic inductance effects.

5.2.4.2 Phase shift

As been introduced earlier, phase shift is due to inductance resistance ratio. The phase difference between estimate flow and true flow is plotted for three devices in **Figure 5.17**.

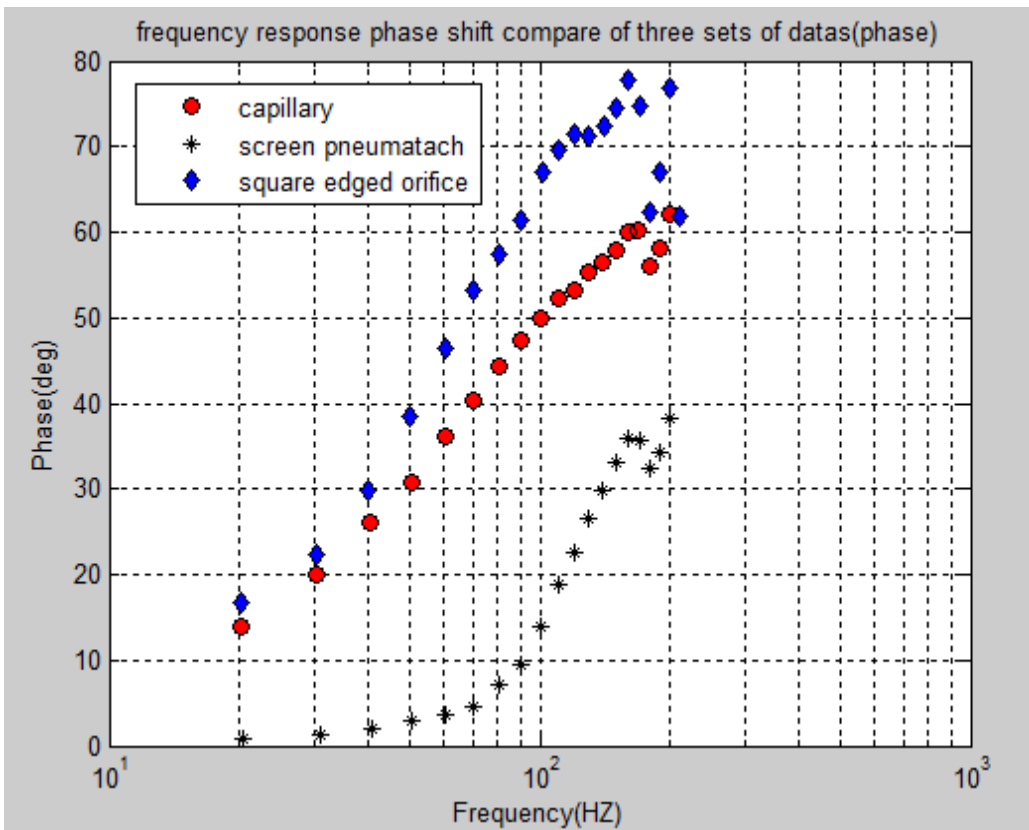


Figure 5.17 Phase shift frequency response of three devices

As been introduced, the maximum phase shift our process can get close to is 90°, from this graph we can see at low frequency about 200HZ, capillary tube reaches about 80°, this indicates a large inductance over resistance ratio. Screen Pneumotach has the best phase shift response.

This phase shift issue is easy to understand, as been introduced earlier, inductance is the major factor to cause the phase shift, this means, with frequency increase, inductance rejects the

change of flow, then the flow rate indicated by flow-meter will not follow the real flow rate correctly, and we define the change over 3db of magnitude the point where estimate flow cannot reflect the real flow, the reason it because of the phase shift, flow indicated by flow-meter will grow into another direction in a complex plane, as frequency become larger and large, we know the maximum phase shift appear when $s \rightarrow \infty$, then phase shift 90° , this means the estimate flow grows into another direction completely, the real flow cannot effect estimate flow anymore.

5.2.5 PSPICE simulation results

In this section, SPICE circuit simulation is used to model the real system, all the parameters are based on true parameters calculated. Even through Resistance of three devices might be different, we use capillary tube parameters as sample. Process circuit is shown in **Figure 5.18**.

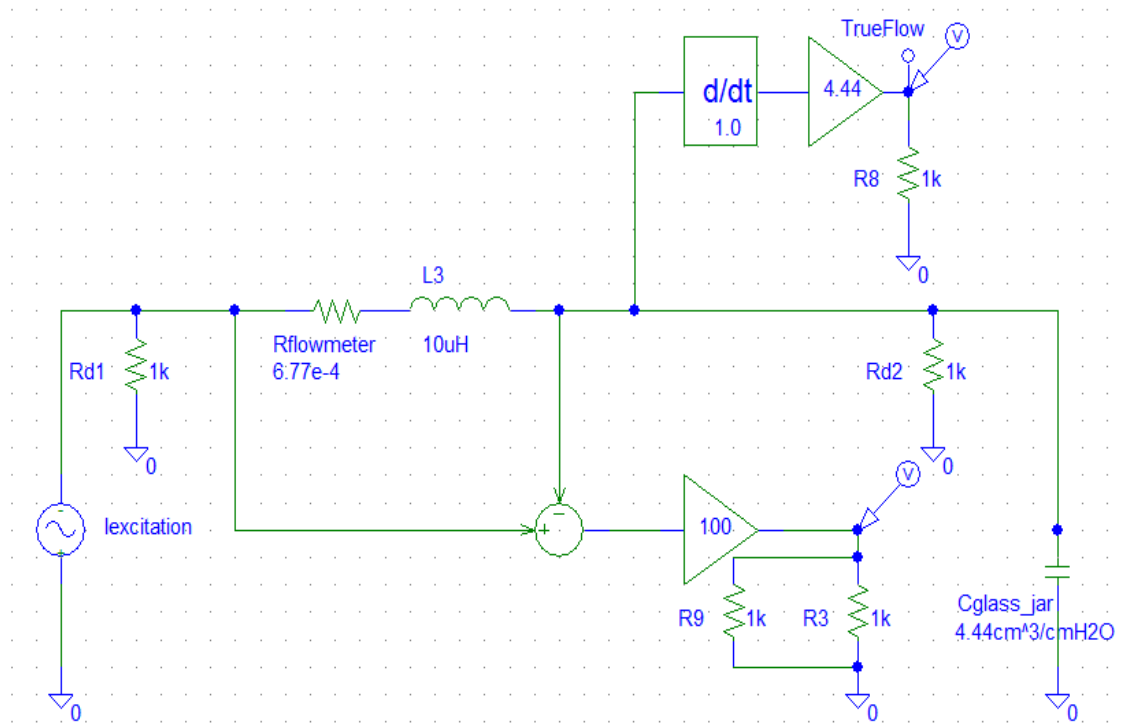


Figure 5.18 SPICE simulation for frequency response process setup

AC simulation results for magnitude and phase is shown in **Figure 5.19**.

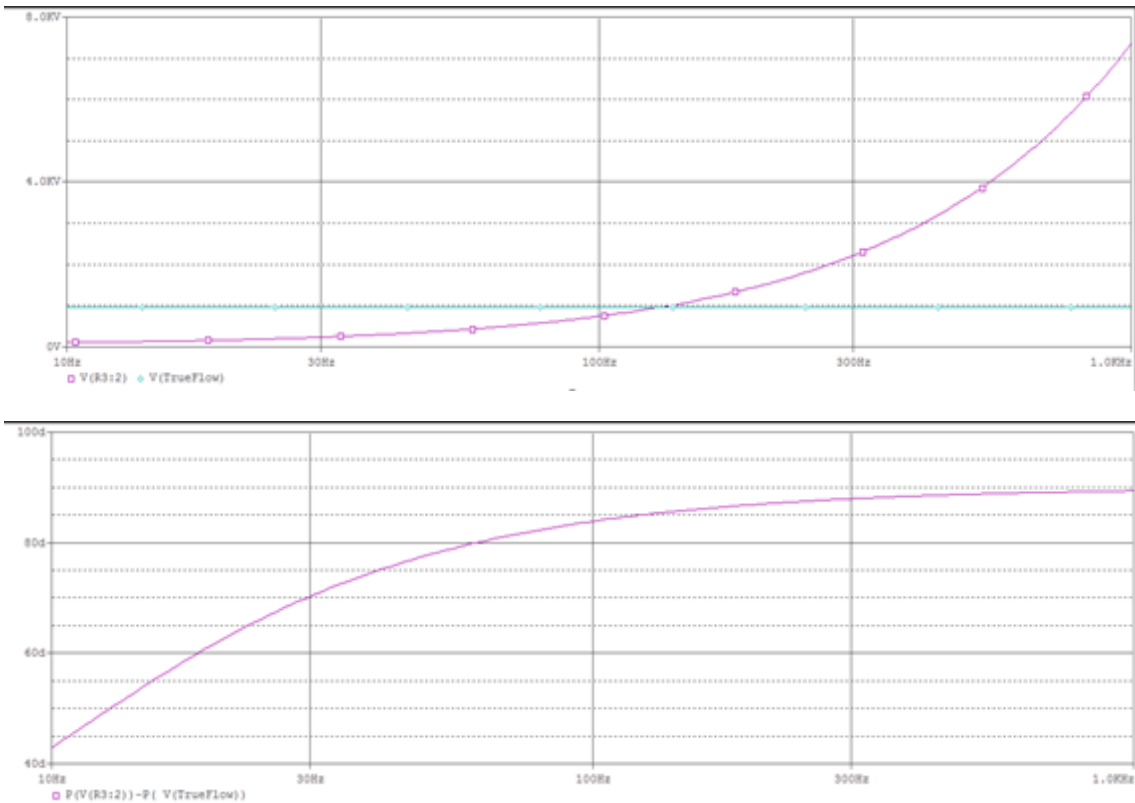


Figure 5.19 AC analysis of magnitude and phase difference

5.2.6 First Order system model

As have been introduced in earlier section, inductance effect is the major reason for phase shift and bandwidth limitation, the equivalent model for capillary flow-meter is shown in **Figure 5.20**.

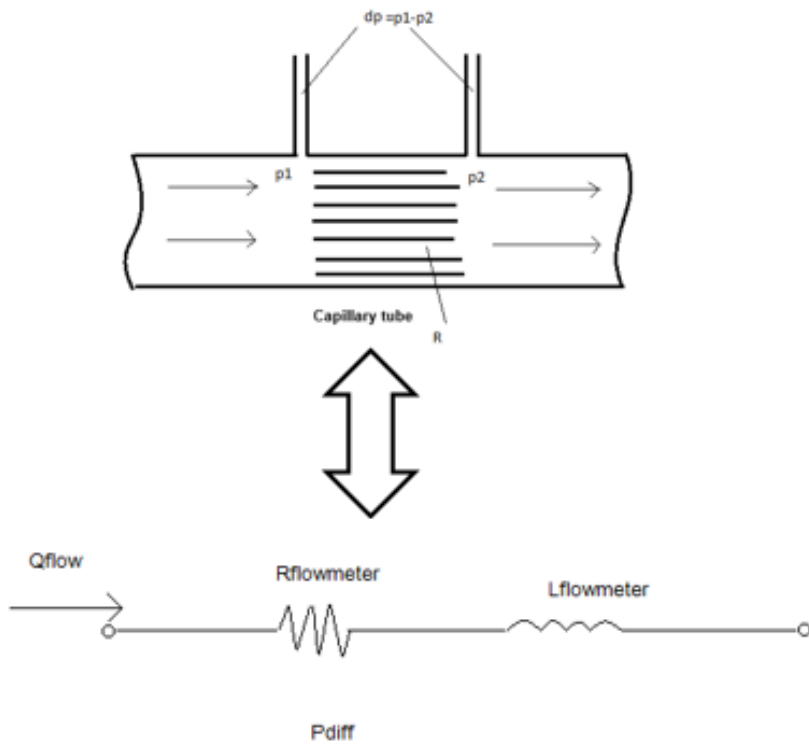


Figure 5. 20 equivalent electrical model for flow-meter

With this equivalent RL model, an equivalent first order transfer function can be obtained:

$$H(s) = \frac{s}{2\pi f_c} + 1$$

Plot this first order system and compare to true data collected, shown in **Figure 5.21**.

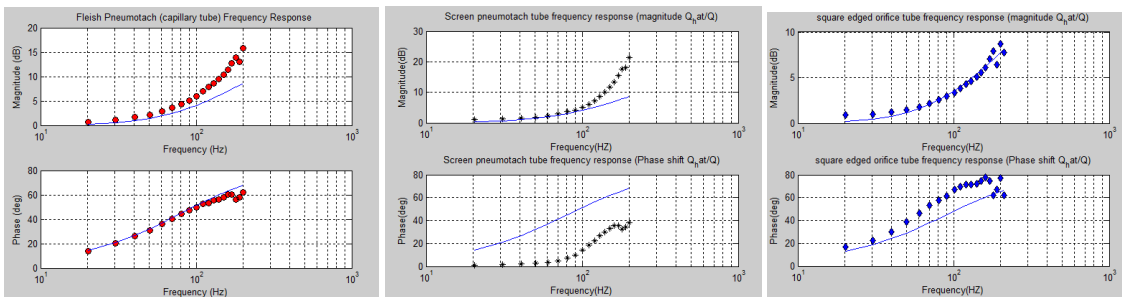


Figure 5. 21 Comparison with first order system

We can see that data fits capillary flow-meter and square edge orifice flow-meter very good, the first order system can approximately explain the behavior of capillary and square edge orifice

flow-meter, to have accurate curve fitting, higher order system have to be used, and behavior needed to be explained.

5.3 Discussion

From the above data results and PSPICE simulation results, we can see that data collected are match to the simulation results. Matlab and LabVIEW program has been made for this experiment, accuracy of this experiment depends on lab environment and investigator operation.

The data we collected shows that nonlinear flow-meter, for this type, have a higher bandwidth than linear flow-meter, both capillary and Screen Pneumotach.

Chapter 6

CONCLUSION AND RECOMMENDATION

The phase and magnitude frequency response generated from Matlab is shown in **Figure 6.1**.

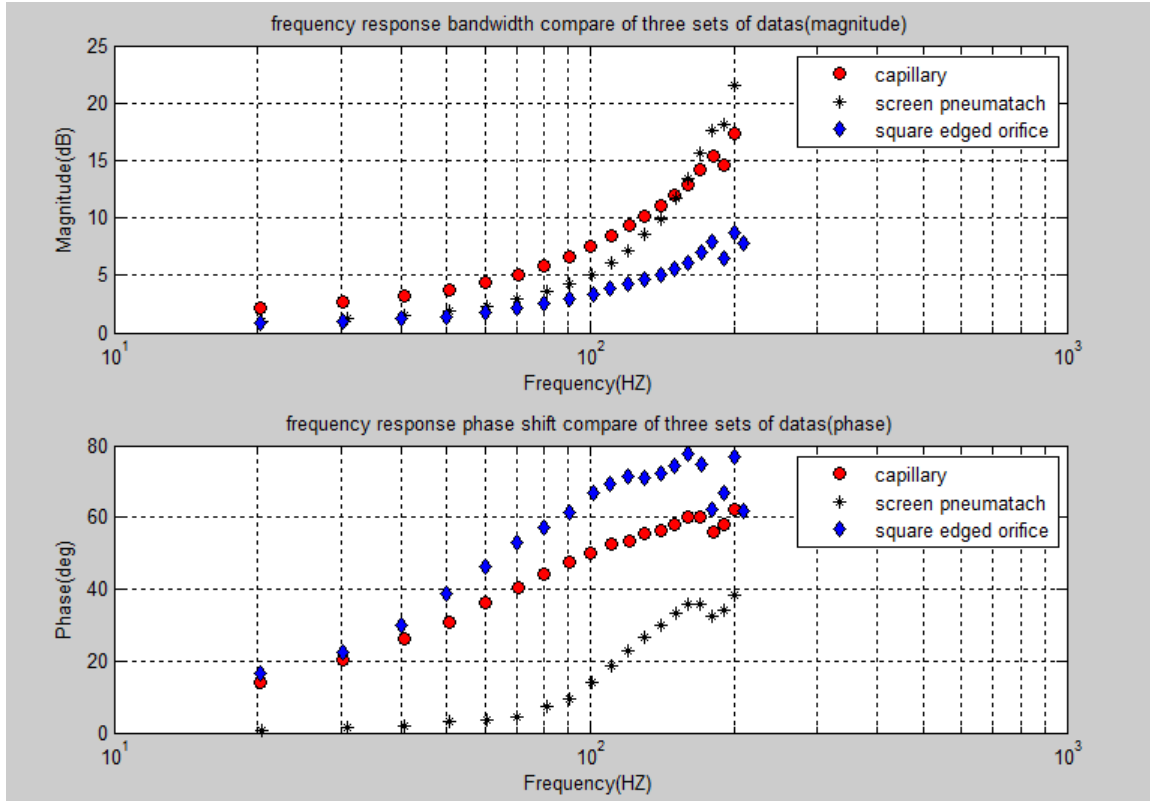


Figure 6.1 frequency response data for three devices

From the data collected, we can make the conclusion that nonlinear flow-meter, specifically, for square edge orifice type has a larger bandwidth around 100 HZ, Screen Pneumotach has a lower bandwidth about 70~80 HZ, capillary has the lowest bandwidth about 40~50 HZ.

Whole process considered most of the second effect, error is been minimized.

Inductance in flow-meter plays a major role in frequency response, our simulation and data yields that inductance is the main reason for bandwidth limitation for flow-meters.

Further research is needed to improve the hardware and software for pneumatic process.

RECOMMENDATIONS

Future research related to following parts might be a plus for continuous research:

Small flow detection in Square edged orifice

Square edged orifice cannot detect small flow accurately, because of the square of flow rate factor in equation, for a small amplitude flow, flow are all going to pass through middle hole of square edged orifice, can barely generate a pressure difference, in this case, noise is going to dominate the behavior, even though this device has a higher bandwidth, in hospital applications, small flow detection is also needed. How to detect small amplitude flow rate is a topic to be dived in.

Inductance effect compensation

With the well explained first order system and frequency response, it is possible to compensate the limited bandwidth and phase shift, it can be done in software program.

Inductance effect detection and improved device

Inductance is the main parasitic dominates the frequency response, a way to detect the inductance fast and convenient is needed, and improved convenient device is needed.

Viscosity effect

In our process, the flow Wet Test Meter detected is moister flow, our method is to moister flow before it enters the flow-meter, however, due to the moister process, dry air viscosity is changed, and viscosity in Poiseuille's equation will affect the resistance.

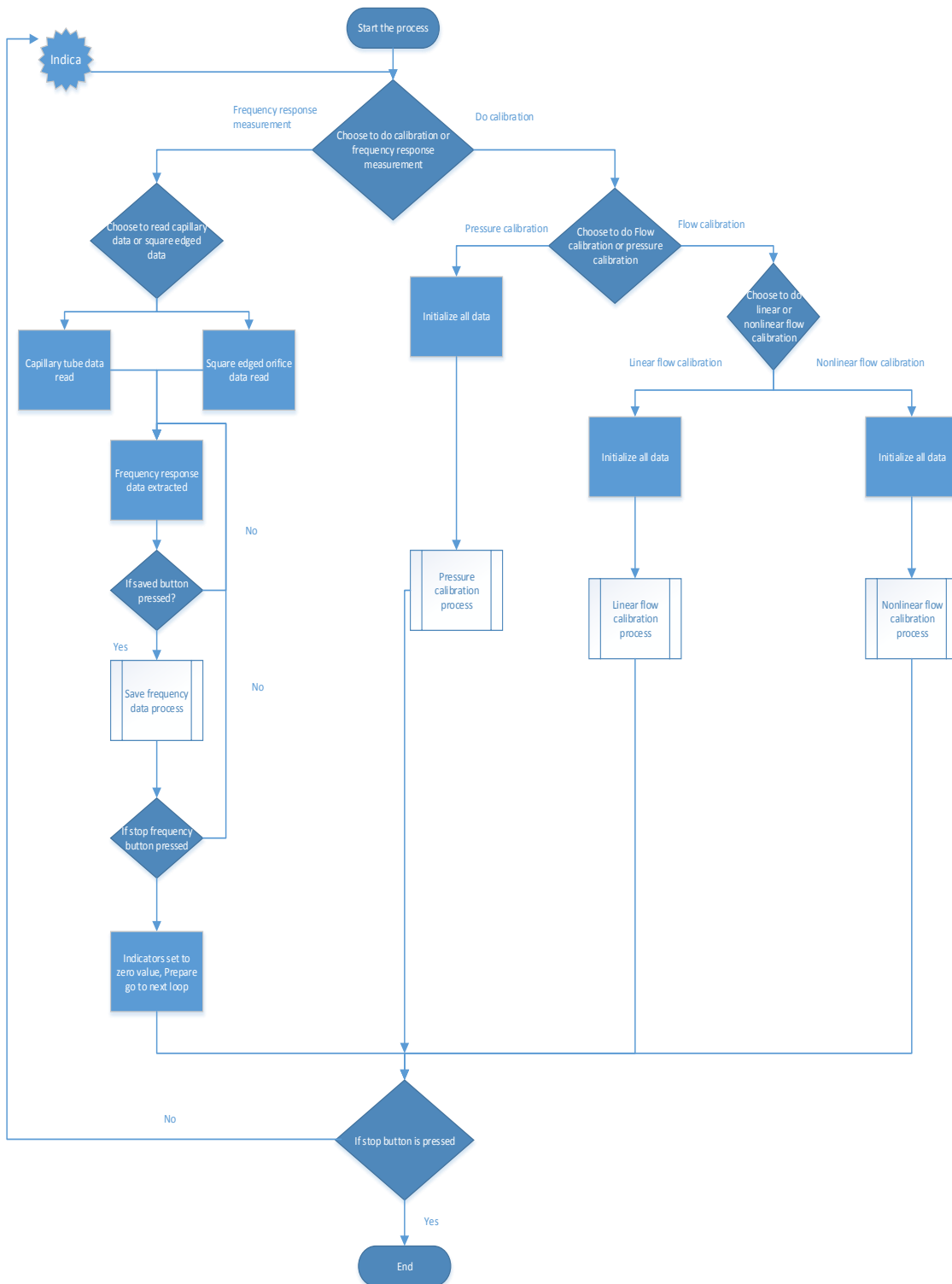
REFERENCES

- [1] Macia, N. (2013). V Latin American congress on biomedical engineering CLAIB 2011 may 16-21, 2011, Habana, Cuba monitoring respiratory parameters as a health status indicator. *IFMBE Proceedings*, 33, 830; 830-833; 833.
- [2] Szeri, A. Z. (1987). Some extensions of the lubrication theory of Osborne Reynolds. *Journal of Tribology*, 109(1), 21-36.
- [3] Qiang, Z. (2005). Mach number and freestream turbulence effects on turbine vane aerodynamic losses. *Journal of Propulsion and Power*, 21(6), 988-96.
- [4] Liu, X. (2007). Low Mach number flow computation using preconditioning methods and compressible navier-stokes equations. *Transactions of Nanjing University of Aeronautics & Astronautics*, 24(4), 271-5.
- [5] Teleaga, I. (2008). Simplified radiative models for low-Mach number reactive flows. *Applied Mathematical Modelling*, 32(6), 971; 971-91; 991.
- [6] Ntamba Ntamba, B. (2012). Pressure losses and limiting Reynolds numbers for non-Newtonian fluids in short square-edged orifice plates. *Journal of Fluids Engineering*, 134(9), 091204-091204.
- [7] Pordal, H. S. (1991). Inviscid steady/unsteady flow calculations. *Computers & Fluids*, 19(1), 93; 93-118; 118.
- [8] Rup, K. (2008). A comparison of measuring capabilities of elbow, coriolis and electromagnetic flow meters. *Archives of Thermodynamics*, 29(4), 141-52.
- [9] Eymard, R. (1994). Mathematical and numerical properties of control-volume, finite-element scheme for reservoir simulation. *SPE Reservoir Engineering*, 9(4), 283-287.
- [10] Segletes, S. (2002). A note on the application of the extended Bernoulli equation. *International Journal of Impact Engineering*, 27(5), 561; 561-76; 576.
- [11] Jones, F. E. (1992). Application of the poiseuille equation to the treatment of laminar flowmeter calibration data. *Industrial Metrology*, 2(2), 91-6.
- [12] Lopata, V. (2013). On the spirometry and spirometers standardization. *2013 IEEE XXXIII international scientific conference on electronics and nanotechnology (ELNANO 2013)* (pp. 316-18)
- [13] Steven, R. (2009). Orifice plate meter wet gas flow performance. *Flow Measurement and Instrumentation*, 20(4-5), 141; 141-51; 151.
- [14] Roberts, J. H. (1926). The Pitot tube. *Colliery Engineering*, 3(29), 292-294.
- [15] Alfonsi, G. (2001). Analysis of streamwise velocity fluctuations in turbulent pipe flow with the use of an ultrasonic Doppler flowmeter. *Flow, Turbulence and Combustion*, 67(2), 137; 137-42; 142.
- [16] Balasubramanian, R. (1991). A non-invasive ultrasound transit time flowmeter. *Proceedings of the Annual Conference on Engineering in Medicine and Biology*, 13(1), 150-151.

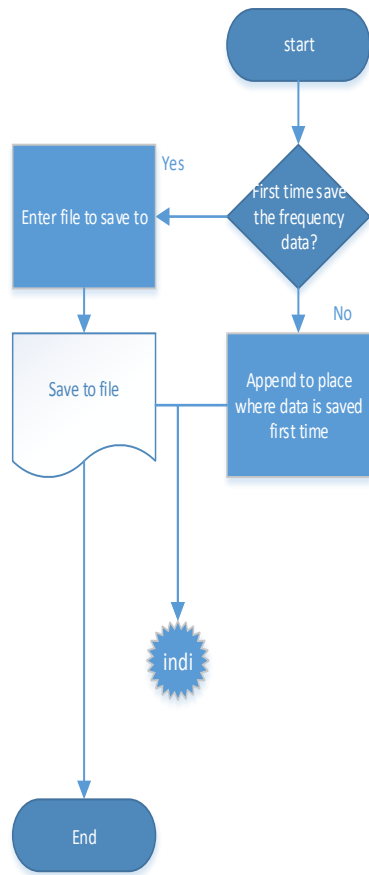
- [17] Piesniewska, G. (1978). Double-chambered thermal flowmeter. *Pomiary, Automatyka, Kontrola*, 24(2), 43-4.
- [18] Leonhardt, S. (2010). Analysis of tidal breathing flow volume loops for automated lung-function diagnosis in infants. *IEEE Transactions on Biomedical Engineering*, 57(8), 1945; 1945-53; 1953.
- [19] Frequency Devices, Product Selection Guide - Low pass Filter Components.
- [20] Abraham, B. (2012). Designing of lab view based electrical capacitance tomography system for the imaging of bone using NI ELVIS and NI USB DAQ 6009. *Bonfring International Journal of Power Systems and Integrated Circuits*, 2(2), 01-06.
- [21] Strang, G. (1976). *Linear algebra and its applications*. New York: Academic Press.
- [22] Macia, N. F. (1988). *Noninvasive, quick obstruction estimation method for the measurement of parameters in the nonlinear lung model*. (Ph.D., Arizona State University). *ProQuest Dissertations and Theses*. (303693416).
- [23] J. Neergaard von, K. Wirz. (1927). Die Messung der Strömungswiderstände in den Atemwegen des Menschen, insbesondere bei Astma und Emphysem, *Z. Klin. Med.*, vol. 105, pp. 51-82.
- [24] Beydon N, Davis SD, Lombardi E, et al. (2007) American Thoracic Society/European Respiratory Society Working Group on Infant and Young Children Pulmonary Function Testing. An official American Thoracic Society/European Respiratory Society statement: pulmonary function testing in preschool children. *Am J Respir Crit Care Med*. 175: 1304–1345.
- [25] Turner, M. J. (1989). Measurement of the frequency response and common-mode gain of neonatal respiratory pressure and flow measurement systems part 1: Apparatus. *Clinical Physics and Physiological Measurement*, 10(3), 219; 219; 002-230; 230.

APPENDIX A

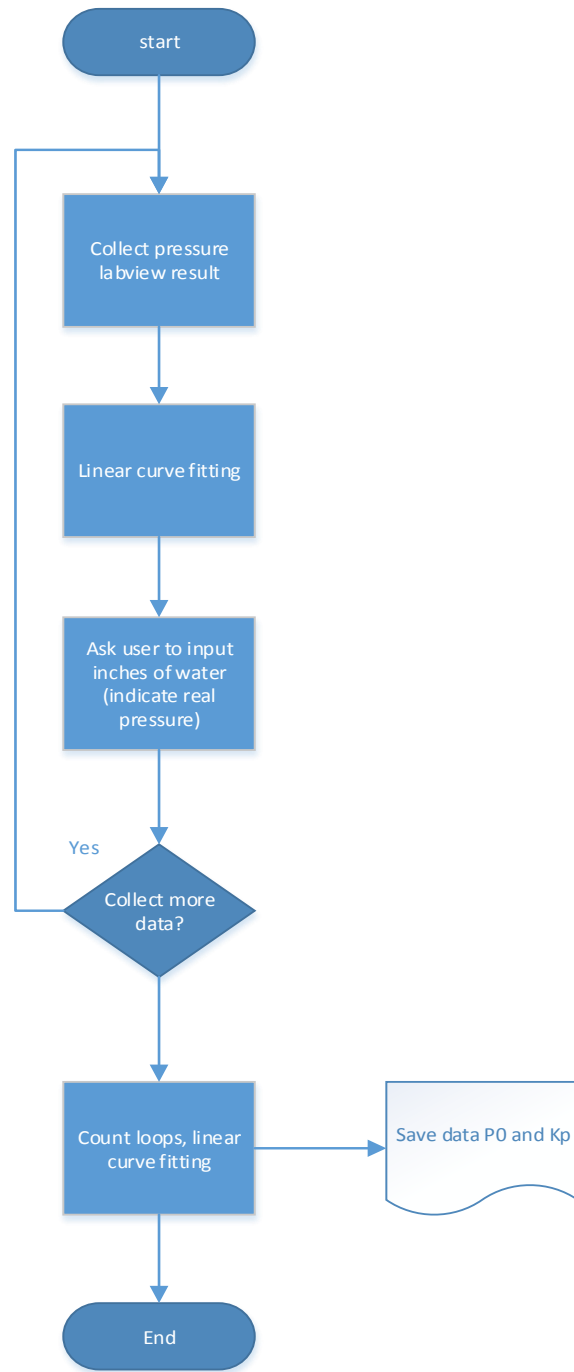
LABVIEW CODE FLOWCHART



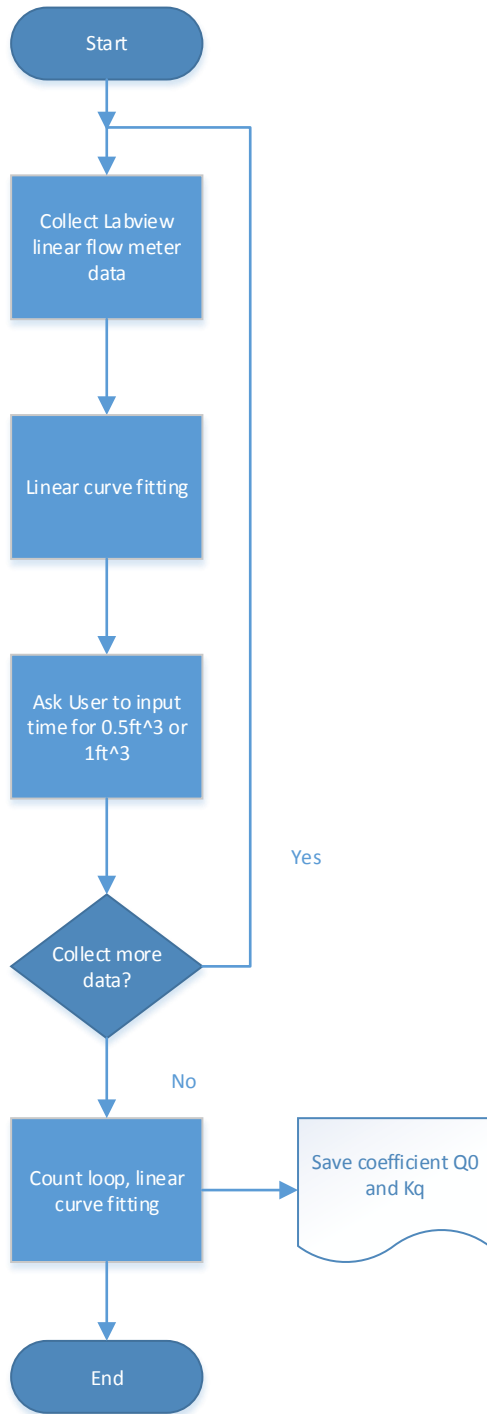
Main loop



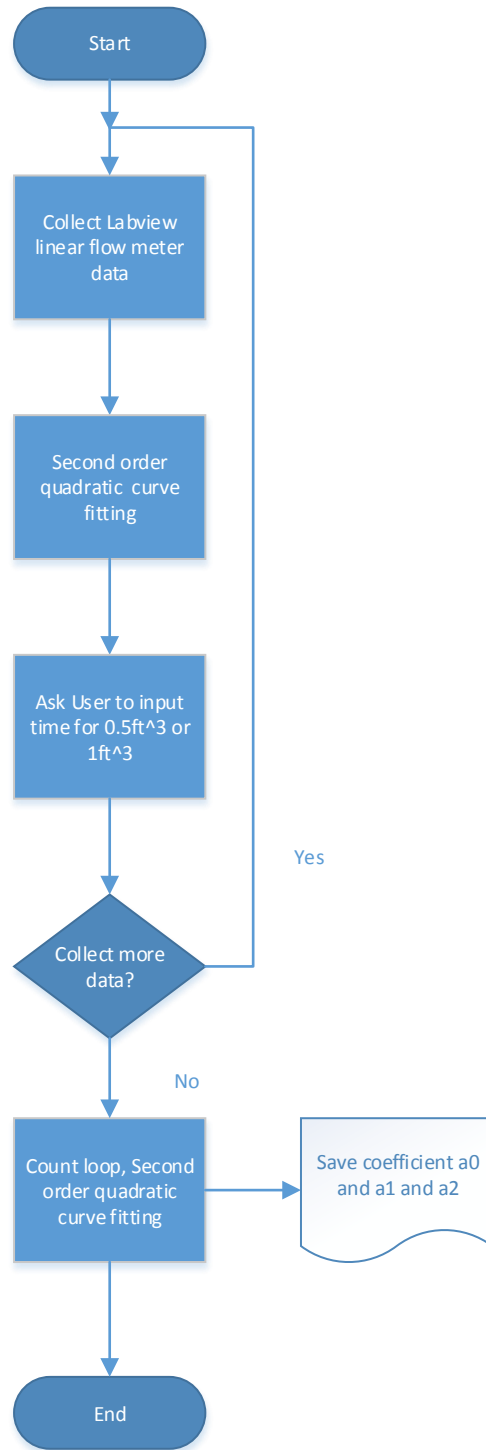
Save frequency data



Pressure calibration



Linear flow calibration



nonlinear flow calibration

APPENDIX B:

SATURATION VAPOR PRESSURE

SATURATION VAPOR PRESSURE OVER WATER
(°F, in Hg) – TABLE
(continued)

Tem- pera- ture	English units									
	.0	.1	.2	.3	.4	.5	.6	.7	.8	.9
*F.	in. Hg.	in. Hg.	in. Hg.	in. Hg.	in. Hg.	in. Hg.	in. Hg.	in. Hg.	in. Hg.	in. Hg.
50	0.36240	0.36375	0.36511	0.36646	0.36783	0.36920	0.37057	0.37195	0.37333	0.37472
51	.37611	.37751	.37891	.38031	.38172	.38314	.38456	.38598	.38741	.38884
52	.39028	.39172	.39317	.39462	.39608	.39754	.39901	.40048	.40195	.40343
53	.40492	.40641	.40790	.40940	.41090	.41241	.41393	.41544	.41697	.41850
54	.42003	.42157	.42311	.42466	.42621	.42777	.42933	.43090	.43248	.43406
55	0.43564	0.43723	0.43882	0.44042	0.44203	0.44364	0.44525	0.44687	0.44849	0.45012
56	.45176	.45340	.45504	.45670	.45835	.46001	.46168	.46335	.46503	.46671
57	.46840	.47009	.47179	.47350	.47521	.47692	.47864	.48037	.48210	.48384
58	.48558	.48733	.48908	.49084	.49260	.49437	.49614	.49792	.49971	.50150
59	.50330	.50510	.50691	.50873	.51055	.51238	.51421	.51605	.51789	.51974
60	0.52160	0.52346	0.52533	0.52720	0.52908	0.53096	0.53285	0.53475	0.53665	0.53856
61	.54047	.54239	.54432	.54625	.54818	.55013	.55208	.55403	.55600	.55797
62	.55994	.56192	.56391	.56590	.56790	.56990	.57191	.57393	.57595	.57798
63	.58002	.58206	.58411	.58616	.58823	.59029	.59237	.59445	.59654	.59863
64	.60073	.60284	.60495	.60707	.60919	.61133	.61347	.61561	.61777	.61992
65	0.62209	0.62426	0.62644	0.62862	0.63082	0.63302	0.63522	0.63743	0.63965	0.64188
66	.64411	.64635	.64859	.65085	.65311	.65537	.65765	.65993	.66221	.66451
67	.66681	.66912	.67143	.67376	.67608	.67842	.68076	.68312	.68547	.68784
68	.69021	.69259	.69497	.69737	.69977	.70217	.70459	.70701	.70944	.71188
69	.71432	.71677	.71923	.72169	.72416	.72664	.72913	.73163	.73413	.73664
70	0.73916	0.74169	0.74422	0.74676	0.74931	0.75186	0.75443	0.75700	0.75958	0.76217
71	.76476	.76736	.76997	.77259	.77521	.77785	.78049	.78314	.78579	.78846
72	.79113	.79381	.79650	.79919	.80190	.80461	.80733	.81006	.81279	.81554
73	.81829	.82105	.82382	.82659	.82938	.83217	.83497	.83778	.84060	.84343
74	.84626	.84910	.85195	.85481	.85768	.86055	.86344	.86633	.86923	.87214
75	0.87506	0.87799	0.88092	0.88387	0.88682	0.88978	0.89275	0.89573	0.89872	0.90172
76	.90472	.90773	.91075	.91378	.91682	.91987	.92292	.92599	.92906	.93215
77	.93524	.93834	.94145	.94457	.94770	.95084	.95398	.95714	.96030	.96348
78	.96666	.96985	.97305	.97626	.97948	.98271	.98595	.98920	.99246	.99572
79	.99900	1.00228	1.00558	1.00888	1.01220	1.01552	1.01885	1.02220	1.02555	1.02891
80	1.0323	1.0357	1.0391	1.0425	1.0459	1.0493	1.0527	1.0561	1.0596	1.0630
81	1.0665	1.0700	1.0735	1.0769	1.0804	1.0840	1.0875	1.0910	1.0946	1.0981
82	1.1017	1.1053	1.1089	1.1125	1.1161	1.1197	1.1234	1.1270	1.1307	1.1343
83	1.1380	1.1417	1.1453	1.1490	1.1527	1.1564	1.1602	1.1639	1.1677	1.1714
84	1.1752	1.1790	1.1828	1.1866	1.1904	1.1943	1.1981	1.2020	1.2058	1.2097
85	1.2136	1.2175	1.2214	1.2253	1.2292	1.2332	1.2371	1.2411	1.2450	1.2490
86	1.2530	1.2570	1.2610	1.2650	1.2691	1.2731	1.2772	1.2812	1.2853	1.2894
87	1.2935	1.2976	1.3017	1.3059	1.3100	1.3142	1.3183	1.3225	1.3267	1.3309
88	1.3351	1.3393	1.3436	1.3478	1.3521	1.3564	1.3606	1.3649	1.3692	1.3736
89	1.3779	1.3822	1.3866	1.3910	1.3954	1.3998	1.4042	1.4086	1.4130	1.4174
90	1.4219	1.4264	1.4308	1.4353	1.4398	1.4443	1.4489	1.4534	1.4580	1.4625
91	1.4671	1.4717	1.4763	1.4809	1.4856	1.4902	1.4949	1.4995	1.5042	1.5089
92	1.5136	1.5183	1.5230	1.5278	1.5325	1.5373	1.5421	1.5469	1.5517	1.5565
93	1.1613	1.5661	1.5710	1.5759	1.5807	1.5856	1.5905	1.5955	1.6004	1.6053
94	1.6103	1.6153	1.6203	1.6253	1.6303	1.6353	1.6404	1.6454	1.6505	1.6556
95	1.6607	1.6658	1.6709	1.6761	1.6812	1.6864	1.6916	1.6967	1.7019	1.7072
96	1.7124	1.7176	1.7229	1.7282	1.7335	1.7388	1.7441	1.7494	1.7548	1.7601
97	1.7655	1.7709	1.7763	1.7817	1.7871	1.7926	1.7980	1.8035	1.8090	1.8145
98	1.8200	1.8255	1.8311	1.8366	1.8422	1.8478	1.8533	1.8590	1.8646	1.8702
99	1.8759	1.8816	1.8873	1.8930	1.8987	1.9045	1.9102	1.9160	1.9218	1.9276
100	1.9334	1.9392	1.9450	1.9509	1.9568	1.9626	1.9685	1.9745	1.9804	1.9863

APPENDIX C

MATLAB CODE FOR DATA GENERATION

```

% data results read by matlab
% Flow-meter results, for linear and nonlinear
% Arizona State University at Polytechnique campus

% linear capillary flow-meter
x_capillary=[20.278 30.20382 40.5576 50.434 60.11888 70.45238 80.05585
90.19674 100.3594 110.3997 120.5549 129.907 140.2849 150.1261 160.1946
169.9388 180.8516 190.1347 200.5953];
y_capillary=[2.164492 2.65133 3.154802 3.703938 4.351695 5.103621
5.838237 6.615129 7.48453 8.418868 9.344293 10.10051 11.00126 11.91608
12.86337 14.15223 15.44004 14.5739 17.34799];
p_capillary=[14.017 20.1124 26.02827 30.79558 36.05448 40.25328
44.30241 47.34131 49.86442 52.36704 53.29949 55.36774 56.4129 57.97954
60.04422 60.27692 55.94093 58.1031 62.14353];

% linear screen pneumatach flow-meter
x_screen=[20.49256 30.80993 40.80799 50.63997 60.51633 70.34643
80.81925 90.18781 100.882 110.4737 120.2235 130.0962 140.3919 150.7419
160.1434 170.0895 180.3145 190.0884 200.1268];
y_screen=[0.987993095 1.233624199 1.542550763 1.841056976 2.3446412
2.896855989 3.571518974 4.22732629 5.058206619 6.065862297 7.173815178
8.572898018 9.937890794 11.73242514 13.43274903 15.58464656 17.63583628
18.0794282 21.47269326];
p_screen=[0.797432 1.281523 1.97341 2.960561 3.643962 4.497628 7.220631
9.516993 13.903659 18.817999 22.624103 26.492867 29.772512 33.103818
35.881978 35.645231 32.476503 34.282209 38.283883];

% nonlinear flow-meter
x_square=[20.215895 30.295146 40.118818 49.961206 60.258837 70.169189
80.053201 90.196077 101.149979 110.159382 120.2278396 130.249105
140.577313 150.265789 160.209692 170.779445 180.408687 190.758577
200.460845 210.242473];
y_square=[0.88288575 0.996420117 1.199572345 1.432615414 1.780766058
2.168725572 2.563274274 2.945414237 3.358516071 3.80963879 4.255537817
4.644685174 5.044119544 5.549611194 6.093259203 7.029614258 7.914844132
6.429851411 8.711731836 7.742627899];
p_square=[16.73513 22.44548 29.90062 38.549428 46.41302 53.189378
57.343085 61.376477 66.928874 69.485914 71.465449 71.19859 72.347628
74.48829 77.803047 74.733648 62.313977 66.971048 76.93587 61.963471];

Scrsz=get(0,'ScreenSize');
figure('Name','Flow-meter frequency response','position',[1 1 Scrsz(3)
Scrsz(4)])

subplot(3,3,1);
semilogx(x_capillary,y_capillary,'o','MarkerEdgeColor','k','MarkerFaceC
olor','r','MarkerSize',6)
title('Capillary tube frequency response (magnitude  $\hat{Q}/Q$ )')
xlabel('Frequency (HZ)')
ylabel('Magnitude (dB)')
legend('capillary','Location','NorthWest')

subplot(3,3,4);

```

```

semilogx(x_screen,y_screen,'*', 'MarkerEdgeColor','k','MarkerFaceColor',
'g','MarkerSize',6)
title('Screen pneumatach tube frequency response (magnitude  $\hat{Q}/Q$  ')
xlabel('Frequency(HZ) ')
ylabel('Magnititude(dB) ')
legend('screen pneumatach','Location','NorthWest')

subplot(3,3,7);
semilogx(x_square,y_square,'d','MarkerEdgeColor','k','MarkerFaceColor',
'b','MarkerSize',6)
title('square edged orifice tube frequency response (magnitude
 $\hat{Q}/Q$  ')
xlabel('Frequency(HZ) ')
ylabel('Magnititude(dB) ')
legend('square edged orifice','Location','NorthWest')

subplot(3,3,2);
semilogx(x_capillary,p_capillary,'o','MarkerEdgeColor','k','MarkerFaceC
olor','r','MarkerSize',6)
title('Capillary tube frequency response (Phase shift  $\hat{Q}/Q$  ')
xlabel('Frequency(HZ) ')
ylabel('Phase(deg) ')
legend('capillary','Location','NorthWest')

subplot(3,3,5);
semilogx(x_screen,p_screen,'*', 'MarkerEdgeColor','k','MarkerFaceColor',
'g','MarkerSize',6)
title('Screen pneumatach tube frequency response (Phase shift  $\hat{Q}/Q$  ')
xlabel('Frequency(HZ) ')
ylabel('Phase(deg) ')
legend('screen pneumatach','Location','NorthWest')

subplot(3,3,8);
semilogx(x_square,p_square,'d','MarkerEdgeColor','k','MarkerFaceColor',
'b','MarkerSize',6)
title('square edged orifice tube frequency response (Phase shift
 $\hat{Q}/Q$  ')
xlabel('Frequency(HZ) ')
ylabel('Phase(deg) ')
legend('square edged orifice','Location','NorthWest')

subplot(3,3,[3 6 9]);
semilogx(x_capillary,y_capillary,'o','MarkerEdgeColor','k','MarkerFaceC
olor','r','MarkerSize',6)
hold on
semilogx(x_screen,y_screen,'*', 'MarkerEdgeColor','k','MarkerFaceColor',
'g','MarkerSize',6)
semilogx(x_square,y_square,'d','MarkerEdgeColor','k','MarkerFaceColor',
'b','MarkerSize',6)
title('frequency response bandwidth compare of three sets of
datas(magnitude) ')
xlabel('Frequency(HZ) ')
ylabel('Magnititude(dB) ')

```

```
legend('capillary','screen pneumatach','square edged  
orifice','Location','NorthWest')  
hold off
```


APPENDIX D

LABVIEW VI HIERARCHY

